Title
Mobile sensor network to monitor wastewater collection pipelines

Author
Lim, Jungsoo

Publication Date
2012

Peer reviewed|Thesis/dissertation

UNIVERSITY OF CALIFORNIA
Los Angeles

Mobile sensor network to monitor wastewater collection pipelines

A dissertation submitted in partial satisfaction
of the requirements for the degree
Doctor of Philosophy in Computer Science

by

Jung S. Lim

2012

ABSTRACT OF THE DISSERTATION

Mobile sensor network to monitor wastewater collection pipelines

by

Jung S. Lim

Doctor of Philosophy in Computer Science

University of California, Los Angeles, 2012

Professor Mario Gerla , Chair

The Wastewater Collection System (WCS) has long been recognized as one of the critical infrastructures in the urban fabric, along with fresh water and power system infrastructure. An aging Wastewater Collection System may jeopardize public and environmental health by contaminating the sources of drinking water and by polluting the natural environment. Although the largest part of WCS failures are caused by aging infrastructure, careless dumping can lead to explosions and cause major catastrophes. Moreover, there is a growing consensus that greenhouse gas (GHG) generated from the wastewater infrastructure represents a significant fraction of GHG emissions. While a WCS failure can cause unimaginable hardship, systematic monitoring of the WCS has made little progress over the years due to several challenges that include invisibility, harsh environment, vast geographical span, and the requirement of minimizing service interruption. Thus far, various schemes have been designed and developed to monitor WCS (e.g., robots, Closed Circuit TV (CCTV)). However, due to the cost and the complications associated with these techniques, only a fraction of WCS are inspected each year.

To address some of these issues we propose a novel WCS monitoring method based on mobile pipeline floating sensors named; SewerSnort together with wireless manhole beacons/base stations. SewerSnort is dropped upstream of the WCS and traverses a path in the WCS network. While traveling downstream, the sensor detects emergency conditions (leaks, spills, illegal dumps, and dangerous methane gas concentration) and notifies base stations along the way. Also, the data is carried to the destination (i.e., treatment plant) where it is analyzed to detect anomalies. In this work, we design a wireless mobile pipeline floating sensor unit SewerSnort which is a fully automated and end-to-end monitoring solution; develop a GPS-free radio-frequency based localization scheme inside pipelines; develop an algorithm to detect WCS functional deficiencies; develop a simulation tool to assist field deployment; and develop a radio propagation model to estimate the radio channel quality inside sewer environment. The simulator provides tools to analyze scenarios; to trace the path of SewerSnort; to develop a mobility model for a convoy of SewerSnorts; and to visualize SewerSnort movement in real-time and monitor the in-sewer incidents. Also, possible applications of SewerSnort to real-world problem such as illegal dumping, improving the accuracy of GHG emission e stimates, and performing preventive WCS monitoring, are presented to mitigate or to address our important environmental issues.

The dissertation of Jung S. Lim is approved.

Jack W. Carlyle

Bruce Rothschild

Mani Srivastava

Mario Gerla , Committee Chair

University of California, Los Angeles

2012

To my parents

and to my sister

TABLE OF CONTENTS

LIST OF FIGURES

LIST OF TABLES

ACKNOWLEDGMENTS

This thesis would not have been possible without the help, support, and patience of my advisor Professor Mario Gerla. He provided me with so many insightful research ideas together with wide latitude to pursue them. His review and feedback on my publications have served an invaluable lesson during my Ph.D program. I also would like to thank Professor Diego Rosso for his advice and guidance, where without his knowledge and assistance this study would not have been successful. Also, I would like to thank Professor Mani Srivastava, Professor Bruce Rothschild, and Professor Jack W. Carlyle for the invaluable advice and guidance, and serving on my qualifying exam and dissertation committees. Lastly, I would like to thank Uichin Lee, YoungTae Noh, Sungwon Yang, Seongwon Han, and many other fellow students in the Network Research Lab.

VITA

Education

2001–2003	M.S., in Computer Science, University of California, Los Angeles, USA
1994–1997	B.S., in Computer Science, California State University, Los Angeles, USA

Work Experience

2001–current	Senior Systems Analyst, City of Los Angeles, Department of Public Works, Bureau of Sanitation, USA
1997–2001	Systems Analyst, City of Los Angeles, Information Technology Agency, USA

Academic Experience

2011–2011	Teaching Assistant (CS 130: Software Engineering), Computer Science Department, UCLA.

PUBLICATIONS

Jung Soo Lim, Jihyoung Kim, Jonathan Friedman, Uichin Lee, Luiz Vieira, Diego Rosso, Mario Gerla, Mani B Srivastava "SewerSnort: A drifting sensor for in situ Wastewater Collection System

gas monitoring" Ad Hoc Networks Journal (Elsevier), Special Issue on Challenged Environments, March 2011

J. Kim, J.S. Lim, J. Friedman, U. Lee, L.F.M. Vieira, D. Rosso, M. Gerla, and M.B. Srivastava, "SewerSnort: A Drifting Sensor for In-situ Sewer Gas Monitoring", In Proc. SECON, 2009, pp.1-9.

Jungsoo Lim, Uichin Lee, Mario Gerla, William J. Kaiser "Sewage Grid: mobile floating sensors that Monitor the Wastewater collection System", IEEE /IFIP WONS 2008, Fifth Annual Conference, Germany

CHAPTER 1

Introduction

1.1 The Problem

In the United States, the Wastewater Collection System (WCS) components are, on average, at least thirty years of age – with some even reaching ninety years of continuous service which far exceeds the lifespan of the WCS components [48]. As the cost associated with maintenance, upgrade, and replacement of the aging WCS is staggering [4], the frequency of system failures is soaring. US EPA estimated that approximately over 500,000 sanitary sewer overflow incidents had occurred in 2001 [68]. In addition, over 1.3 trillion gallons of untreated wastewater was discharged to the rivers or the oceans in 2001 alone [68].

Although one million miles of national WCS is designed to handle up to 50 trillion gallons of municipal wastewater per day, thus well above the 18 to 19 trillion gallons of wastewater generated daily in the US, the capacity is significantly reduced by functional deficiencies [69] caused by the aging infrastructure. Functional deficiencies such as blockage, infiltration, and inflow (I/I), reduce the effective capacity by more than 50% [40].

Most WCS failures are caused by aging infrastructures. However, careless dumping can also lead to catastrophes. The disastrous series of sewer gas explosions in Guadalajara, Mexico in 1992, which caused death of 206 people and left almost unrecoverable damages to the city [72], demonstrates the devastating effects of illegal dumping (in this case refinery oil derivatives) in the sewer lines. Unfortunately, illegal dumping is the most frequently committed environmental

crime [30] and it causes financial burden to our community[1]. Especially, any accidental discharge of untreated sewer contaminated by toxic chemicals to the public or to the natural environment is extremely hazardous to our community.

In addition, there is a growing consensus that sewer gas contributes a significant fraction of greenhouse gases (GHG) such as carbon dioxide (CO_2) and methane (CH_4) [20, 55]. Organic material transported by the sewer accumulates along the bottom (forming a sediment) and walls (forming a coating known as bio-film). Biochemical reactions that occur in these sediments and films produce hydrogen sulfide (H_2S, corrosive and poisonous), methane (CH_4, explosive and a major climate change contributor), carbon dioxide (CO_2, a major climate change contributor), and other volatile substances (collectively known as in-sewer gases) [27]. These in-sewer gases represent a considerable fraction of the greenhouse gases (GHG) released in the environment [20, 55].

Large worldwide efforts are underway to quantify these emissions and to elaborate strategies for prevention of gaseous formation [32]. Some of these efforts are sponsored by major utilities and non-profit organizations including the research funded by the Orange County Sanitation District, and by the Orange County Water District with the WateReuse Foundation. The latter two programs, both headed by Dr. Rosso, aim at quantifying and minimizing the process carbon footprint. Unfortunately, the current state of sewer monitoring technology forces a reliance on punctual measurement [75], with insufficient data density for high-resolution modeling. This has thus far forced the exclusion of sewer networks from the scope of the above projects. Therefore, there is a critical need for fundamental research to develop the appropriate tools for accurate in-sewer emission modeling, for full scale implementation of emission mitigation techniques, and for inclusion of sewer networks in process carbon-footprint analysis.

Thus, there is a critical need for fundamental research to develop an innovative approach for detecting and monitoring wastewater collection system.

[1] According to the October 8, 2006 USA TODAY article "Illegal Dumps Alter Western Landscape" by Benjamin Spillman: "... In California alone, illegal dumping on private and public land costs at least $87 million annually, ..."

1.2 The Challenges

Monitoring WCS poses unique challenges. First, the entire sewer pipelines are buried deep underground. A problem is not noticed until it becomes an "ecological failure." Second, due to the WCS harsh environment the sewer is not fit for human inspection. The areas that can be inspected are mainly limited to manholes. However, manhole-based sensor readings are poor indicators of toxic or flammable gas concentration due to fresh air drafting through the manhole, a problem known as "chimney effect." Moreover, manholes are being progressively sealed to reduce maintenance and odorous release; thus, leaving WCS segments of up to 100 m unchecked. Third, the geographical distance to be monitored is immense. For example, a large municipality like Los Angeles has a WCS spanning over 12,000Km [49]. Forth, the interruption of sewer service, when possible, causes tremendous inconvenience to the public and is typically minimized or avoided. However, inspecting sewers in operation is extremely complicated due to various dynamics. Also, the results are largely site-specific and may be open to interpretation. Lastly, the heterogeneity of the network and the multiplicity of potential threats make its monitoring problem-driven as opposed to routine maintenance. In general, sewer investigations are driven by infiltration or exfiltration, or odorous release, in general difficult if not impossible to predict. To date, there is no available model for accurately predicting release of sewer gases in a spatially distributed network, and existing as ventilation models are unsatisfactory when compared to field measurements [74].

Because of all the above reasons, only a small fraction of the WCS is inspected each year - typically, from 0.4% to 2% [69]. Closed Circuit TV (CCTV) inspection, which is the most widely used physical assessment method, is performed on 0.1% to 2% of the WCS each year [69]. The average distance between flow-meters is over 5 miles, hardly enough to map the behavior of a complex system like an urban WCS [69]. Moreover, flow measurements of such magnitude confine the error at best within 10% [24]. It is no surprise that the simulations, which interpolate the measured data points and model what may happen inside the sewer pipeline, often predict nonexistent problems (or totally miss existing threats) due to inadequate spatial sampling frequency.

Thus, accurate and effective WCS modeling, prediction, and fault detection requires a new inspection methodology that overcomes invisibility, harsh environment, and geographic spread. Such new inspection methodology should not depend on human intervention. Rather, it should automate the entire process. The new approach must support in-sewer gas monitoring continuity for the entire WCS network. To meet the above requirements, we propose a novel WCS inspection methodology based on mobile unmanned floating sensor platforms. In this work, we address the following challenges:

- **Emergency preparedness :** Unlike current inspection methods, which require lengthy preparation and provide only very limited spatial resolution, an "always on" solution is required to monitor the health of the WCS at short notice and along any path.
- **"Chimney effect" resolution:** The air flow through the manhole makes accurate gas measurement from manhole-mounted sensors impossible. A new approach that sample gas density along the pipeline is required.
- **Comprehensive Inspection:** Since manholes are being progressively closed up to reduce maintenance cost and odorous release and the distance between manholes is ever increasing, extended lengths of WCS segments are unchecked. To address this issue, a new monitoring technique needs to be developed.
- **Detection and localization of functional deficiencies:** A new approach should not only effectively detect functional deficiencies, but also accurately estimate their location. Traditional navigation aids, like Global Positioning System (GPS), are unavailable since the entire wastewater collection system is buried underground.

1.3 The Contributions

To overcome such challenges we envision a novel WCS monitoring method based on mobile pipeline floating sensors named, SewerSnort together with wireless manhole beacons/base sta-

tions. SewerSnort is dropped upstream of the WCS and traverses a path in the WCS network. While traveling downstream, the sensor detects emergency conditions (leaks, spills, illegal dumps, and dangerous methane gas concentration) and notifies base stations along the way. Also, the data is carried to the destination (i.e., treatment plant) where it is analyzed to detect anomalies.

In this work, we design a low cost mobile floating sensor node SewerSnort II together with wireless sensing network to monitor WCS and to notify emergency conditions. SewerSnort II is dispensed upstream of the WCS and traverses a path in the WCS network. While traversing the path, SewerSnort II acquires operational data along with geographical information messages sent from beacons installed beneath manholes. When SewerSnort II detects emergency conditions during its journey, it uploads the collected data to base stations. Upon the completion of journey, SewerSnort II may be extracted at a wastewater treatment plant, pumping station, or sewer manhole using a screening device similar to the one used at the pumping station. The data acquired by SewerSnort II can be collected through traditional public network infrastructure systems such as municipal Wi-Fi, an emerging low-power high-availability mesh networking systems such as Streetline [62]. Additionally, the data in SewerSnort II can be manually retrieved through short-range wireless communication upon retrieval since physical contact with the probe once deployed in the sewer is not advisable due to surface contamination and biohazard.

The proposed system would allow frequent and comprehensive WCS inspection, early detection of problems, and innovative detection methodology of functional deficiencies. In addition, the system would allow targeting more accurate sewer flushing timetable which substantially improves service uptime, reduces the maintenance expense, enhances illegal toxic chemical dumping enforcement, reduces the risks of contaminating the source of drinking water, and reduces the risks of polluting our natural environment. As envisioned, this work makes the following contributions to exploit a mobile sensing network in the study of computer science:

- A mechanical and electrical design of a floating mobile sensor platform which is fully automated and end-to-end monitoring solution

- The development of a GPS-free underground localization scheme using beacon unique geo-ID's transmitted through probing messages with radio frequency (RF) power measurements (RSSI) from beacon-to-SewerSnort II radio transmissions
- The development of a network system to opportunistically notify emergency conditions of wastewater collection system
- The development of innovative fault detection schemes for infiltration/inflow, exfiltration, and blockage by exploiting their side effects
- The development of simulation tools to assist a field deployment of the system
- The development of analytical radio signal propagation model inside sewer environment to estimate the wireless communication channel quality and to maintain the network connectivity among floaters during the journey

CHAPTER 2

Background

2.1 Wastewater Collection System

A Wastewater Collection System collects wastewater generated from households or industries and transports them to treatment facilities or disposal sites. The system is categorized as a separate sewer system or a combined sewer system depending on whether sanitary wastewater is separated from storm water.

The separate sewer system (typical of the Western United States and of newer developments) has two wastewater drainage systems in parallel; i.e., a sanitary sewer discharging wastewater to a wastewater treatment plant and a storm sewer discharging storm water to a receiving water basin.[1] The combined sewer system (typical of the Eastern United States and of older developments) drains both sanitary and storm water to a wastewater treatment plant. There are two types of sanitary sewers based on hydraulic characteristics and purposes; gravity and pressure sewers. The gravity sanitary sewers transport wastewater by gravity and are commonly used to collect wastewater from wastewater sources (residential, commercial, industrial sources). Gravity sewers are used when the natural slopes are sufficient enough to convey a flow. The pressure or pumped sewer transports wastewater using pressure to collect wastewater from residential sources where the construction of a gravity sewer is unsuitable (e.g., uphill slopes). It is also possible to use a combination of gravity and pressure sewers.

A typical separate sanitary collection system illustrated in Figure 2.1 is organized as follows:

[1] A receiving water basin denotes a stream or river that has water flowing in it, or a lake, pond, dugout, or slough that has water standing in it.

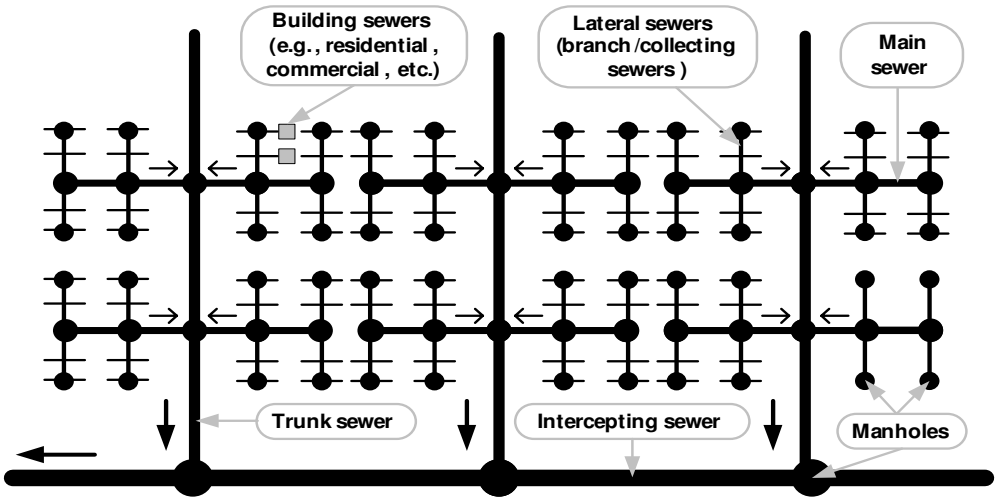

Figure 2.1: Illustration of a sewer system

- *Lateral sewers* (also called branch or collecting sewers) are used to collect wastewater from buildings (entry points) and convey it to the main sewer. They are usually located underneath streets or utility easements.

- *Main sewers* are used to convey wastewater from lateral sewers to larger sewers (trunk or intercepting sewers).

- *Trunk sewers* are large sewers that are used to convey wastewater from main sewers to the treatment or disposal facilities or to large intercepting sewers.

- *Intercepting sewers* are large sewers that are used to intercept a number of main and trunk sewers and convey wastewater to the treatment or disposal facilities.

- *Manholes* are used for sewer cleaning and inspection. They are located where the pipe system changes direction, grade, or diameter, at junctions, and, for small diameter sewers ($d < 1.2m$) at intervals no greater than $120m$.

2.2 In-sewer processes

In-sewer processes that occur during conveyance of wastewater are physical, chemical and biological in nature. Physical processes are related to the build-ups and erosion of sewer sediment. Chemical and physico-chemical processes occur due to the gas transfer over the air-water interface (e.g., emission of hydrogen sulfide) and the chemical oxidation and reduction of sulfur-carrying compounds. In biological processes, bacteria degrade organic compounds (C, H, O) for synthesis and energy harvest, leading to transformations of wastewater compounds and changes in the biodegradability of the wastewater, and to the release of gases in the sewer air space.

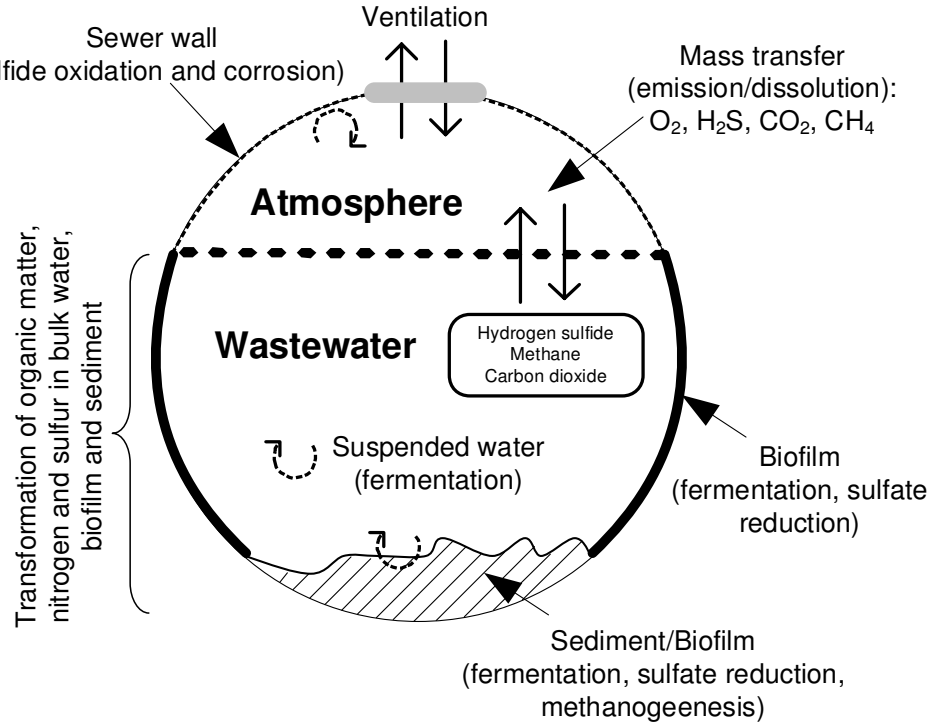

Figure 2.2: Illustration of in-sewer processes

As shown in Figure 2.2, in-sewer biological processes happen in five phases [27]: suspended water, biofilm (slime layer), sediment, atmosphere, and the sewer wall. These phases interact and exchange relevant substances across the phase boundaries. An in-sewer bio-process will have

different behavior based on microbial redox conditions(quantifiable using an oxidation-reduction potential [ORP] probe): aerobic respiration when dissolved oxygen is present, anoxic respiration when nitrate/nitrite ions are present and anaerobic respiration when none of these (oxygen, nitrate/nitrite ions) are present.[2] The shift from anaerobic to anoxic metabolism can be engineered by adding nitrite to the sewer, in order to curb sulfur reduction and odor formation [32]. In Table 2.1, we summarize different redox conditions and relevant sewer gases generated in various types of sewers. Aerobic/anoxic respiration produces carbon dioxide, whereas anaerobic respiration generates numerous volatile substances that vaporize or evaporate at atmospheric pressure such as hydrogen sulfide (product of sulfate reduction), carbon dioxide (product of fermentation), and methane (product of methane-genesis).

Table 2.1: Sewer Gases Under Different REDOX Conditions

Redox conditions	Possible Sewer Types	Sewer Gases
Aerobic (+oxygen)	Partly filled gravity sewer Aerated pressure sewer	Carbon dioxide (CO_2)
Anoxic (-oxygen,-nitrate)	Pressure sewer with nitrate	Carbon dioxide (CO_2)
Anaerobic (-oxygen,-nitrate,+sulfate)	Pressure sewer Full-flowing gravity sewer Gravity sewer (low slope, sediment)	Hydrogen sulfide (H_2S) [sulfate reduction] Carbon dioxide (CO_2) [fermentation] Methane (CH_4) [methane-genesis]

In particular, hydrogen sulfide diffused into a thin liquid film on the sewer surface (see Figure 2.2) can be oxidized to sulfuric acid (H_2SO_4) by microbial reactions [27]. Then, sulfuric acid may react with the alkaline cement ($CaSO_4$) in the concrete pipes causing corrosion.

Each of these in-sewer processes can be analytically modeled using differential equations [73,

[2]A microbial "respiration" process consists of two steps (called redox process): *oxidation* of organic matter and *reduction* of an electron acceptor. In other words, bacteria break down organic matter and transfer electrons from the electron donor (organic matter) to the relevant electron accepter (e.g., oxygen, nitrate/nitrite ions, sulfate ions)

76]. The models typically consider various factors that influence reactions [73]. For instance, a sulfate reduction model takes the following factors as inputs: quantity of sulfate, Chemical Oxygen Demand (COD), temperature, pH, area-to-volume ratio (i.e., biofilm and sediment), flow velocity, and anaerobic residence time [76].[3] In practice, however, accurately fitting a model to in-sewer processes is greatly challenging, for the present approaches make in-situ measurement extremely laborious and substantial data collection must be performed to count and to understand the spatio-temporal variability of the underlying model parameters while biological processes are correlated [73].

2.3 Sewer functional deficiencies

2.3.1 Blockages

Blockages as illustrated in Figure 2.3(a) are composed of organic and/or inorganic matters. When the organic matters are decomposed, methane (CH_4) and hydrogen sulfide (H_2S) are produced anaerobically [15]. Thus, sewer gas formation is a key indicator of sediment accumulation. Nevertheless, sewer gas formation and release are not spatially linked, i.e. formation may occur in a section where the air-space is in negative pressure and air is drafted in the local manholes, with potentially distant release downstream or upstream of the formation zone depending on gaseous pressure gradients. Whereas liquid formation occurs in the zone of debris accumulation and/or of anaerobic activity, the gas-phase composition of sewer gas in the surrounding area may depart from equilibrium due to rapid transport of the sewer gas in the air-space. It is therefore crucial to monitor both the liquid- and gas- phase composition of sewer gases to identify the spatial distribution of formation and release.

[3] Chemical Oxygen Demand (COD) is defined as the quantity of a specified oxidant that reacts with a sample under controlled conditions.

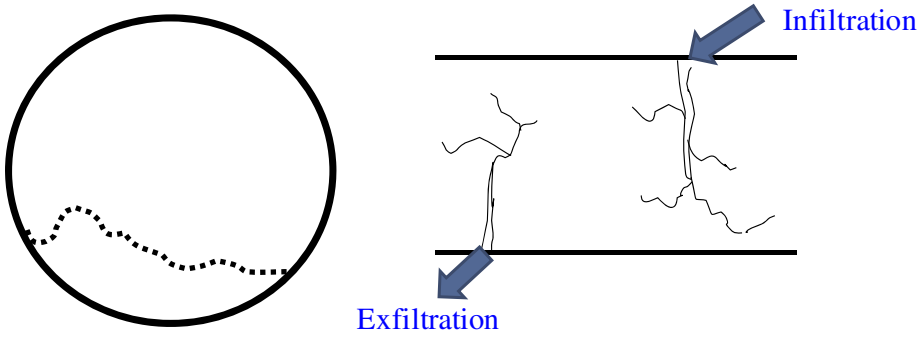

(a) Blockages (b) Cracks

Figure 2.3: Illustration of sewer functional deficiencies: (a) Blockages and (b) Infiltration/Exfiltration

2.3.2 Infiltration and Inflow

Infiltration/Inflow (I/I) as illustrated in Figure 2.3(b) is groundwater or storm water gets into sewer system through cracks as shown in Figure 2.4. I/I increases the flow level and can cause overflows. In general, groundwater/storm water exhibits much distinctive characteristics from sewer. For example, depending on the type of soil at the water table, the concentration of total dissolved solid (TDS) in the sewer is diluted by I/I since TDS in groundwater is typically less than 800 mg/l while sewage has typically 1,000 mg/l or more of TDS [64]. Since the concentration of TDS can be estimated by the amount of dissolved ions[4], I/I can be effectively detected by measuring conductivities along the pipeline.

2.3.3 Exfiltration and Leakages

Exfiltration is sewage escaping a WCS through infrastructural cracks. Although untreated wastewater leakages are the major cause of groundwater contamination, monitoring exfiltration has been greatly challenging due to their invisibility. Exfiltration is not visible even during closed-circuit television (CCTV) inspection, but may be detected by exploiting its side effects. In case of ma-

[4]The conductivity of rainwater is near zero and groundwater has 200 umhos/cm while sewage has about 2000 umhos/cm. [22]

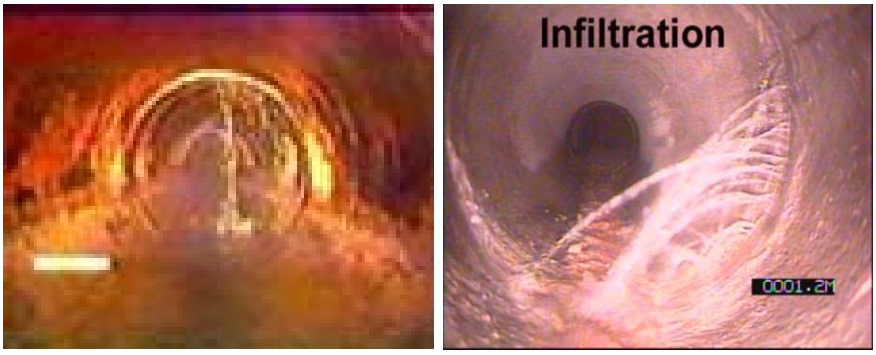

Figure 2.4: Images of infiltrations

jor cracks, acoustic detection of seeping/gushing water can be used. Also, the escaping fluid may cause flow reduction. Mechanically, the "flow slow down" causes organic/inorganic materials to be accumulated round the defective area. In addition, spatially monitoring changes in liquid level in the sewer with a floating sensor may help detecting exfiltration. Currently, exfiltration is estimated by using tracer experiments based on mass balance analysis. In seismically active regions such as California, infrastructural cracks and elements loss of alignment continuously progress, requiring a continuous and spatially distributed monitoring tools (such as the one proposed here).

2.4 Environmental and health impacts of sewer gas

High concentration of sewer gas is a warning signal of system failure and can be an indicator of hazardous environments (i.e. endangering public health and contaminating our natural environment). Sewer gas not only generates obnoxious odor, but also contains harmful toxic gases such as hydrogen sulfide H_2S and carbon dioxide CO_2 which endanger public safety. Moreover, by considering the growing consensus that sewer gas represents a significant fraction of GHG, the sewer gas substantially pollutes our natural environment.[5] However, the current effort to quantify GHG emissions from wastewater conveyance and treatment industries has largely overlooked the sewers because of the lack of basic knowledge about sewer internal dynamics and access imitations of the

[5] According to New York Mayor's report in 2007, 17% of GHG emission was caused by sewer [47]

current sewer inspection technologies. Especially when we consider the fact that a significant fraction of wastewater components nowadays (e.g., soaps, detergents) are petrochemical derivatives with definite impact on GHG, acquiring accurate gas concentration distributions in sewer becomes more critical than ever before.

Up until now, the current sewer models have been based on punctual measurements of methane gas, with immense loss of the opportunity of measuring a suite of components throughout the sewer network. Thus, the proposed method to solve this important environmental problem makes it feasible to probe the entire WCS and to overcome the limits of the current sewer gas emission models that rely on only punctual measurements.

CHAPTER 3

Related Works

Wireless sensor networks have been widely utilized in various environmental monitoring systems. Among the wealth of research contributions, this chapter reviews only the few that are most significantly related to our work.

3.1 Advanced pipeline monitoring systems

Mobile robots can perform sewer inspection (e.g., anomaly detection) by autonomously navigating a pipeline. They are typically equipped with lights and cameras for pipeline profiling, and various sensors (e.g., sonar, infrared, laser) for autonomous navigation. To name a few prototypes, there are KURT developed by Kirchner et al. [34] and KANTARO by Ahrary et al. [2]. KURT, a six-wheeled robot equipped with sonar, has two types of tasks which are classified as basic or complex. The basic task is to collect the field data and the complex task is to react based on the pre-loaded internal map and the pre-installed program. However, when this six-wheeled robot drifts in a sewer pipe and toppled over, the pre-loaded internal map and the instructions for tasks are no longer useful.

Mobile robot research in sewers has been focused on localization using an internal map and feature detection (e.g., manholes and inlets). Teichgräber et al. [65] proposed SEK, a "cable-guided" floating inspection tool that conducts camera inspections, recording major abnormalities such as erosion, deposits, obstacles and leaks in the gas space. SEK differs from SewerSnort in that (1) SewerSnort is an "unteathered" lightweight drifter that monitors in-sewer gases, and (2) SewerSnort performs localization using the beacons installed beneath sewer manholes.

Wireless sensor networks have recently utilized in sewer monitoring [61, 29]. PipeNet [61] uses a network of fixed wireless sensors to detect and locate leaks in the "full flowing" water transmission pipeline. The system collects pressure, flow velocity, and acoustic/vibration data at the fixed points along the pipelines. Then, an analytic algorithm is applied to detect and to locate the leaks. Nonetheless, the leak detection algorithm for water supply pipeline of PipeNet, does not apply for WCS since WCS is designed to carry open channel flow and sewer is primarily open channel flow which has a free flow surface and free space for air flow passages inside pipeline while fresh water transmission line carries pipe flow which fluid is completely filled up in a conduit. In addition, installing sensor at every few meters may infeasible in a WCS system, especially when we consider a large municipality like Los Angeles, which the WCS spans over 12,000Km [49]. The IDEAS laboratory in Purdue university used a wireless sensor network for developing a system to prevent Combined Sewer Overflow (CSO) in South Bend, IN [29]. The system transmits an alert alarm through a wireless channel to facilitate automatic flow diversion when the flow level reaches the threshold. In addition, a system to inspect sewer using a buoy was invented and patented by Stenstrom *et al.* [60]. A tethered buoy electronic tracking system for localization was proposed together with a sewer buoy to inspect sewer.

3.2 Current industry practices

Apparently, the major limitations of the current inspection approaches are the complications associated with the methodology, the access limitation, and the expensive operational cost and maintenance expense.

3.2.1 Physical condition assessment methods

- Human inspection [71] - trained personnel visits a site, and by visual inspection they identify existing or potential problem area. The human inspection is not only hazardous to personnel and to people in the surrounding areas, but also unable to detect most of the functional

deficiencies.

- Dyed water testing [71] - an inspector floods the suspected pipe segment with fluorescent dyes and radioactive tracers to identify potential leaks.
- Lamping [71] - an inspector takes pictures of sewer pipe by lowering a still camera and "lamp" into a manhole to identify any defects in the pipe. The reachable distance is limited by the length of their wire.
- Sonar [71] - the sonar technology is used to generate an image of the interior of the pipeline. The test requires heavy and expensive equipment, yet the quality of image is poor in general.
- Sewer Scanner and evaluation technology (SSET) [71] - SSET is to provide more complete images of the interior of the pipeline than the sonar technology. A 360 degree scanner is used to produce a full digital picture.
- Closed circuit television (CCTV) [71] - A closed-circuit camera with light captures the images of the pipeline interior. CCTV provides much more data than any other physical condition assessment methods, and it is the most widely used method; yet, it cannot be used on pipeline with odd shape or less then 36" diameter [70].

3.2.2 Flow monitoring system

While the physical condition assessment methods provide only temporary and instantaneous data, the flow monitoring system provides a permanent and continuous data by installing a fixed sensor at the interested locations. However, the flow monitoring system, combined with wireless technology, is designed only to control the sanitary sewer overflow, neither to detect nor to locate the functional deficiencies of the WCS system [71].

3.3 Mobile robot localization in sewers

Mobile robot localization may be classified as relative, absolute, or a mixture of both. Relative localization is based on dead reckoning using gyroscope and compass. As the robot moves, its actual position may deviate from dead reckoning estimate due to the accumulation of errors (e.g., wheel slippage). Thus, periodic absolute localization is crucial to long-term performance.

Absolute localization requires either active beacons that transmit to the robot a signal with position information (e.g., GPS), or known landmarks recognizable by the robot. The most popular approach is relative localization with landmark recognition. Unfortunately, in sewers, there are only a few local features such as manholes, junctions, pipe joints and inlets that can be used as landmarks for localization [45]. Consequently, landmark detection in sewers experiences uncertainty with regard to detection and identity. Bayesian models can be used exploiting the conditional probability of the estimated location with respect to the observation and to the a priori probability distribution. Popular Bayesian methods include Kalman filtering [46], Markov [18], and Particle filtering (or Monte Carlo localization) [17].

In our system we build a GPS-free localization scheme based on received signal strength indicator (RSSI) ranging technique using beacons to locate and to track a floating sensor node. A beacon installed under sewer manholes transmits geographical identification data (i.e. geo-tag) on a IEEE 802.15.4 channel. Then, the sensor node localizes itself through the beacon message and RSSI data associated with its packet. Since RSSI based technique can be implemented without any special hardware support and can provide relatively accurate location information, it is a natural choice for the work. In addition, we enhance our localization scheme by taking into account unique characteristics of WCS environment.

CHAPTER 4

The Use of Floater

4.1 Discovery of emergency

4.1.1 Prevention of gas explosion

Although most of system failures are caused by aging infrastructure, malicious attacks such as terrorism or sabotage can result catastrophic disaster. The disastrous series of sewer gas explosions in Guadalajara, Mexico on Wednesday, April 22, 1992, which caused death of 206 people and left almost unrecoverable damages to the city [72], demonstrates the potential impact of terrorist attack using underground sewer lines.

To deliver prompt alarms in case of possible explosion or astronomical explosive gas concentration, a SewerSnort may upload collected data to base stations while traversing WCS before it reaches to the destination. An urgent data can be transmitted to a beacon node installed under a manhole cover. Then, the beacon node can relay the received data to a gateway node deployed on a nearby lamppost which will eventually deliver the data to a central node so that the possible gas explosion can be prevented.

4.1.2 Detection of illegal dumping

Unfortunately, people dump hazardous and unauthorized substance into sewer to avoid "disposal fee" or just for their convenience. However, illegal dumping of highly flammable solvent in sewer can create devastating disaster as we have seen in the past. In addition, illegal dumping of toxic

chemicals can be extremely hazardous to the public and our natural environment.

However, detecting illegal dumping in WCS can be much more difficult than detecting functional deficiencies. In general, functional deficiencies are mainly caused by aging infrastructure and can be detected at any time, but illegal dumping is caused by human and can be detected only when it happens. In order to detect illegal dumping a frequent WCS inspection is required. However, the cost and the complications associated with the current inspection methods make a frequent inspection infeasible. On the other hand, a low cost floater requires minimal preparation time and operational cost. In addition, sample data which indicates a possible illegal dumping can be uploaded to a nearest base station[1] and initiates an appropriate action to be taken. Detailed scenario analysis of illegal dumping detection is explained in Section 9.2.1.

4.2 Monitoring of greenhouse gas (GHG) emission

In-sewer processes are responsible for biodegradation of organic compounds, generation of obnoxious odor, and production of sewer gases, and should be monitored in a spatially distributed manner to allow proper modeling of GHG emission. However, the knowledge regarding processes occurring in sewer has been limited to punctual measurements of methane gas [20, 21], with immense loss of critical data.

The proposed mobile pipeline floating sensor would allow comprehensive WCS inspection and provide with needed data to improve the accuracy of GHG emission modeling.

[1] In some cases, toxic chemical upsets pH level (i.e. acetic acid classified as carcinogen has pH 1.0). Thus, pH fluctuations can be an indicator of illegal dumping. In addition, toxic metal such as mercury or metal wastes causes significant increase of conductivity.

4.3 Detection of functional deficiencies

4.3.1 Blockages

The deposits that cause blockage are typically composed of organic/inorganic components, where they produce methane (CH_4) gas and hydrogen sulfide (H_2S) gas [15] when they are decomposed. Thus, sewer gas formation and high concentration of hydrogen sulfide gas are a key indicator of sediment accumulation or blockage. However, sewer gas formation and release are not spatially linked, i.e. formation may occur in a section where the air-space is in negative pressure and air is drafted in the local manholes, with potentially distant release downstream or upstream of the formation zone depending on gaseous pressure gradients. While liquid formation occurs in the zone of debris accumulation and/or of anaerobic activity, the gas-phase composition of sewer gas in the surrounding area may depart from equilibrium due to rapid transport of the sewer gas in the air-space.

Thus, as pointed out previously, the floater can monitor both the liquid- and gas- phase composition of sewer gases concentration along to pipeline between manholes to identify the spatial distribution of formation and release and provide insight for infrastructural diagnostics [15].

4.3.2 Infiltration and Inflow

Infiltration and Inflow (I/I) is groundwater/storm water gets into sewer system through cracks. As pointed out previously, I/I increases the flow level and can cause overflows. Groundwater/storm water has a very different chemistry than sewer water. For example, depending on the type of soil at the water table, the concentration of Total Dissolved Solid (TDS) in the sewer is diluted by I/I since TDS in groundwater is typically less than 800 mg/l while sewage has typically 1,000 mg/l or more of TDS [64]. Since the concentration of TDS can be estimated by the amount of dissolved ions[2]. Thus, I/I can be effectively detected by measuring conductivities along the pipeline.

[2]The conductivity of rainwater is near zero and groundwater has 200 umhos/cm while sewage has about 2000 umhos/cm. [22]

In addition, the total organic carbon (TOC) measured in sewer is much higher than TOC measured in groundwater.[3] Thus, sampling data throughout the entire pipe segment with a floating sensor can provide a novel, comprehensive, and efficient I/I detection method.

4.3.3 Exfiltration and leakages

Exfiltration causes untreated wastewater to escape the WCS due infrastructural cracks. As pointed out previously, monitoring exfiltration has been greatly challenging due to its "invisibility." However, we can exploit a side effect of exfiltration, namely flow reduction due to escaping fluid. Mechanically, the "flow slow down" causes organic/inorganic materials to be accumulated around the defective area. Also, an acoustic detection of seeping/gushing water can be used in case of major cracks.

[3] In general, TOC in sewer is 10 to 170 mg/L and TOC in groundwater is < 20 mg/L [10].

CHAPTER 5

System Overview

5.1 System design requirements

In system design, the main objective is to monitor the health of WCS effectively, pro-actively, and comprehensively; therefore, the acquired knowledge about in-sewer process would assist detecting illegal dumplings, delivering prompt alarms in case of emergencies, improving the accuracy of GHG emission modeling, and preventing WCS failure. In order to monitor the entire WCS while addressing the unique challenges in WCS, the system should fulfill the following requirements:

- **System should provide 24/7 "readiness."** In order to support **emergency preparedness**, the system should be deployable with minimum preparation time and effort. To monitor the health of the WCS at short notice and along any path the system should be fast to deploy, uncomplicated to use, and painless to manage.

- **System should address "Chimney effect" in WCS.** In order to address "Chimney effect", the system should be able to collect data between manholes. To access area between manholes, the system should be independent of the pipe profile (material, shape, or size.) The most widely used WCS inspection technologies such as Closed Circuit TV (CCTV), Sewer Scanner and Evaluation Technology (SSET), or sonar only works with a limited set of the pipe materials and shape deployed in WCS's [71]. In addition, system should resolve the accessible distance limitation. Especially, since manholes are being progressively closed to reduce maintenance cost and odorous release, the distance between manholes is ever increasing. Since all current physical assessment methods suffer from strict limitations on the

reachable distances, a new approach is required.

- **System should support comprehensive inspection.** In order to a provide comprehensive inspection, system should be scalable. A large metropolitan city like Los Angeles has a WCS composed of over 12,000 Km of pipelines [49]. In addition, system should be deployable with reasonable cost such that the deployment, maintenance, and operational expense should be kept affordable. For example, on average CCTV costs $2.26/foot and SSET costs $3.47/foot. In other words, one comprehensive examination for Los Angeles costs $8.27 million using CCTV or $12.7 million using SSET.

- **System should locate functional deficiencies.** In order to detect and locate the functional deficiencies along the pipeline, we need to annotate the data with location information. However, Global Positioning System (GPS) signal is unavailable to aid measuring the proximities of sampling points inside pipeline since the entire wastewater collection system is buried underground and GPS signal is unreachable. Thus, we need to develop a new localization scheme.

5.2 WCS monitoring using mobile floating sensors

To address the above system design requirements and to overcome the challenges, we propose the use of mobile floating sensors to monitor in-sewer gases and to acquire other operational data as illustrated in Figure 5.1. Unlike conventional inspection techniques, we use a mobile pipeline floating sensor named SewerSnort II and wireless network together with fixed sensors placed at strategic points to monitor the health of WCS (Throughout the paper, we will use SewerSnort II and SewerSnort interchangeably).

A SewerSnort is dropped upstream and traverses a path of the WCS network. While it travels down the pipeline, SewerSnort collects operational data using various on-board sensors. Once a SewerSnort is deployed, we need to keep track of its position. Since the Global Positioning System (GPS) transmits signals from very high altitudes using only 50W transmitters by microwave-

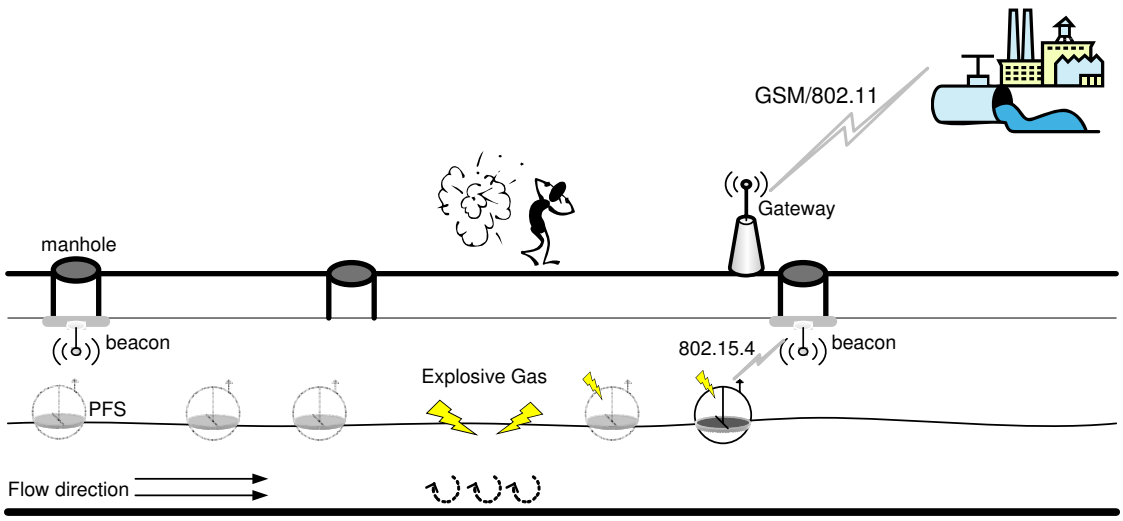

Figure 5.1: Illustration of mobile pipeline floating sensor monitoring scenario

frequency carriers, the GPS signal does not readily penetrate the ground.

Thus, we propose a GPS-free localization scheme by exploiting beacons and Received Signal Strength Indicator (RSSI). First, preprogrammed beacons are installed underneath sewer manholes in the region of interest. Then, beacons broadcast messages which include their physical locations and time-stamps by pre-determined interval. Second, a SewerSnort listens to the beacons and collects RSSI values from received beacon messages, while traversing down pipes. Then, a SewerSnort estimates its proximity based on beacon messages and the strength of their respective signals (via off-line processing).

The collected data is stored on-board memory and retrieved when the SewerSnort reaches its destination. SewerSnort may be extracted at a wastewater treatment plant, pumping station, or sewer manhole using a screening device similar to the one used at the pumping station. In emergencies, to reduce delays, the collected data can be opportunistically uploaded to a nearby base station/gateway as illustrated in Figure 5.1.

Also, SewerSnort can be deployed at strategic locations by analyzing the sewer map and inspection demands. The strategic points are typically located at an entry point to the sewer. In addition, SewerSnort dispensing schedule can be configured based on the application scenario.

For instance, if engineers want to understand how in-sewer gas level changes over time, they can dispense floaters at regular intervals for continual sampling.

The use of mobile pipeline floating sensor together with wireless network is a simple solution, yet it yields great features as follows:

- Unlike the conventional robotic WCS inspection systems which are complicated to setup and operate, a mobile floating sensor is easy to use and requires minimal setup time. Also, the conventional inspection robotic systems are bulky, heavy, and require external power. However, the proposed floating mobile sensing unit is small, light, and battery-operated (e.g., $< 30cm$ in diameter, and $< 300g$ in weight) and can operate during any flow rate conditions.

- One of the main advantages of mobile floating sensor is their immunity to pipe profile. A mobile floating sensor is not affected by the pipe profile. Whether the pipe is made of brick, concrete, or clay, the SewerSnort is insensitive for the materials of pipeline. Also, the shape of pipeline does not affect SewerSnort data collection. In addition, SewerSnort can access to area difficult to reach if not impossible with the current industry WCS inspection technology.

- The use of mobile floating sensor together with wireless network makes possible to inspect the entire WCS without running wires. In addition, SewerSnort and the beacons require a minimal operational and maintenance expense while they make comprehensive proactive WCS inspection feasible.

5.3 Feasibility

The fluid flow in a pipe is classified as laminar or turbulent, and the sewer flow is considered as laminar in general. The laminar flow is a stable and streamlined flow; yet, the turbulent flow has highly irregular and random motion. To determine the type of flow we use its Re value:

$$\text{Re} = \rho \upsilon \delta / \gamma$$

whereρ is the fluid density, υ is the fluid velocity, δ is geometrical length associated with flow, and γ is the viscosity. The term viscosity is used to characterize the degree of internal frictions in the fluid. Also, the amount of energy lost to internal friction relates to the flow velocity. For pipe we have:

Laminar flow:	$Re < 2000$
Transitional flow:	$2000 < Re < 4000$
Turbulent flow:	$4000 < Re$

The sewer flow is considered as laminar based on the following facts. First, sewer contains high concentration of suspended solid which creates internal frictions. The concentration of suspended solid in sewer has not been systematically measured. However, approximately 100 milligram per liter (mg/l) of suspended solid exists in the effluent after the primary treatment in the wastewater treatment plant, while the tap water contains less than 1 mg/l [43]. Second, the slope of pipeline is rather mild to control the flow velocity since the flow velocity of a pipeline is mainly governed by slope of pipe and gravity. For instance, the sewer network design manual of Bureau of Engineering at Los Angeles specifies 0.003 radian (or 0.1719 $^\circ$) for the pipe slop [58]. Third, concrete, which creates relatively more internal friction than copper, glass, plastic or ion, is the widely used material for sewer pipeline. According to the Nikuradse's definition of mean height of roughness; copper and glass are 0.003, iron is 0.15, plastic is 0.03, and concrete is 6.0 where the higher number is, the rougher surface is. Thus, in general the sewer flow is classified as laminar which steady and stable enough not to significantly affect sampling data.

CHAPTER 6

System Design

6.1 Design of mobile pipeline floating sensor "SewerSnort II"

In our previous work [33], we designed an inner tube hull that can roll along the pipeline sidewall (Figure 6.1(a)). The sensing unit is placed in the middle of the inner tube to prevent wastewater from submerging it. Also, the hull is tall enough to sustain the sensor above waterline in the event when high turbulence capsizes the floater.

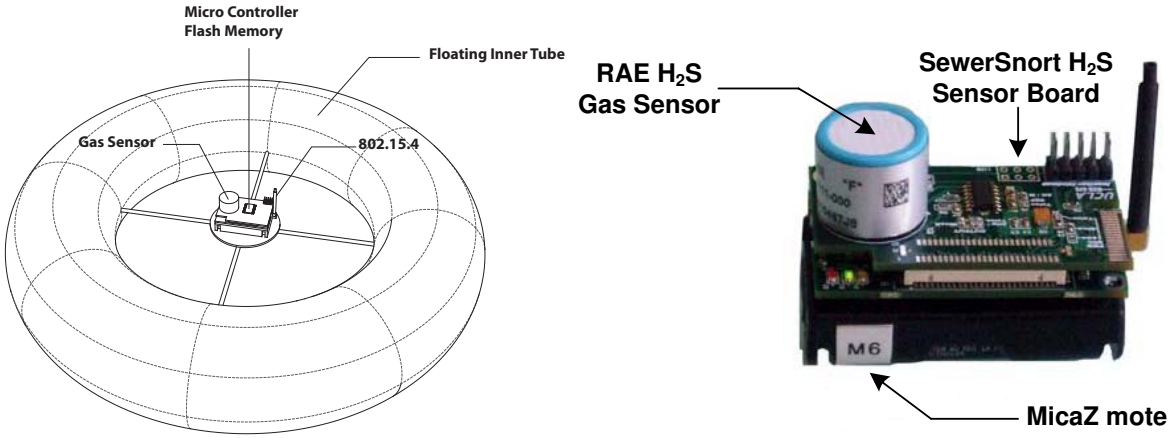

(a) SewerSnort

(b) The gas sensor board with a MicaZ mote

Figure 6.1: SewerSnort floater design. The size of a tube can be adjusted based on the size of pipe

When a surface vessel moves through a constricted waterway, the current velocity gradient of open channel flow may push the vessel toward the bank. This phenomenon is known as the "bank suction" effect [16]. While a vessel moves down, an asymmetric flow around the vessel causes pressure differences. Such pressure differences may result lateral forces that pushes the

vessel to the bank. While a lateral force pushes the vessel toward the bank, the direct force from flow pushes the end of the vessel which causes yawing movement. The strength of lateral force is depending on many parameters such as the depth of water, the width of waterway, the velocity of flow, and the speed of vessel. When we consider the flow depth, the size of pipe, and flow velocity, we do not expect considerable pressure differences around the floating sensor while it traverses down pipeline. Especially, when the speed of floater is zero (i.e. no on-board motion control), no significant later force will be generated toward the floating sensor. Thus, the inner tube hull may roll along the pipeline sidewall.

Also, we designed a SewerSnort hydrogen sulfide (H_2S) gas sensing unit as a proof of concept. We used electrochemical sensors to detect H_2S gas. Electrochemical sensors detect a specific gas by generating electrical current proportional to the concentration of gas and reacting with itself. This electric current is generated between the sensor's anode and cathode electrodes as illustrated Figure 6.2.

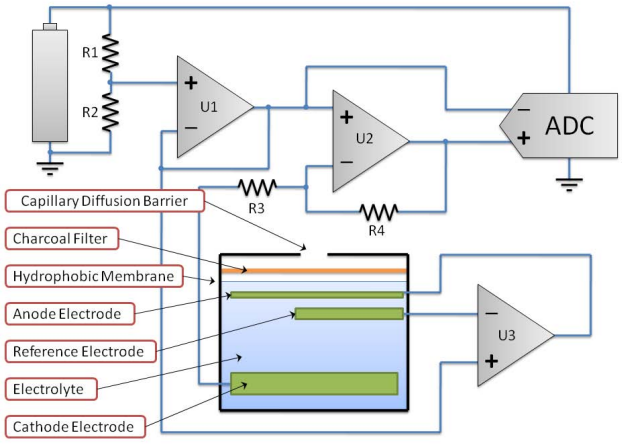

Figure 6.2: Simplified schematic of the electrochemical gas sensor and analog signal conditioning elements. This differential ratiometric approach consumes $< 15\mu W$ in our current implementation. Electromagnetic compatibility elements are not shown for clarity.

Our SewerSnort floaters are equipped with an RAE 032-0102-000 electrochemical sensor element [53] and a custom Analog Front End (AFE) that provides bias and signal conditioning

functions. The oxidation reaction that takes place at the anode is:

$$H_2S + 4H_2O \rightarrow H_2SO_4 + 8H^+ + 8e^- \tag{6.1}$$

Water is provided inside the sensor as an electrolyte into which the electrodes are immersed and sealed in by a gas-permeable hydrophobic membrane as shown in Figure 6.2. As a proof of concept, we mainly focused on the high selectivity on specific gas and moderate sensitivity on detection. [1] In order to accurately detect the gas from electrochemical sensors, maintaining stable and constant voltage at the anode electrode is critical. Although, the SewerSnort operates mainly by battery power, the travel distance and time can be scheduled beforehand; thus, we can budget the needed power accordingly. We account all required resources including power and storage spaces in Section 6.3.

6.1.1 Amended design of mobile pipeline floating unit

In our previous work [33], we mainly focused on monitoring in-sewer gases. However, in this work, we expand our coverage to liquid side as well as air space. In this work, we design a sensing unit named "SewerSnort II" that models a sphere to allow data acquisition from fluid as well as air space (we will use SewerSnort II and SewerSnort interchangeably throughout the paper). First, we divide the sphere into two regions. The lower region is filled with substance heavier than air (i.e. oil), but lighter than water so that it can float along the pipeline. On the other hand, the upper region is filled with air so that it does not topple over in sewer. Second, we install the sensors for air space on upper hemisphere (i.e. gas sensors) and the sensors for liquid on lower hemisphere (i.e. conductivity and pH sensors) as illustrated in Figure 6.3. Lastly, we install sonar directly on the bottom center of SewerSnort and the infrared around the partition between upper and lower hemisphere to measure flow depth as illustrated in Figure 6.3.

For the wet region, we use conductivity, pH, or salinity sensor to detect WCS anomalies. For example, inflow and infiltration (I/I) can be detected by measuring conductivity along the

[1] The data sheet of RAE 032-0102-000 [53] reports that it is highly selective against carbon monoxide, nitric oxide, hydrogen, etc.

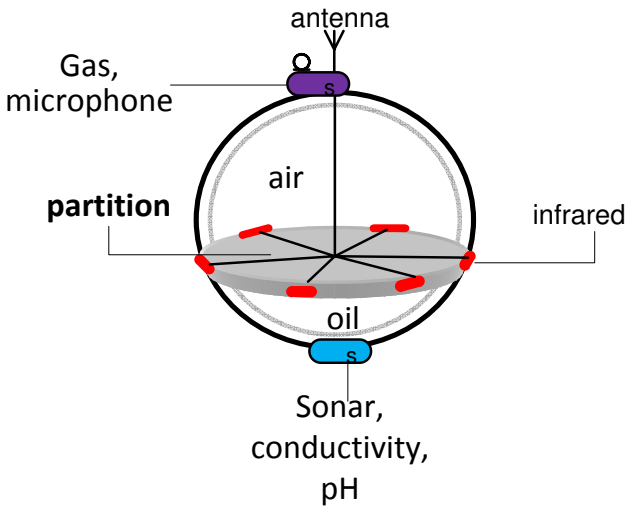

Figure 6.3: SewerSnort design scheme

pipeline. I/I is groundwater/storm water gets into sewer system through cracks and, as pointed out previously, it increases the flow level which can result overflows. Also, I/I can be detected by measuring the total organic carbon (TOC) along the pipeline since the TOC measured in sewer is much higher than TOC measured in groundwater. [2] In addition, particularly for the area near the beach, intrusion of seawater through the cracks can be detected by measuring the level of salinity.

For the dry region, we use methane (CH_4) gas sensor, hydrogen sulfide (H_2S) gas sensor, temperature sensor, and microphone to detect WCS functional deficiencies. For example, blockages can be detected by measuring methane (CH_4) gas or hydrogen sulfide (H_2S) gas. The deposits that cause blockage are typically composed of organic/inorganic components, where they produce methane (CH_4) gas and hydrogen sulfide (H_2S) gas [15]. Thus, high concentration of hydrogen sulfide gas is a key indicator of blockage. As pointed out in Section 1.2, sewer gas measurements has been primarily limited to manholes up until now. However, our probing of gas concentration along the pipeline between manholes can provide much more insight for infrastructural diagnostics [15]. In addition exfiltration can be detected by measuring sewer gases. Exfiltration is untreated wastewater escaping WCS through infrastructural cracks. Although exfiltration is the major cause

[2] In general, TOC in sewer is 10 to 170 mg/L and TOC in groundwater is < 20 mg/L [10].

of environmental contamination, as pointed out in Section 2.3.3, monitoring exfiltration has been greatly challenging due to its "invisibility." However, we can exploit its side effect, namely flow reduction due to escaping fluid. Mechanically, the "flow slow down" causes organic/inorganic materials to be accumulated around the defective area; hence, these accumulated materials produce substantial amount of sewer gases. Moreover, major cracks can be identified through acoustic detection of seeping/gushing water sound generated by escaping flow.

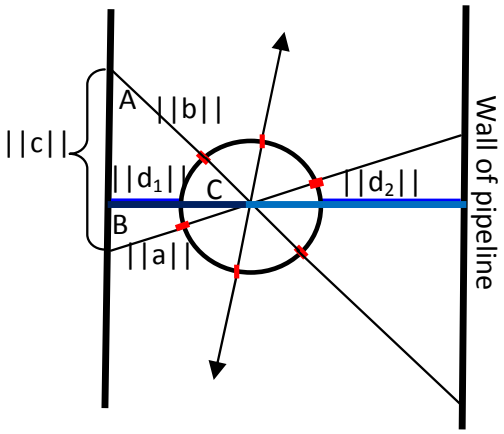

Figure 6.4: Top view of the partition

Also, we install at least six infrared emitters/receivers around the partition apart by equal degree as illustrated in Fig. 6.4. Then, together with sonar we can estimate the severity of sediment accumulations. (To our best knowledge, there is no known technology that can comprehensively estimate the level of sediment accumulations from the entire WCS.) From the six infrared emitters/receivers we are guaranteed to collect at least four range measurements regardless the position of SewerSnort II on flow surface as illustrated in Figure 6.4.

Using the range measurements and the law of sine and cosine, we calculate $\|d_1\|$ in Figure 6.4 as

$$\|d_1\| = \frac{\|a\|\|b\| \sin C}{\sqrt{\|a\|^2 + \|b\|^2 - 2\|a\|\|b\| \cos C}} \tag{6.2}$$

where $C = 60^\circ$ (i.e. 360° / 6, each infrared transceiver is apart by 60°), $\|a\|, \|b\|$ are infrared measurements. With the same method, we calculate $\|d_2\|$. Since the radius $\|R\|$ of pipe is known,

we calculate the flow level $\|L\|$ using $\|d\| = \|d_1\| + \|d_2\|$ as

$$\|R\|^2 = \left(\frac{\|d\|}{2}\right)^2 + (\|R\| - \|L\|)^2 \tag{6.3}$$

and,

$$\|L\| = \|R\| - \sqrt{\|R\|^2 - \left(\frac{\|d\|}{2}\right)^2}. \tag{6.4}$$

However, this approach does not factor in the level of the accumulated sediments. The flow level $\|L\|$ includes sediment. Thus, by continuously measuring the flow depth using sonar and comparing the sonar measurements with flow level $\|L\|$ calculated based on infrared range measurements as illustrated in Figure 6.5 , we can comprehensively estimate the severity of sediment accumulations along the pipeline and to best our knowledge this is the first effort to comprehensively measure the sediment accumulation along the sewer pipeline.

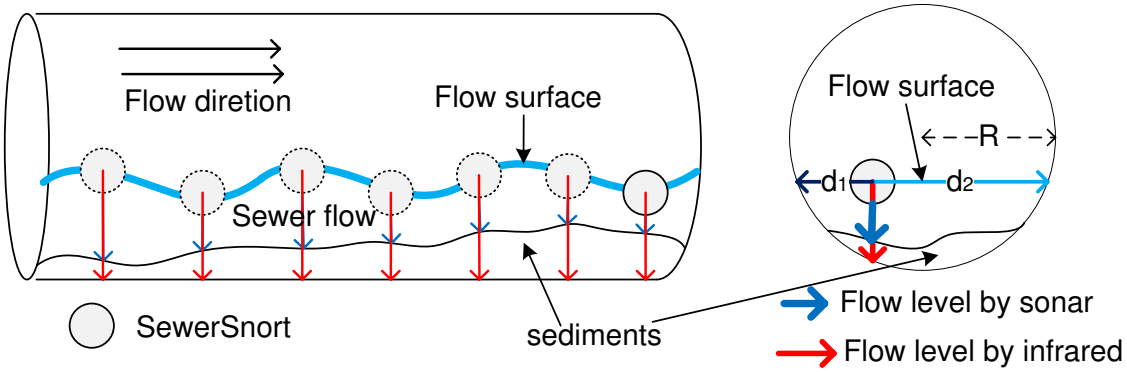

Figure 6.5: Illustration of sediment accumulation detection

6.1.2 Degree of Freedom

The possible movements of SewerSnort II inside pipeline are listed in Table 6.1, and illustrated in Figure 6.6. As stated in Section 6.1.1, we divide a sphere into two parts, upper hemisphere and lower hemisphere. The upper hemisphere is filled with air while the lower hemisphere is filled with substance heavier than air, but lighter than water such as oil; therefore, SewerSnort will not be

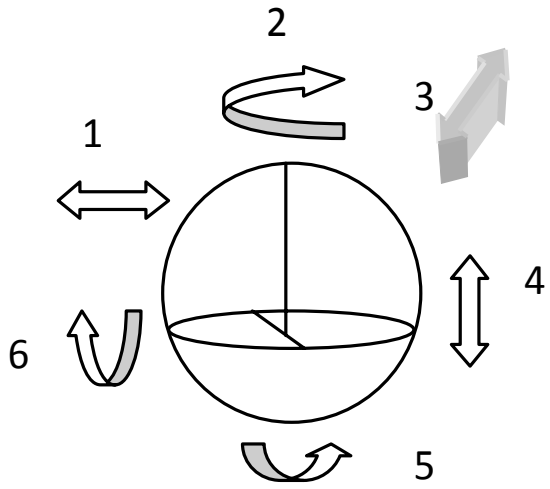

Figure 6.6: SewerSnort: 6 Degree of Freedom

Table 6.1: The name and description of movements

Number	Name	Description	Movement
1	Swaying	Moving left and right	Possible
2	Yawing	Turning left and right	Possible
3	Surging	Moving forward and backward	Mainly forward only
4	Heaving	Moving up and down	Limited
5	Pitching	Tilting up and down	Limited
6	Rolling	Tilting side to side	Limited

toppled over while it traverses pipeline. Thus, the mobile floating sensor is effectively prevented from rolling. Also, the lower hemisphere will not be able to move out of water surface without any on-board motion control for floater; thus, the mobile floating sensor is prohibited from moving up and down (i.e. heaving) or tilting up and down (i.e. pitching) on the flow surface.

On the other hand, the mobile floating sensor may roll along the sidewall of pipeline as described in Section 6.1. The lateral force caused by asymmetric flow around floater may move the floater from left to right or from right to left (i.e. swaying) while the direct force of flow makes the floater rolling (i.e. yawing) along the wall of pipeline. In addition, the mobile floating sensor mainly moves forward (i.e. surging) since the flow travels from upstream to downstream. SewerSnort will never cycle through the same path unless it encounters a major infrastructural flaw. Nonetheless, such cases will not be covered in this study.

Although swaying and yawing are possible movements of the SewerSnort, we can collect adequate amount of data to calculate the flow level regardless the position of SewerSnort inside pipeline since we design a SewerSnort as a sphere with at least six or more infrared emitters/receivers horizontally installed around the partition.

6.1.3 Sensing unit platform

In our previous work [33], the H_2S gas sensing unit was implemented on MICAz mote due to its low cost and wide availability. However, in addition to MICAz mote, varieties of sensing unit platforms are widely available commercially and academically. In this section, we present a brief overview of the main components and the functionalities of sensing unit platforms. Primarily, a sensing unit is capable of (1) collecting environmental data without any human interaction, (2) processing and carrying data, and (3) transmitting information through wireless communication channel to a designated place. Also, in general, a sensing unit is composed of three main components as followings:

- **Mote**: Mote is composed of microcontroller, analog-to-digital converter (ADC), radio con-

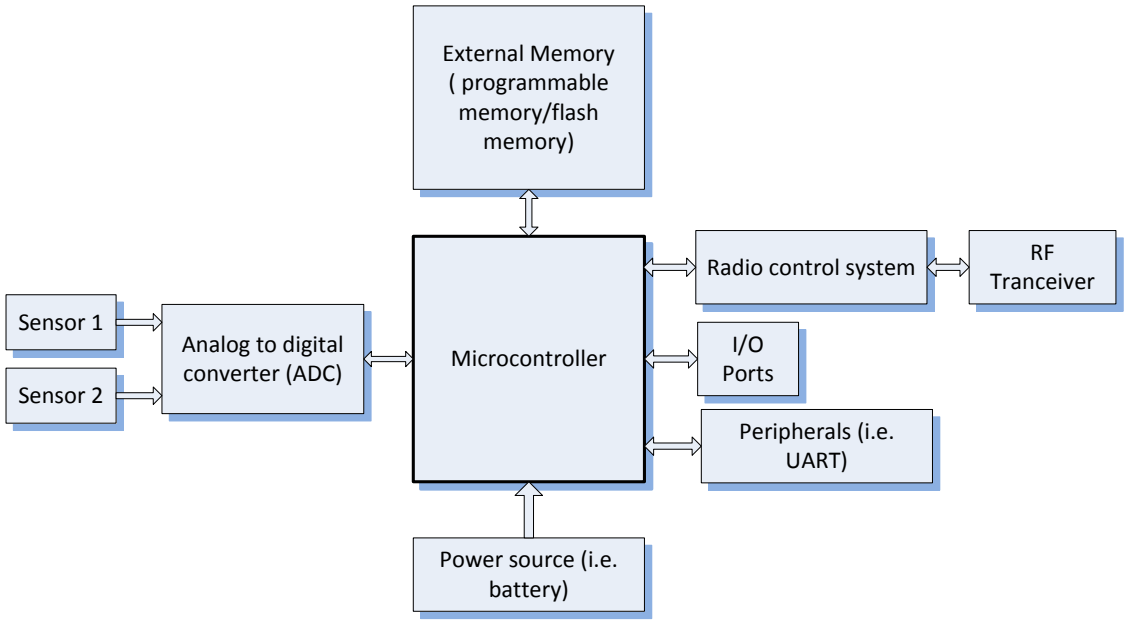

Figure 6.7: Mote block diagram

trol system with RF transceiver, programmable memory for program, flash memory for storage space, power supply unit(usually battery), I/O ports and various peripheral devices (i.e. UART) as illustrated in Figure 6.7. The mote is an autonomous unit which collects data, processes data, and transmit/store information. Some of widely available mote platforms are MICAz, Iris, Telos, and Imote2 [42] as shown in Figure 6.8(a), 6.8(b), and 6.8(c).

- **Sensor board**: Sensor board provides an interface between mote and sensor. Sensor board is mounted on a mote and can be connected to custom made or purchased sensors. In addition, sensor board is embedded with multiple types of sensors such as accelerometer, microphone (acoustic), and light. Some of widely available sensor boards are MTS300/400 and MDA100/300 which are used in the MICA mote family [42] as shown in figure 6.9(a), 6.9(b). Although, sensor board connects sensors to a mote, some of sensing unit platform (i.e. Telos platform) is integrated into wireless communication module.

- **Programming board**: Programming board provides interfaces to connect a mote to a computer or to a network. The interface includes serial port, USB port, Ethernet port, or IEEE

802.11(WiFi) port. Programming board, also known as a gateway, is used to program mote or to retrieve data from mote. Some examples of programming board are MIB510/520/600 [42].

(a) IRIS Mote (b) MICAz Mote (c) TelosB Mote

Figure 6.8: MEMSIC MICA Mote family (a) and (b) and (c)

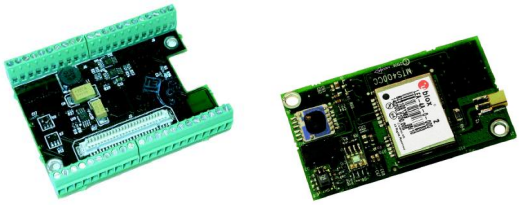

(a) MDA 300 (b) MEMSIC MTS 400 Sensor board

Figure 6.9: MEMSIC Sensor Boards (a) and (b)

Sensing unit in WSN operates mainly by battery power. Thus, a CPU on the sensing unit platform is based on standard 8 or 16 bit micro-controller with processor speed between 4 - 16 MHz to minimize power usages. Also, sensing unit is equipped with small amount of flash memory typically 512 KB - 1MB since flash memory uses less energy for read/write than SRAM. The Table 6.2 summarizes the major characteristics of widely available mote platforms.

Although a sensing unit has inherently less processing power and storage space compare to other wireless devices such as cell phones and laptops with 802.11, sensing component in sensing

Table 6.2: Sensor Mote Platform

Mote Type	CPU speed (MHz)	Program memory (KB)	RAM (KB)	RF (MHz)	Transmission rate (Kbits/sec)
MICA2	16	128	4	433/868/916	38.4 kbaud
MICAz	16	128	4	2.4 GHz	250
Cricket	16	128	4	433	38.4kbaud
IRIS	16	128	8	2.4 GHz	250
TelosB	16	48	10	2.4 GHz	250
Imote	12	512	64	2.4 GHz	100
Imote2	13 - 416	32 MB	256	2.4 GHz	250

unit is tightly coupled with radio transmitting component; therefore, data can be effectively transmitted over wireless communication channel. In addition, a sensing is small in terms of physical size, inexpensive, and not relying on pre-existing infrastructure. Thus, collecting data from area difficult to access or for vast geographical area becomes possible.

In addition, the recent advancement in micro electro-mechanical systems (MEMS) technology and ubiquitous wireless communication made ever easier and possible to measure an array of environmental data which were difficult if not feasible. Moreover, numerous vendors manufacture many types of sensors that are commercially available and have made possible to accommodate various types of environmental monitoring system with minimal development or just configurations of a system [42, 44].

6.1.4 Wireless communication platform

6.1.4.1 IEEE 802.15.4 and ZigBee

IEEE 802.15.4 is a standardized communication platform in wireless sensor network (WSN). It provides a standardized physical layer (PHY) and medium access control (MAC) layer specifica-

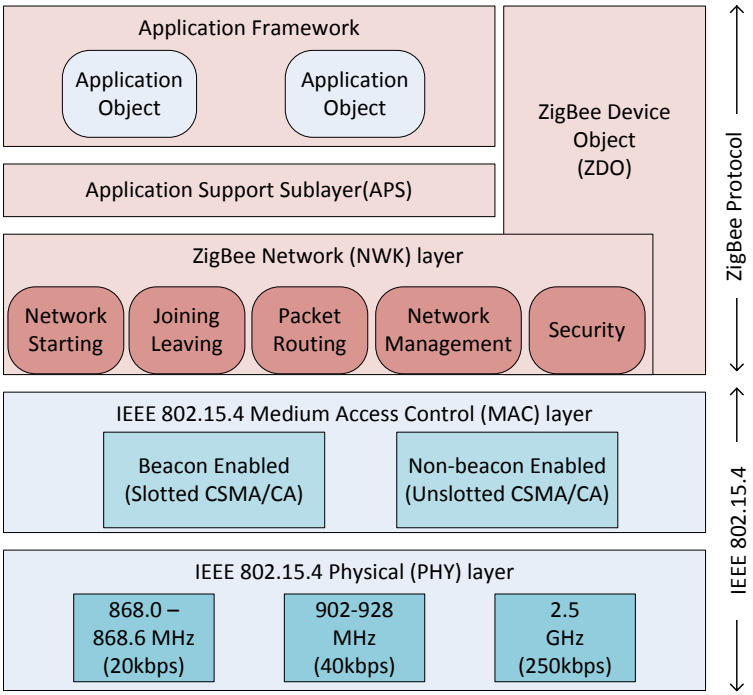

Figure 6.10: IEEE 802.15.4 and ZigBee Protocol Stack

tion. The motivation of IEEE 802.15.4 is to provide low-cost and low-speed ubiquitous communication of nearby devices with little to no underlying infrastructure. The IEEE 802.15.4 is designed for low data rate, low power consumption, and low complexity based on the requirements of WSN.

On top of IEEE 802.15.4 PHY layer and MAC, ZigBee protocol is developed to provide various advanced features for sensor nodes [77]. ZigBee protocol is comprised of ZigBee network (NWK) layer, the application support sublayer (APS), the application layer framework, the manufacturer-defined application objects, and the ZigBee device objects (ZDO) as illustrated in Figure 6.10.

IEEE 802.15.4 Protocol

1. **Physical Layer:** IEEE 802.15.4 PHY layer supports activation/deactivation of the radio transceiver, detection of received signal energy level, detection of link quality, channel section, clear channel assessment, and transmiting/receiving packets across the physical medium. IEEE 802.15.4 PHY layer operates based on direct sequence spread spectrum

(DSSS) with range of 5$\tilde{5}$00m depending on environment at frequency band as followings:

- 868.0-868.6 MHz: used in Europe, allows one communication channel with data rate 20kbps
- 902-928 MHz: used in North America, allows up to thirty channels with data rate 40kbps
- 2400-2483.5 MHz: used in worldwide, allows up to sixteen channels with data rate 250kbps

2. **Medium Access Control (MAC) Layer:** IEEE 802.15.4 MAC layer uses Carrier Sensing Multiple Access/Collision Avoidance (CSMA/CA) protocol. However, unlike IEEE 802.11, Request-To-Send/Clear-To-Send (RTS/CTS) protocol is not used for IEEE 802.15.4 MAC mainly due to relatively low data rate where collision may less likely occur. IEEE 802.15.4 MAC layer provides various operation modes depending on the needs. For a periodic transmission, it offers beacon mode. When only intermittent transmission is needed, it operates on disconnection mode where nodes are not attached to network when there is no data to transmit in order to conserve energy. In addition, to support the low latency transmission, it operates on guaranteed time slot (GTS) mode which an assigned time slot in Superframe is allocated for a specific node. Also, IEEE 802.15.4 MAC provides four different frame types namely, beacon frame, data frame, ACK frame, and MAC Command frame.

3. **Network Layer:** IEEE 802.15.4 Network layer is responsible of starting/establishing a network, joining/leaving network, configuring its stack, assigning address, synchronizing with other nodes by listening for beacons or polling nodes, and routing packets. IEEE 802.15.4 Network consists of two types of nodes. One is a full function device (FFD) and the other is reduced function device (RFD). FFD is capable of functioning as a personal area network (PAN) coordinator, a router, or a regular node. On the other hand, RFD cannot be a coordinator or a router, and it can communicate only with FFD node. The main purpose of RFD is to reduce the cost by having fewer hardware requirements. IEEE 802.15.4 supports three

types of network topologies namely, star topology, mesh topology, and cluster-tree topology.

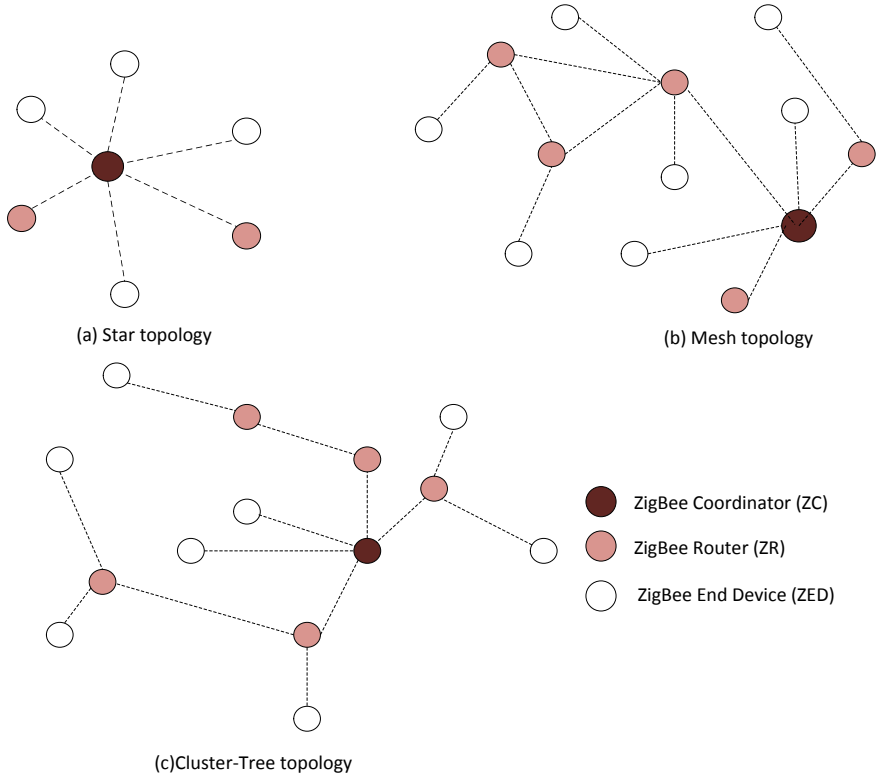

Figure 6.11: ZigBee network topology structures

ZigBee Protocol

1. **ZigBee Device Object (ZDO)**: ZigBee consists with three types of ZDO namely, ZigBee Coordinator (ZC), ZigBee Router (ZR), and ZigBee End Device (ZED).

   – ZigBee Coordinator (ZC): A ZigBee network is required to have one ZC. ZC works as a Personal Area Network (PAN) Coordinator. ZC starts/configures a network. When a network is operating under beacon-enabled mode, a ZC will broadcast beacons.

   – ZigBee Router (ZR): ZR listens the beacons from its parent and broadcasts its own beacons to synchronize nodes in the network. ZR participates in multi-hop routing and ZR can also act as a PAN coordinator.

- ZigBee End Device (ZED): ZED can communicate only with ZC or ZR, but not with other ZED. Also, ZED does not participate in routing. ZED is comparable to RFD in IEEE 802.15.4.

2. **ZigBee Network (NWK) Layer**:NWK layer is responsible of initiating a network, associating/disassociating a network, assigning addresses, configuring nodes, routing packets, and managing security. NWK layer supports three types of network topology namely, star topology, mesh topology, and cluster-tree network topologies similar to IEEE 802.15.4 as illustrated in Figure 6.11.

6.1.4.2 Communication channel quality inside pipeline

Wireless communication channel inside pipeline exhibits slightly different characteristics than terrestrial wireless communication channels because of the constraint on channel propagation caused by the pipe wall. Radio frequency (RF) wave propagation inside pipeline is influenced by waveguides and boundary condition in addition to attenuation and multi-path fading. Also, the vertical RF wave propagation will be limited by the wall of pipeline while the horizontal RF wave propagates to far region.

In the past, analytical wireless communication channel propagation models for underground mine and road/subway tunnels were developed to describe the characteristics of radio wave propagation in such constricted area [3, 14, 38]. Particularly, from the previous study [3], Ian Akyildiz *el.al.* developed an analytical signal propagation channel model for inside rectangle tunnel environment and validated their model with the field experiments. With their model and the field validation, they found that the characteristics of the radio frequency propagation inside tunnels can be described based on operating frequency, tunnel size, antenna polarization, antenna position, and electrical parameters as follows:

- **Operating frequency** - When transmitter and receiver are close inside tunnel, the received signal strength attenuates rapidly and fluctuates rapidly. However, when the receiver moves

away from the transmitter, the signal attenuation is gradual and fluctuation decreases. It is because of the fact that the higher order electromagnetic modes attenuate rapidly and only few low-order mode can reach far distance. Hence, the signal with higher frequency can reach further than the signal with lower frequency inside tunnel.

- **Tunnel size and antenna polarization** - As tunnel size becomes wider and higher, the signal attenuates more slowly. Also, as the width of tunnel gets larger, the signal attenuates more slowly for the horizontal polarized antenna.

- **Antenna position** - The best position of antenna for signal transmitting/receiving is the center of tunnel. When both a transmitter and a receiver are located near the center, the rate of the signal attenuation is the lowest. As either or both of them moves toward the wall, the signal attenuates much faster.

- **Electrical parameters** - In general, the electrical parameters of air in tunnel is not considerably different from the parameters of normal air.

Thus, in Chapter 10, we account for the impact on radio propagation of the cross section of the sewer pipe as well as for the effect of pipe bends on propagation. Then, we propose an analytical radio propagation model for sewer environment to develop an efficient wireless communication network in such restricted environment.

6.2 Localization

While SewerSnort is collecting a data, the data needs to be associated with sampling location information to spot the functional deficiencies. Localization protocols for Wireless Sensor Network (WSN) are classified as range-based localization protocol or range-free localization protocol. Range-free localization protocol estimates its proximity based on the connectivity information among nodes. For example, the convex position estimation (CPE) [11] algorithm estimates the location of nodes using a subset of the beacon nodes which know their accurate location informa-

tion. A node exchanges probing messages with its neighbors to populate the connectivity table of its neighbors. Then, considering the transmission ranges and the connectivity information with its neighbors, a sensor node deduces very rough location information for itself.

On the other hand, the range-based localization protocol estimates the location based on various ranging techniques. In range-based protocol, the beacon nodes which have accurate location information broadcast beacons and the regular nodes estimate their location by measuring the distance or the angle between them and the beacon nodes by applying multilateration or triangulation techniques respectively. For range-based localization protocol, there are mainly four ranging techniques, namely received signal strength indicator (RSSI) based technique, time of arrival (ToA) based method, time difference of arrival (TDoA) based scheme, and angle of arrival (AoA) based approach. Although the range-based localization protocol provides much more accurate location information than the range-free localization protocol, the range-based localization protocol may require special hardware. However, RSSI based technique does not require any special hardware support or has minimal hardware requirements. Since a sensor node is equipped with a radio and in most cases a sensor node can report the received signal strength of incoming packets, RSSI based technique does not require any special hardware support or has minimal hardware requirements.

In addition, specific localization scheme to locate a sewer robot was developed. Ahrary *et. al.* developed a localization system for an autonomous robot in the sewer system [2]. The localization was achieved by computing the distance of pixels from the image files which were taken from robot. A camera attached to a robot takes pictures, and the distance of neighboring pixels are computed to estimate its location. However, this approach not only suffers from the computational complexity, but also is not scalable since there is no way of distinguishing from one sewer manhole (SMH) to the other in this scheme.

In this work, we build a GPS-free localization scheme based on RSSI ranging technique to locate and to track a mobile floating sensor node. Since RSSI based technique can be implemented without any special hardware support and can provide relatively accurate location information without complicated calculations, it is a natural choice for the work. Radio-frequency (RF) based

localization has been widely used for indoor positioning via triangulation using measured signal strengths from multiple beacons [5, 39]. To this end, we can use either an empirically measured signal strength [5, 39] or a theoretical model that captures signal attenuation over distance [5, 50]. In the literature, it was shown that a theoretical model well estimates the distance when the line-of-sight (LoS) is dominant; otherwise, the map based approach is preferable (e.g., indoor office environments) [5]. Also, recent measurement studies by Howitt et al. proposed a radio wave propagation model for concrete storm drain pipes operating at 2.4 - 2.5GHz frequency band [25]. By using this model, we estimate the location of the mobile floating sensor node inside the sewers. Unlike previous methods of "online" location tracking methods [5, 39, 50], we perform "off-line" signal processing on the measured signal strength samples to better estimate the trajectory of a floating sensor node.

6.2.1 Theoretical RSSI-based Localization

The relation between the received energy and the distance from a sender to a receiver is given by

$$RSSI(d)_{rx} = P_{tx} - PL(d_0) - 10\eta \log \frac{d}{d_0} + X\sigma \tag{6.5}$$

for the log-normal channel model [54], where $RSSI(d)_{rx}$ is received power at distance d, P_{tx} is transmitted power, $PL(d_0)$ is the path loss for a referenced distance d_0, η is a path loss exponent, and $X\sigma$ is noise. The transmitting power and the path loss can be measured during the calibration period. A η is specific to the environment and determined empirically[3]. In addition, various approaches of estimating η have been proposed in [37, 63]. However, in order to apply the log-normal channel model in a real world, a de-noising process is needed beforehand.

6.2.2 De-noising RSSI samples

Although destructive/constructive reflections have a small impact on measured RSSI values when there exists a dominant LoS [35], they cause rapid fluctuation. To de-noise the raw RSSI data we

[3]In general, η = [2, 4] depending on the environment. The noisier it is, the higher η is.

choose to use the Empirical Mode Decomposition (EMD) [26]. The EMD effectively filters out noise from the non-stationary time series signals such as RSSI data from SewerSnort.

Briefly, EMD is a data-driven signal processing technique. EMD decomposes signals into n empirical modes first and produces the residue which is the mean trend or constants. EMD algorithm is comprised of successive steps as follows:

1. Identify all local maxima and all local minima.
2. Connect all local maxima using cubic spline line as an upper envelope.
3. Repeat step 2) for all local minima as a lower envelope.
4. Compute the mean as
$$m(t) = \frac{E_{max}(t) + E_{min}(t)}{2}. \tag{6.6}$$
5. Extract the local detail h_1 as
$$h(t)_1 = X(t) - m(t), \tag{6.7}$$
where X(t) is a RSSI data at time t.
6. Repeat step 1 - 5 by treating the local detail $h(t)_i$ from the previous sifting as the raw data until
$$h(t)_m = h(t)_{m-1} - m(t)_m. \tag{6.8}$$
For example, h_1, the detail obtained after the first sifting, becomes data for the second sifting as
$$h(t)_2 = h(t)_1 - m(t)_2. \tag{6.9}$$
7. Then, the intrinsic mode function component of the data becomes
$$C(t) = h(t)_m \tag{6.10}$$
C(t) is a de-noised RSSI data at time t.

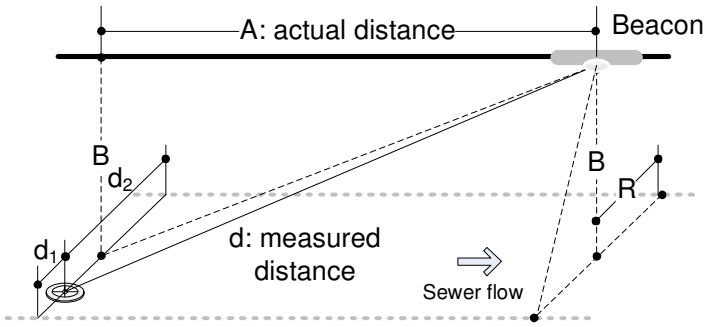

Figure 6.12: Distance estimation in sewers

6.2.3 RSSI-based SewerSnort localization

To design a RSSI-based SewerSnort localization scheme, we define a geo-spatial coordinate system using beacons. First, beacons are installed underneath sewer manholes in the area of interest. Second, the beacons periodically broadcast messages containing geo-tag which corresponds to a specific physical location. [4] Third, upon receiving the beacons, a SewerSnort decodes the message to determine the beacon's identity while the average signal envelope power of the beacon packet – the RSSI – is measured. Then, a SewerSnort stores geo-tag along with the averaged RSSI data. Forth, we de-noise the collected RSSI data using EMD, Then we estimate the proximity of the sampling points using the residue from EMD.

The relationship between RSSI and inter-radio distance can be approximated by the radio wave propagation model for concrete storm drain pipes as in [25]:

$$RSSI(d)_{rx} = P_{tx} - \alpha_{(r,\sigma)} \times d - A_{CL} \tag{6.11}$$

where $RSSI(d)_{rx}$ is the received power at distance d, P_{tx} is the transmitted power in ***dB***, $\alpha_{(R,\sigma)}$ is the multi-mode attenuation loss (***dB/m***) which is dependent on radius (R) and conductivity (σ) of a concrete pipe, and A_{CL} is the antenna coupling loss given in ***dB***. A value of A_{CL} changes based on a position of a beacon inside a pipe [25]. For example, assuming one beacon is installed

[4] Numerous techniques for low power medium access control exist and could be leveraged to reduce battery drain. These include supplemental "wake-up" RF circuitry [51] and low-power ultra-low drift clocking systems [57] to support extremely low duty-cycle time-division protocols [56]

at the center of pipe, and the other beacon is installed on the ceiling of pipe. Then, the value of A_{CL} where a beacon is installed at the center is smaller than the value of A_{CL} where a beacon is installed on the ceiling assuming that a SewerSnort is located at the bottom of a pipe. Thus, by anchoring positions of beacons on the ceiling of pipes, it is possible to calculate the depth of the water if we know the value of A_{CL} of the pipe. Also, the value of A_{CL} and $\alpha_{(R,\sigma)}$ are depending on the radius (R) and conductivity (σ) of the concrete pipe and these values are empirically derived from multiple experiments [25].

Now, from equation 6.11 we can measure the distance from a beacon to SewerSnort. However, we want to compute the actual distance "A" as illustrated in Figure 6.12 based on the distance that we measured from equation 6.11. Since we install a beacon at the ceiling of the pipe and swaying is a possible movement for SewerSnort as described in Section 6.1.2, $A^2 \geq d^2 - (2R)^2$ in any event. To compute "A" we need to know d_1, d_2 and "B." We know the the radius of a pipe (R). Also, from the section 6.1, we can compute d_1, d_2, and flow level. Since radius R is known and flow level L can be computed, we can compute $B = 2R - L$.

Then, A can be computed as

$$A = \sqrt{\left(d^2 - \left(\frac{|d_2 - d_1|}{2}\right)^2\right) - (2R - L)^2}. \tag{6.12}$$

Alternatively, we can estimate d_1, d_2, and "B" by considering "bank suction" effect as explained in section 6.1. When lateral force caused by pressure differences pushes a SewerSnort to the wall of pipeline, d_1 may becomes 0 and

$$\frac{(d_2 - d_1)}{2} = \frac{d_2}{2}. \tag{6.13}$$

Also, the current flow level ($2R - B$) can be estimated by tracking the changes of RSSI. Since RSSI will be increased as SewerSnort approach to the beacon and RSSI will be maximized when the SewerSnort passes by the beacon, we can estimate B as

$$B = R + \sqrt{R^2 - (\frac{d_2}{2})^2} \tag{6.14}$$

Thus, the distance "A" also can be estimated as

$$A = \sqrt{(d^2 - (\frac{d_2}{2})^2) - B^2}. \tag{6.15}$$

6.2.4 Enhancement of location estimation assisted by flow velocity

The location of a SewerSnort can be estimated using Equation (6.11) and de-noise procedure. However, the dynamic nature of signal propagation inside the pipe under mobile environments can influence the accuracy of de-noised RSSI data as we have seen in our experiments (Section 8.3). Under this circumstance, such SewerSnort mapping can produce abrupt jumps and reverse of directions which results in high errors. Knowing that the sewer flow is laminar and exhibits spatio-temporal coherence as illustrated in the feasibility analysis section, abrupt changes of a floating sensor node proximity are not likely to happen in practice. On the basis of such characteristics, we propose to utilize the flow velocity in addition to Equation (6.11) and the de-noised RSSI data to improve the accuracy. Also, we exploit the fact that the RSSI values peak right below beacon nodes and manhole's locations are known. Thus, whenever a peak is detected, localization error can be corrected, and location estimation restarts from the beacon node's location.

SewerSnort location estimates can be improved using flow velocity as follows. For a given beacon node, we first de-noise the measured RSSI samples. From de-noise data, we find the peak and use the beacon's location as a departure position. Assuming that the SewerSnort has traveled at a constant velocity V, we substitute the distance d in Equation (6.11) with Vt where t is time, i.e., $RSSI(Vt)_{rx} = P_{tx} - \alpha_{(a,\sigma)} \times Vt - A_{CL}$. Recall that all the variables in Equation (6.11) except the velocity V are known. Thus, we can find the velocity V that minimizes the sum of square errors between the modified model and the de-noised RSSI data.

In the event that a SewerSnort has received RF signals from two adjacent beacon nodes while drifting (denoted as A and B), we have two different velocity estimates (V_A: moving away from A, and V_B: approaching to B). Since error is minimized right below a beacon node, both speeds are used to estimate locations as follows: from A, V_A is used for t_A unit times (A to B), and from B, V_B

is used for t_B unit times (B to A). Say the distance between A and B is d_{AB} and drifting duration is t_{AB}, then, the following conditions must be satisfied to properly align estimated location from both directions: (1) $V_A t_A + V_B t_B = d_{AB}$ and (2) $t_A + t_B = t_{AB}$. Hence, we have $t_A = \frac{d_{AB} - v_A t_{AB}}{V_B - V_A}$, and $t_B = \frac{v_B t_{AB} - d_{AB}}{V_B - V_A}$. However, note that there is a sudden speed change in this scheme (say after t_A unit times).

For a given pipe, parameters in Equation (6.11) such as $\alpha_{(a,\sigma)}$ and A_{CL} are affected by the changes of water depth. Calibrating these model parameters under a set of different water depths is greatly laborious task when there is a sewer flow. An alternative is to estimate the average speed between two beacon nodes, namely d_{AB}/t_{AB}. In this case, there is no sudden change of speed within a pipe segment formed by these consecutive beacons (e.g., A and B), yet can result in higher errors compared to the previous approach. Nonetheless, this approach can be very useful for handling the case when the distance between two consecutive manholes is too far to receive beacon messages or an intermediate beacon is failed.[5]

6.3 Resource requirements

In this section, we account all required resources for SewerSnort and beacons in respect of storage space and energy. Due to high sampling frequency, the needed storage space will grow rapidly. Also, as the travel distance increases, the energy consumption for collecting samples (i.e. gas, conductivity, or sonar) will grow very rapidly. Thus, in addition to estimating the required resources, we describe various techniques of optimizing the resource usages. The acquired data from SewerSnort can be compressed aggressively so that the required storage can be significantly reduced. In addition, we can strife for conserving energy by adjusting sampling frequencies and defining multiple levels of events.

[5] In practice, we do not anticipate an extended unreachable distance, because the average distance between sewer manholes is 71.93m [48] and the transmission range of 802.15.4 radio is 30m indoor and 70m outdoor [77].

6.3.1 Storage requirements

The acquired data can be packed and stored onboard all the way through the journey and retrieved after SewerSnort is retracted. Even though the amount of data, with high sampling frequency, will grow rapidly, the required storage can be reduced significantly by aggressively compressing and storing the difference from the previous value.

Table 6.3: Estimated storage requirements for the upper region sample types

Type	Data size
Sample Data - gas	2 bytes
Sample Data - microphone	2 bytes
Total (sample data)	4 bytes
Calculated Data - flow level	1 byte
Total (calculated data)	1 byte
GeoTag	2 bytes
Timestamp	4 bytes
Signal strength (RSSIval)	1 byte
Total (beacon)	7 bytes

First, we summarize the approximate storage requirements for the acquired data of the upper region as listed in Table 6.3. Then, we can compress data by taking their characteristics into account.

Since, the sensor measurements are collected totally asynchronously from the beacon sensing, we account the storage requirement for the upper region as

$$\text{Required storage} = (5 \text{ bytes} * f) + (7 \text{ bytes} * I), \tag{6.16}$$

where f is sampling frequency and I is beacon interval. For example, if f = 1 sample/1s [6] and I

[6] In general, the sewer flow velocity is approximately 0.2m/s - 1m/s. Thus, the sampling frequency of 1s provides a reading for every 20 cm - 100 cm, and this is sufficient for "Meter" type accuracy. Since factual traveling path of floater may unprecedented, this velocity does not account for the nonlinear traveling path of floater.

= 1 beacon/1s, we collect 43,200 bytes/hr = 14,400 (sampling) bytes/hr + 3,600 (calculated data) bytes/hr + 25,200 (beacon message) bytes/hr. In general, 24 hours is sufficient for a floater to travel from upstream to a wastewater treatment plant [71]. Thus, a SewerSnort may collect up to 1MB for the entire trip. However, the required storage can be reduced significantly by compressing data and storing a difference from the previous value.

For example, considering the fact that the range of H_2S real-world sample data is no greater than 100 ppm and the environment does not change drastically from one region to the right next [7], we can use delta-compression. Since delta between two consecutive samples can be stored in one byte, we can truncate meaningless leading 8 bits without loss of information. Thus, we can reduce the storage requirements for sample data by half. Also, a beacon message can be extensively compressed by considering the fact that GeoTag is sequential and timestamp has small delta between adjacent timestamps. Thus, we can truncate leading 8 bits from a delta of GeoTag and leading 24 bits from a delta of timestamp without losing data. In addition, same GeoTag will be repeatedly stored until the next GeoTag is detected. Thus, we can store only when we detect a new GeoTag value. Consequently, a beacon message can be compressed into 2 bytes and number of beacons deployed. After compressing the data, we have 18,000 bytes/hr = 7,200 (sampling) bytes/hr + 3,600 (calculated data) bytes/hr + 7,200 (beacon message) bytes/hr and number of GeoTag (depending on number of beacons deployed). Assuming five thousand beacons were deployed, we will have 437KB in 24 hours.

Table 6.4: Estimated storage requirements for the lower region sample types

Type	Data size
Sample Data - conductivity	2 bytes
Sample Data - sonar)	2 bytes
Sample Data - pH	2 bytes
Total (sample data)	6 bytes

Second, we summarize the approximate storage requirements for the lower region as listed in

Table 6.4. Then, we compress data by considering their characteristics. Since the lower region will not collect beacon messages and will only collect sample data, the required storage is 6 bytes/s. To estimate the sampling location of the lower region, we set the timer to synchronize with the upper region sensors. Then, the location information from the upper region can be used for the samples collected from the lower region. When we collect 1 sample/s, we collect 21,600 bytes/hr = 6 bytes * 3600 (samples) or 518,400 bytes/24 hours. However, we can reduce the storage requirement significantly. Since pH data can be stored in 1 byte, we can reduce the required storage to 432KB/24 hours.

6.3.2 Energy requirements

We account the approximate energy requirements for beacon and SewerSnort. We assume that neither sophisticated energy management protocols nor energy management architecture from OS or hardware is implemented. Also, the power requirements of sensors and of other components (i.e. microcontroller) may somewhat differ depending on the model.

6.3.2.1 Beacon

We define the required energy for a beacon as

$$E_{interval} = E_{transmit} + E_{sleep} \tag{6.17}$$

, where $E_{interval}$ is the energy required for one interval, $E_{transmit}$ is the energy required to send a beacon message, and E_{sleep} is the energy required during sleep mode. Assuming that we use UDP (IPv4) and IEEE 802.15.4 [77], the estimated energy to send a beacon packet is as follows:

$$E_{interval} = (\text{Interval} * 928\mu s) * 0.001mA(E_{sleep}) + 27.283mA(E_{tx}) * I \tag{6.18}$$

For example, if a beacon interval is 1 second, we need 27.29mAs (milliamp-second) per interval. With a pair of AA batteries providing 2700mAh, the beacon can last 98.9 hours or 4.12 days.

Table 6.5: Estimated energy consumption for beacon

Radio (CC2420 chipset [77]:)	
Data transmission rate	250 kbps
Power consumption	
Transmission mode	17.4mA
Sleep mode	1μA
Protocol:	
Size (UDP Header 64 bits + IP Header 160 bits + 802.15.4 header 112 bits + pay load 56 bits)	392 bits
Transmission time w/802.15.4 (Packet 1,568μs + preamble 1.296μs)	1569μs
Battery:	
Configuration	2S AA
Chemistry	NiMH
Nominal Voltage	2.4V
Packet (From Beacon)	
Energy per Packet	27.29mAs = 65.5mJ
Beacon Interval	1sec
Total Lifetime	4.12 days

6.3.2.2 SewerSnort II

The required energy for a SewerSnort is much more than for a beacon. For the upper region the required energy is defined as

$$E_{SewerSnort} = E_{sampling} + E_{storing} + E_{radio} + E_{mc} \tag{6.19}$$

, where $E_{sampling}$ is the energy required for sampling, $E_{storing}$ is the energy required to write the data into non-volatile memory, E_{radio} is the energy required for listening to the beacons, and E_{mc} is the energy required for being active on the microcontroller. The required power varies widely by sensor type as shown in Table 6.6. A SewerSnort equipped with a flash memory, an IEEE 802.15.4 radio, and various sensors would require the energy listed in Table 6.6 assuming the microcontroller is fully active during the journey.

Table 6.6: Estimated power requirements for sensors

Sensor type	Power requirements
CH_4 gas (methane)	40mA
H_2S gas (hydrogen sulfide)	40mA
O_2 gas (oxygen)	160mA
Microphone	15mA†
Ultrasonic	80mA
Conductivity	35mA†
Temperature	0.5mA
pH	10mA
Salinity	15mA

†It varies depending on the sensitivity.

With a pair of 2700mAh batteries, a sensing unit in the upper region of SewerSnort could last approximately 24 hours. Lifetime can be extended with a larger battery pack and more sophisticated power management. This worst-case analysis demonstrates that even on inexpensive and

limited energy reserves a SewerSnort would be more than capable of one day long missions. We expect that, as the system is developed, multi-day missions would become possible.

Table 6.7: Estimated energy consumption for upper region

Component	Power requirements
$E_{sampling-gas,microphone}$	45mA
$E_{listening}$ (beacon)	19.7mA †
$E_{micro-controller}$	8mA †
Total	72.7mA + $E_{storing}$ ‡

†It can be changed depending on processor/radio platform. This is for MICAz with a low-power microcontroller ATmega 128L and 802.15.4 radio [77]. ‡It depends on the amount of data. ATmega 128L uses 1μJ/Byte to store at on-board flash memory. Assuming that we collect 18 bytes, we use less than 10 μAs.

For the lower region, we account the required energy as listed in Table 6.8. With a pair of 2700mAh batteries, the lower region of sensing unit could last approximately 16.5 hours. However, a larger battery pack can be installed to supply additional energy to extend the lifetime.

Table 6.8: Estimated energy consumption for lower region

Component	Power requirements
$E_{sampling-sonar,pH,conductivity}$	125mA
Total	125mA + $E_{storing}$ †

†It depends on the amount of data. ATmega 128L uses 1μJ/Byte to store at onboard flash memory. Assuming that we collect 18 bytes, we use less than 10 μAs.

Although a floater can carry all acquired data to the destination, we may upload a portion of data to a base station for an emergency. When a floater uploads data, the energy cost can be estimated as

$$E_{total} = E_{tx} * (\text{M bits} + \text{Headers}) \tag{6.20}$$

, where E_{tx} is energy required to transmit one bit, and M is total bits to be uploaded. For example, if 2KB (payload 2,048 * 8 bits + UDP Header 64 bits + IP Header 160 bits + 802.15.4 header 112 bits) are uploaded, we would deplete approximately 76.5mAs and free 2,048 bytes in flash memory assuming that there is no retransmission and we spend 5mJ/bit to upload while 1μJ/byte to read/write flash memory using IEEE 802.15.4 and MICAz flash memory [77]. Depending on the urgency and on the amount of data to be uploaded, we may equip a floater with additional batteries.

6.4 Power conservation

Since SewerSnort relies mainly on battery power, even minimal energy savings without compromising the accuracy of information will be helpful. In an effort to save energy resource, SewerSnort can adjust the sampling frequencies without losing any critical data. In addition, to prolong the lifespan of a beacon, we can put beacons into sleep mode most of the time. By carefully scheduling the travel time of a SewerSnort, we can synchronize the wake up time of the beacons so that we can maximize the sleep time of beacons. Before the field deployment, a scenario can be developed and tested using simulation tools provided in Chapter 9; thus, we can schedule the journey of a floater to minimize the required resources and maximize the lifespan of beacons.

6.4.1 Adaptive sampling frequency

The sampling frequency of SewerSnort can be adjusted without losing any critical data. When a floater collects sample, it compares the sample data with the previous one. If the difference is less than the pre-determined threshold, a floater increases the sampling frequency by 1 unit (i.e. 1 second) if the sampling frequency is less than the absolute maximum frequency. However, if the difference between two consecutive samples is greater than the threshold, set the sampling

frequency to 1 unit. For example, assume that we set the threshold of H_2S data to 1 ppm and the time unit u = 1 second. At time t SewerSnort collects 2 ppm, and at time $t+f$ (f is current sampling frequency and $f \geq 1second$) SewerSnort collects 2.2 ppm; then, the next sampling will be done at $t + (2f + 1second)$ if $f < MaxInterval$. However, at time t SewerSnort collects 2 ppm, and at time $t + f$ SewerSnort collects 3 ppm; then, the next sampling will be done at $t + (f + 1second)$. The logic is illustrated with flowchart in Figure 6.13.

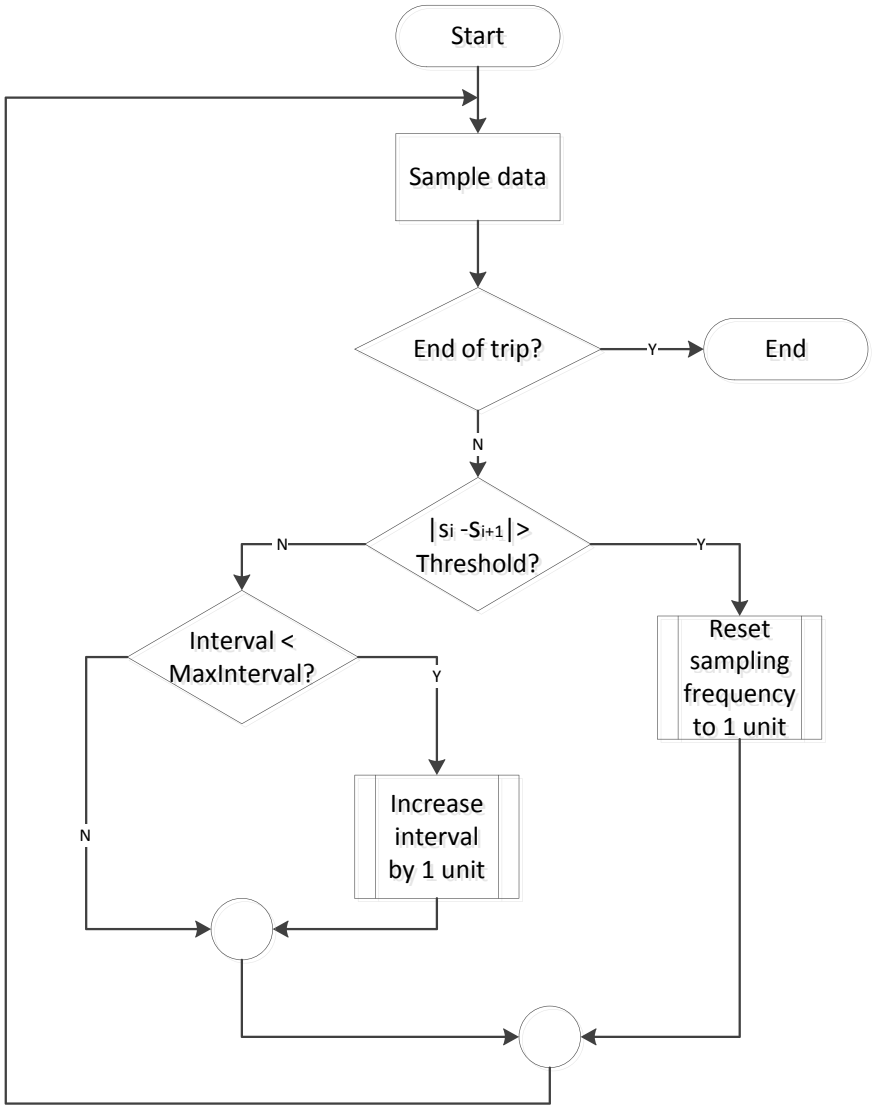

Figure 6.13: Adaptive sampling frequency (The unit can be any predetermined interval(i.e. 1 unit = 1 second).)

6.4.2 Adaptive beacon interval

Using the SewerSnort path analysis report from the simulation tool in Chapter 9, we can estimate when SewerSnort will pass by certain route. As illustrated in Figure 6.14, we can estimate the (longitude, latitude) of SewerSnort along with the estimated travel time. Thus, we can wake up the necessary beacons as needed or maintain the sleep mode so that we can extend the lifespan of the beacons.

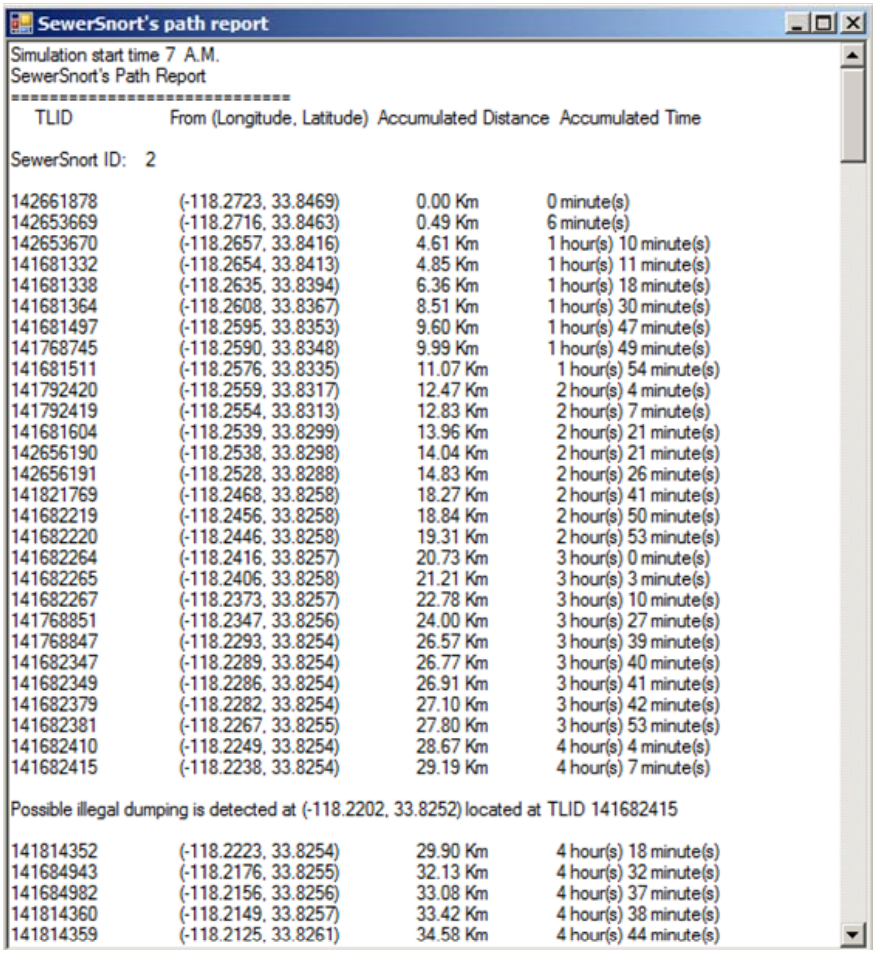

Figure 6.14: Example of SewerSnort path analysis

6.5 Emergency notification

Although most of system failures are caused by aging infrastructure, malicious attacks such as terrorism or sabotage can result catastrophic disaster. The disastrous series of sewer gas explosions in Guadalajara, Mexico on Wednesday, April 22, 1992, which caused death of 206 people and left almost unrecoverable damages to the city [72], demonstrates the potential impact of terrorist attack using underground sewer lines.

To deliver prompt alarms in case of emergency spills, fraudulent dumps, or astronomical explosive gas concentration, SewerSnort may upload collected data to base stations on a street level while traversing WCS before it reaches to the destination. As illustrated in Figure 6.15, urgent data can be transmitted to a beacon node installed under a manhole cover. Then, the beacon node can relay the received data to a gateway node deployed on a nearby lamppost which will eventually deliver the data to a central office (to make a decision and take an action on it).

For wireless communications, ZigBee can be used between a beacon and a gateway if the distance is within the radio range of ZigBee. Alternatively, WiFi can be used if the distance is not within the ZigBee radio range. Finally, a gateway node can transmit data to the central office either via wireless access networks such as GSM or wired access networks such as Digital Subscriber Line (DSL) and Passive Optical Network (PON).

Although severe signal attenuation between a beacon node and a gateway is encountered since the beacon node is located below ground (i.e., beneath the thick metal manhole cover as shown in Figure 6.16) and it makes the data communication challenging, a number of schemes has been designed and developed in an effort to address this communication challenge. One solutions is employing the techniques used to enable wireless underground sensor networks where the sensor nodes buried underground can report sample data to nodes on the surface wirelessly [28]. The other alternative is using an external antenna (over the surface) from the underground beacon node. We install external antennas on the surface of manhole covers to transmit data from underground to aboveground. However, the external antennas (or surface nodes) can be easily destroyed be-

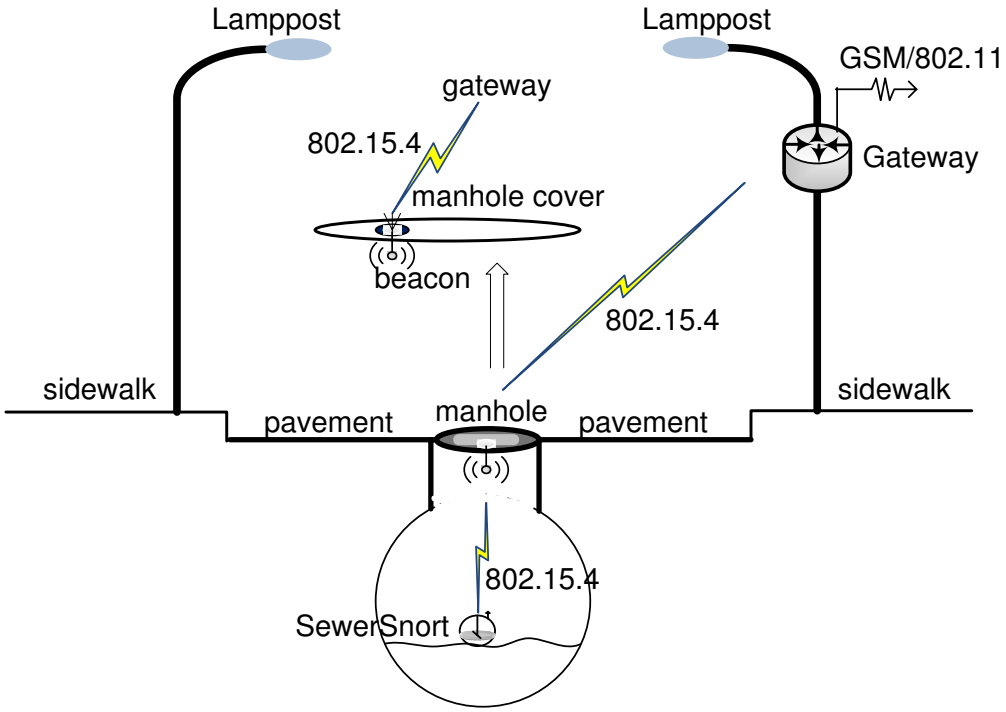

Figure 6.15: Illustration of gateway/base station

Figure 6.16: Images of manhole cover

cause manholes are typically located on human accessible roads and antennas can be run over by vehicles/pedestrians or be scrapped with snow plows.

In order to address this problem, we can leverage the following two approaches proposed in the recent studies. Mastarone et al. [41] proposed to install a thin slot antenna into a conventional cast-iron manhole cover (by milling the manhole cover and placing a coaxial RF connector in the hole). However, this approach cannot fully protect an antenna from the harsh environment of the active roadbed and the continuous feeding of wire erosion. Thus, Jeong et al. [31] built a noble composite manhole cover with fiberglass fabric below which a thin slot antenna is attached to isolate from the external physical environment yet to efficiently radiate electromagnetic waves.

6.6 Fault recovery

Since a SewerSnort is carried by sewer flow and has no on-board motion control during the journey, the SewerSnort is unable to move around the obstacles when the SewerSnort gets stuck with blockages. To rescue a stranded SewerSnort, it is necessary to estimate its position. Considering that a base station can hear probing messages from the floaters when the floaters pass by, we can keep a log of probing messages at the base station and use it to locate the lost SewerSnort. For example, as illustrated in Fig 6.17, base station 5 heard floater 7, but base station 6 did not; therefore, floater 7 is stuck between base station 5 and base station 6. For a better estimate of the lost

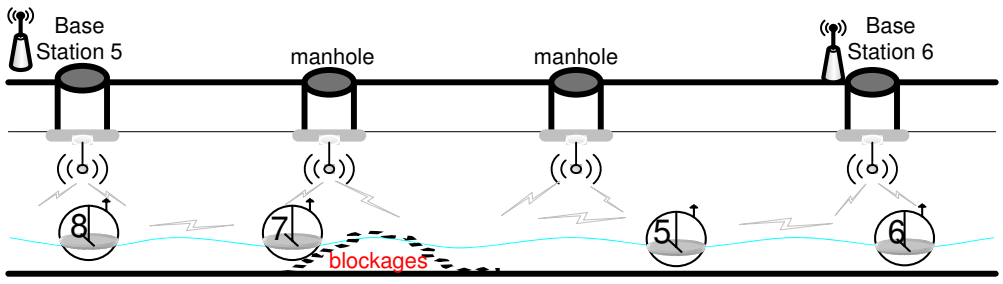

Figure 6.17: Illustration of fault recovery

position, we can deploy a “convoy” of SewerSnorts that they can hear from the neighbors. When a

Table 6.9: Example of message log of SewerSnort

SewerSnort ID	Timestamp of the last packet received
0	16:23:40
1	16:25:10
2	**12:10:15**
...	...
n	16:30:00

SewerSnort receives proving messages, SewerSnort keeps a log of the latest timestamp of probing messages as illustrated in Table 6.9. Upon retracting the surviving SewerSnorts at the end of the journey, we can estimate the approximate positions of the lost SewerSnorts based on the log. For example, in Table 6.9, we can approximate that node id 2 may have been stuck or run out of power around at 12:10:15.

CHAPTER 7

Data Analysis

7.1 Measurement Error Control

In general, the sewer flow is believed to be laminar and the environment does not change drastically from one region to the right next [13]. Hence, the linear least square fitting is an ideal choice for controlling the measurement errors in sampling data such as CH_4, H_2S, pH, or conductivity. In addition, the linear least square fitting provides smooth, continuous, and differentiable function which can aid to detect anomalies efficiently. First, we remove obvious outliers from raw data. Then, we apply Minimum Mean Square Error (MMSE) as followings:

We define $\mathbf{y}, \mathbf{a}, \mathbf{h}$, and $u_m(x)$ as

$$
\begin{aligned}
y &= (y_1, y_2 \ldots y_n)^T && \text{(sample data)} \\
a &= (a_0, a_1 \ldots a_m)^T && \text{coefficient vector} \\
h &= (u_m(x_1), u_m(x_2) \ldots u_m(x_n)) && \text{n x m matrix} \\
& u_m(x) = 1 + x + x^2 + \ldots + x^m
\end{aligned}
$$

and express them as a normal equation.

$$y = ha \tag{7.1}$$

Let (x_t, y_t) be a pair of coordinates where a x_t is time and y_t is a sample data taken at time x_t. Based on Minimum Mean Square Error (MMSE) theorem, there exists a polynomial $P_m(x)$ which has degree m that is less than the number of samples and minimizes the sum of mean square

error [6]. Since we want to minimize the square errors, we let $y = P_m(x)$ and find the coefficients of $P_m(x)$ as

$$a = (h^T h)^{-1} h^T y. \tag{7.2}$$

Now, using $P_m(x)$, we control the measurement quality and detect the functional deficiencies.

7.2 Detection of Functional Deficiency

To identify a trend such as increasing flow or decreasing flow effectively, we divide the pipeline into segments with equal length (i.e. 1m). Then, we let $s_0, s_1, s_2 \ldots s_n$ be the segments in order as they are located in the pipeline.

Now, we compute a mean value m_i of each segment $s_i (i = 0, 1, \ldots, n)$ using $P_m(x)$ as

$$m_i = \frac{1}{|a_i - a_{i-1}|} \int_{a_{i-1}}^{a_i} P_m(x) \mathrm{d}x, \tag{7.3}$$

where segment $s_i = [a_{i-1}, a_i]$ as illustrated in Figure 7.1 and 7.2.

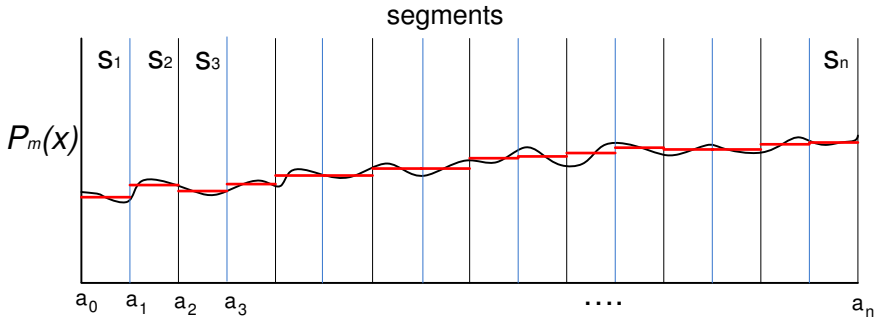

Figure 7.1: Increasing flow

Then, we can deduce that it is increasing if $\ldots m_{i-1} \leq m_i \leq m_{i+1} \ldots$ as illustrated in Figure 7.1, and decreasing if $\ldots m_{i-1} \geq m_i \geq m_{i+1} \ldots$ as illustrated in Figure 7.2. In addition, we compute a variance of sonar data. We deduce that it is fluctuating if $var(sonar) > threshold$.

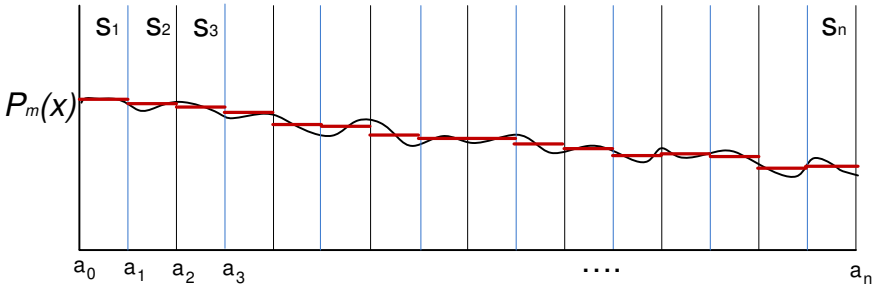

Figure 7.2: Decreasing flow

Air flow in conduit and molecular diffusion phenomena in nature cause dispersion of sewer gases. As a SewerSnort approaches near to the source, the concentration of gases will increase. On the other hand, as it moves away, the concentration may decrease. Also, chemical diffusion occurs in the presence of concentration gradient in nature. The high concentration of toxic chemicals dumped in sewer system will be diluted through chemical diffusion. However, until the system reaches to an equilibrium state, we can detect a range of concentrations along the pipeline.

Thus, using the Equation 7.3 and exploiting their side effects, we detect functional deficiencies as follows.

- Pipe blockages: The deposits that cause blockage are typically composed of organic/inorganic components, where they produce methane (CH_4) gas and hydrogen sulfide (H_2S) gas [15]. Thus, high concentration of hydrogen sulfide gas is a key indicator of blockage. Thus the increase of H_2S gas can be a key indicator of blockages. Also, the fluctuation of sonar data can be a indicator of blockages caused by inorganic components.

- Infiltration/Inflow (I/I): I/I is groundwater/storm water gets into sewer system through cracks. As pointed out previously, I/I increases the flow level and can cause overflows. Groundwater/storm water has very different chemistry than sewer. Hence, I/I can be detected by measuring conductivity along the pipeline. In addition, the total organic carbon (TOC) measured in sewer is much higher than TOC measured in groundwater.[1] Thus, the increase of

[1] In general, TOC in sewer is 100 to 170 mg/L and TOC in groundwater is $<$ 20 mg/L [10].

conductivity or decrease of TOC can be a key indicator of I/I.

- Exfiltration : Exfiltration causes untreated wastewater to escape the WCS. As pointed out previously, monitoring exfiltration has been challenging due to its "invisibility." We exploit a side effect of exfiltration, namely flow reduction due to escaping fluid. Mechanically, the "flow slow down" causes organic/inorganic materials to be accumulated around the defective area. Also, as pointed out previously, an acoustic detection of seeping/gushing water can be used in case of major cracks.

Based on the characteristics of functional deficiencies and the above data analysis approach, we develop a decision tree to detect the functional deficiency as shown in Fig. 7.3. In addition, the above data analysis approach can effectively quantify the severity of functional deficiencies, which assists directing efforts to the critical areas, for the severity of problem is more of concern than the existence of problem in real world.

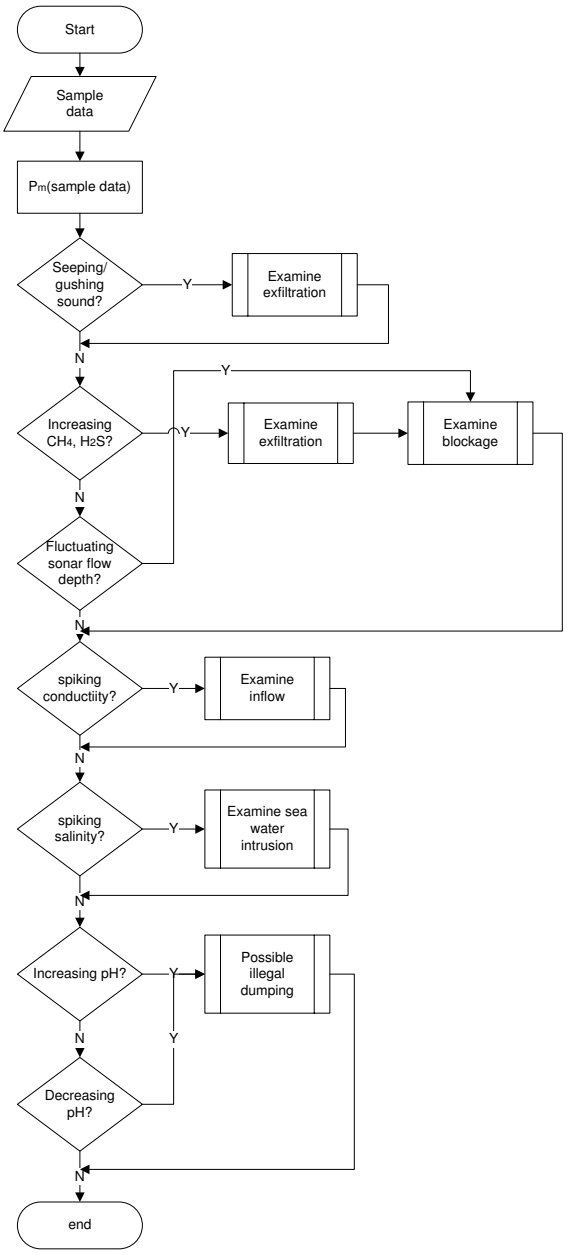

Figure 7.3: Decision tree to detect functional deficiencies

CHAPTER 8

Experiments and Simulations

8.1 SewerSnort gas sensor board evaluation

In our previous work [33], we implemented H_2S gas sensor board as a proof-of-concept. In general, data acquisition modules of industrial grade electrochemical sensor cost in the ranges of thousands of dollars (far outside viability for SewerSnort). Alternatively, we implemented our custom H_2S gas sensor board to demonstrate that our low-power and low-cost sensor board performs sufficiently well to detect the functional deficiencies. In addition, we validated the end-to-end capability of our custom H_2S sensor board by comparing it with that of QRAE PLUS Multi-Gas Monitor [53]. QRAE is an off-the-shelf gas monitor that is equipped with the same type of RAE H_2S electrochemical sensor element. The sensing fidelity of electrochemical sensor is fundamentally limited by the electrochemical element itself. For our chosen element [53], the maximum sensitivity[1] to H_2S is $0.75\frac{\mu A}{ppm}$, yet internal fluctuations and variations over temperature limit the accuracy to $\pm\frac{1}{2}ppm$.

We chose a value of 4.7Ω for the transconductance element R_3 (Figure 6.2) and a gain of 1000 ($R_4 = R_3 \times gain$) as it minimizes offset and Johnson thermal noise, while resolving $0.5ppmH_2S$ changes into an output signal above the quantization threshold of the 10-bit ratiometric Analog-to-Digital Converter (ADC) in our chosen low-cost and low-power processing node (a Crossbow MicaZ). The transfer function for a $1ppm$ signal ($0.75\mu A$) follows:

$$\frac{mV}{ppm} = 0.75\frac{\mu A}{ppm}R_3\frac{R_4}{R_3} \approx 3.5\frac{mV}{ppm} \tag{8.1}$$

[1] In this context, Parts Per Million (ppm) denotes the number of particles of a desired gas per one million particles of the background gas or gases

For evaluation, we placed the QRAE and SewerSnort monitors in an airtight container and introduced a $10ppm$ H_2S gas via a sealed injection tube. Figure 8.1 presents the measured gas concentration in ppm. The figure shows that the measurement results from our AFE are within 0.5ppm of the QRAE on average – e.g. below the sensor element's internal uncertainty.

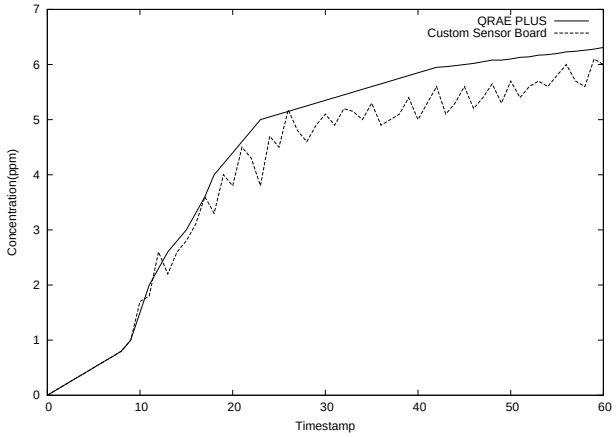

Figure 8.1: Measured gas concentration using the QRAE industrial gas monitor and our SewerSnort AFE. The results agree almost exactly given that the sensor element uncertainty is $\pm 0.5ppm$.

8.2 Theoretical RSSI-based localization scheme evaluation

To validate the theocratical RSSI-based localization scheme, we performed experiments in a corridor with size of 3mx2.5mx100m (Width x Height x Length), using MICAz mote with IEEE 802.15.4 radio as illustrated in Figure 8.2(a). A beacon was placed on the center of ceiling at 5m down from the center of corridor and sent a beacon message every second. Then, a SewerSnort carried by an Amigobot traveled from one end to the other end with constant speed. While moving down the corridor, the SewerSnort collected the RSSI value of beacons. An example of the raw RSSI data is shown in the Figure 8.2(b). Also, we found η was approximately 2.3 for the testbed environment. To de-noise the raw data we applied the EMD algorithm. We identified a local maxima $X_{max}(t)$ as

$$X(t-1) < X_{max}(t) > X(t+1), \tag{8.2}$$

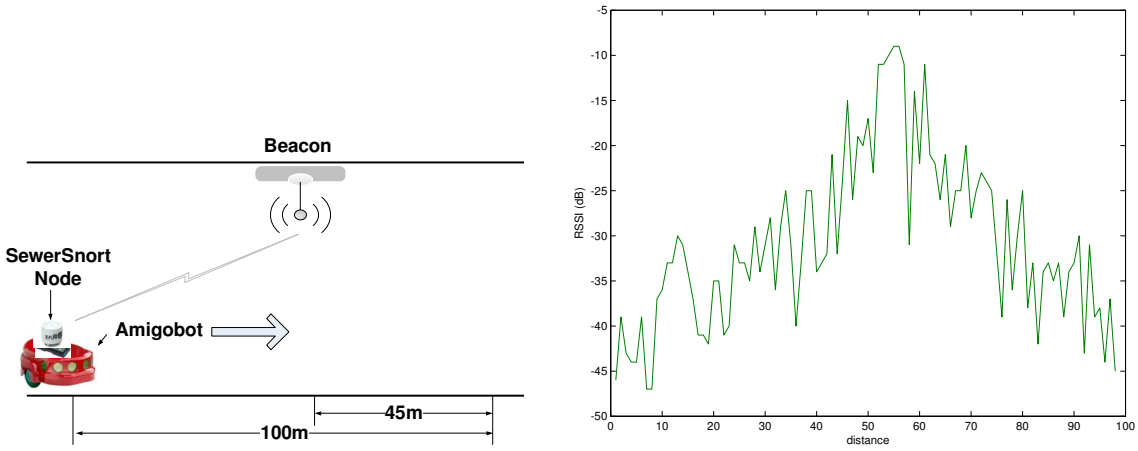

(a) Localization experiment scenario

(b) Raw RSSI data

Figure 8.2: Localization evaluation scenario and raw RSSI data (a) and (b)

and a local minima X_{min} (t) as

$$X(t-1) > X_{min}(t) < X(t+1), \tag{8.3}$$

where X (t) is RSSI value at time t.

Also, we used cubic Bezier curve and Bernstein polynomials to connect all local maxima and all local minima for the upper envelope and for the lower envelop respectively as follows:

$$E(x) = \sum_{i=1}^{n} \binom{3}{i} X_i (1-t)^{3-i} t^i t = [0,1]. \tag{8.4}$$

After the 4^{th} iteration of sifting, we reached to the termination condition. The Figure 8.3 shows the final residue. Overall, the mean absolute discrepancy was 1.87m. In general, the problem of WCS spans over several meters. In addition, the "Meter" type accuracy is sufficient in most pipeline diagnostics applications. The localization scheme with 10m resolution is sufficient to solve the real-world problem and the proposed RSSI based approach can adequately fulfill the requirements.

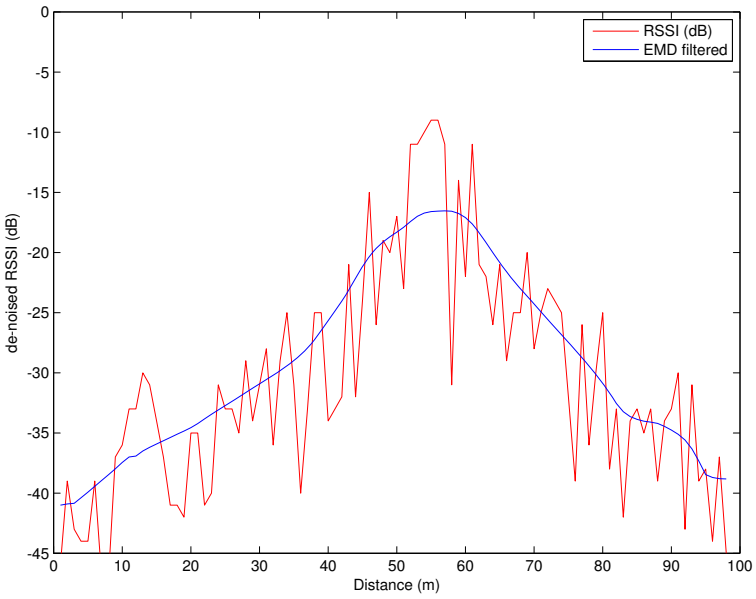

Figure 8.3: Comparison with measured RSSI and De-noised raw RSSI data

8.3 SewerSnort evaluation in a mobile environment

The SewerSnort gas sensor board was interfaced with the MicaZ mote. Since the MicaZ mote had a 2.4 GHz IEEE 802.15.4 compatible radio, we also used it as a beacon node. We developed a TinyOS driver for the SewerSnort gas sensor board. The driver stores the following information in its flash memory: the gas measurements, the beacon messages that include the position of a beacon node, and the received signal strength of the beacon messages.

In the experiments, we first tried to derive the values of A_{CL} and $\alpha_{(R,\sigma)}$ in Equation (6.11) for 10m concrete pipes with diameters of 1.5m and 1.8m. In order to estimate A_{CL} and $\alpha_{(R,\sigma)}$ for each pipe, we used a robust linear algorithm in Matlab. We placed a beacon at the beginning of the pipes, and measured the RSSI values from 0m to 10m, incrementing the measure point by 0.5m. Each measure collected 20 RSSIs, where every RSSI was averaged over a set of 500 samples. Thus, every measure required 10000 samples. We configured the beacon to send out a beacon packet every 10ms, at the highest transmission power of the MicaZ. Figure 8.4 and Figure 8.5

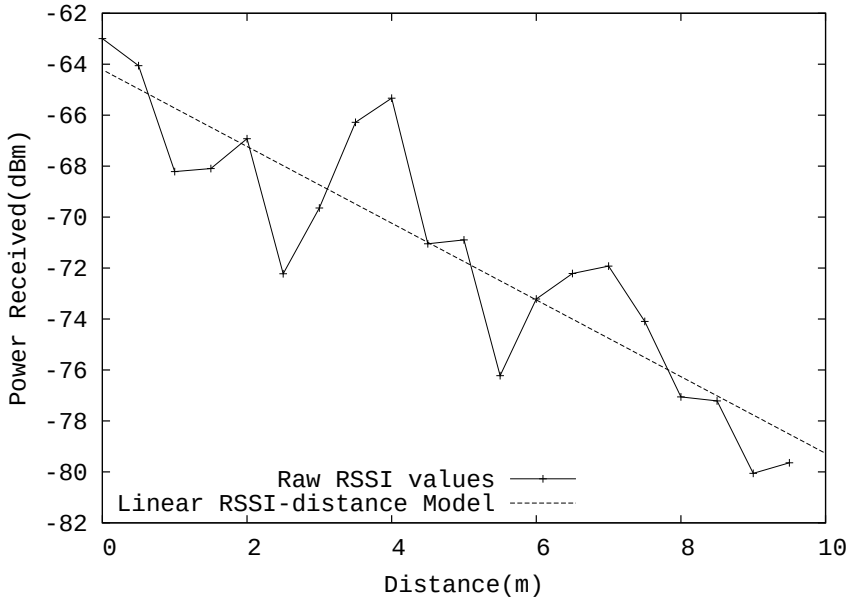

Figure 8.4: Average received power results for 1.5m pipe

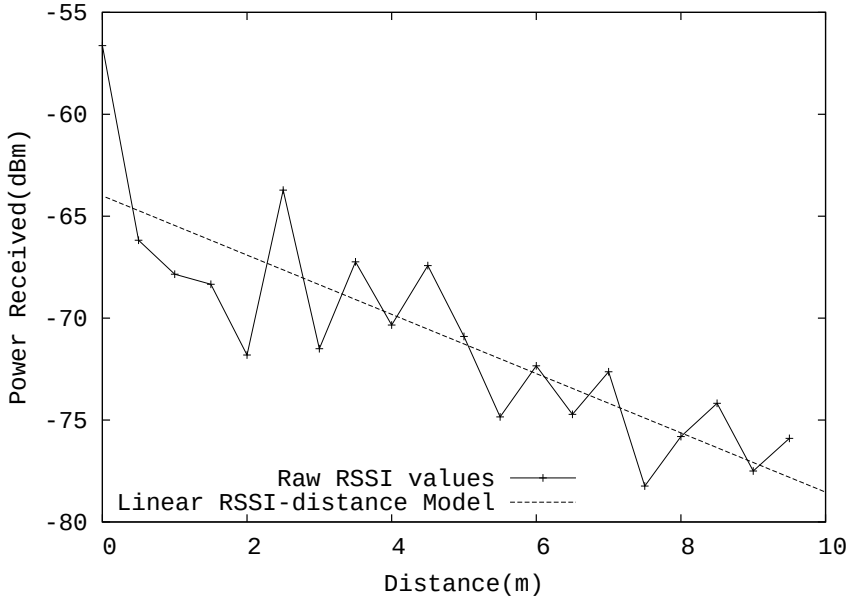

Figure 8.5: Average received power results for 1.8m pipe

show results of linear regression using Equation(6.11).

After obtaining A_{CL} and $\alpha_{(R,\sigma)}$ for Equation (6.11), we considered the mobility scenario of the SewerSnort. We mimicked the mobility of a SewerSnort by using an Amigobot robot, a programmable, wirelessly controllable mobile robot. The SewerSnort node was placed on top of the Amigobot. We programed the Amigobot to move from one end to the other with a constant speed of 1m/s in a straight line. A H_2S gas cylinder ($10ppm$) was placed 3.5m away from the starting point. The overall scenario is summarized in Figure 8.6(a). In the experiment, mainly the sensor's sensitivity was examined and there was no effect of wind or ventilation.

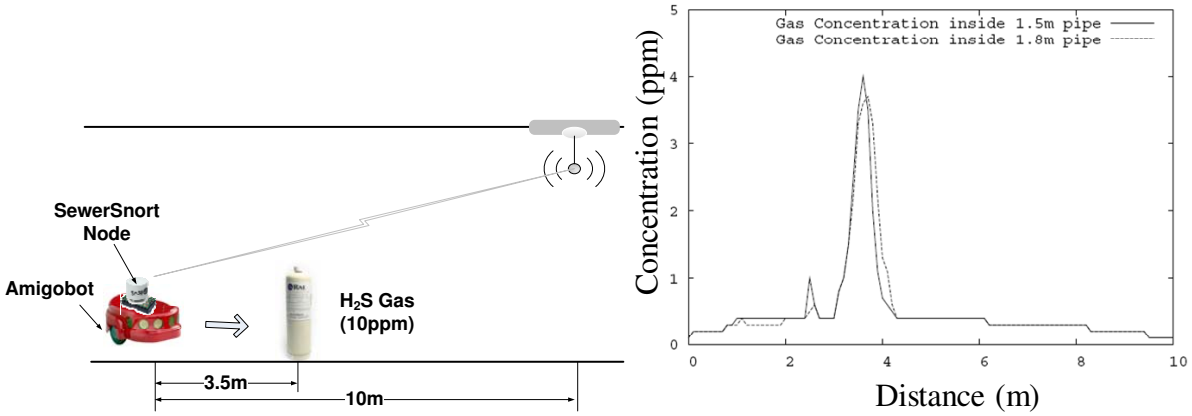

(a) Experiment scenario

(b) Measured H_2S gas concentration (ppm)

Figure 8.6: Gas sensor board evaluation scenario and results (a) and (b)

Figure 8.6(b) shows that the measured gas concentration starts rapidly increasing around the 3.4m and then drastically decreasing after the 3.7m. This range includes the position where we place the gas cylinder. The reason why we observe lower concentration than $10ppm$ is due to gas diffusion in the air. A spike located at around 2.5m in 1.5m pipe is due to randomness of the gas diffusion. For localization, we apply the EMD algorithm to denoise the RSSI measurement data in Figure 8.7 and Figure 8.8. We identify all local maxima $X_{max}(t)$ as $X(t-1) < X_{max}(t) > X(t+1)$ and all local minima $X_{min}(t)$ as $X(t-1) > X_{min}(t) < X(t+1)$ where $X(t)$ is RSSI value at time t. We then use cubic Bezier curves and Bernstein polynomials to connect all local maxima and all local minima for the upper envelope and for the lower envelop respectively as

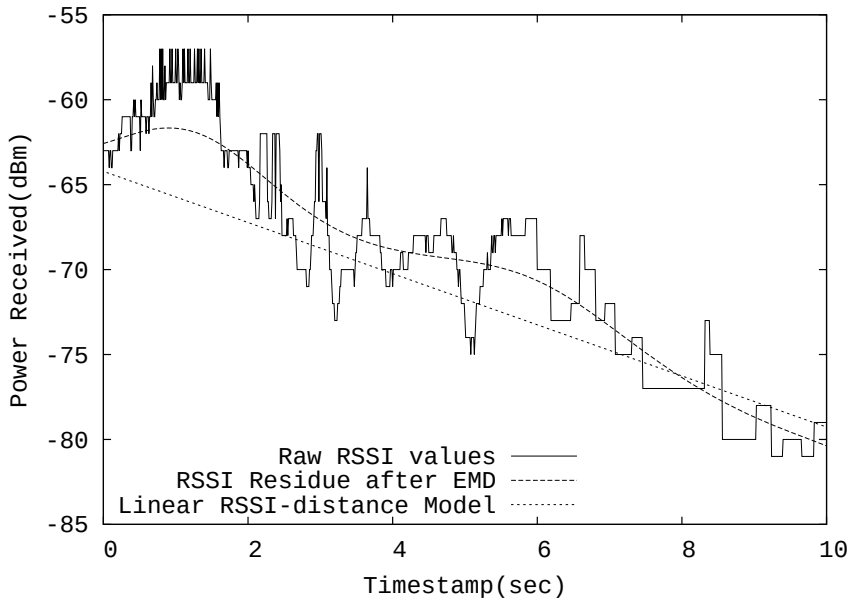

Figure 8.7: Comparison with measured RSSI, EMD filtered RSSI, and Linear RSSI-distance Model (1.5m pipe)

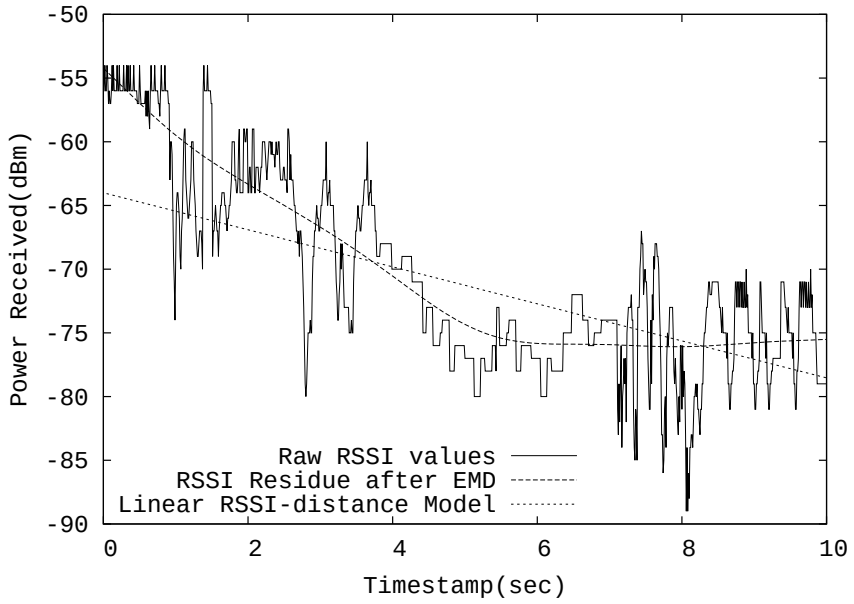

Figure 8.8: Comparison with measured RSSI, EMD filtered RSSI, and Linear RSSI-distance Model (1.8m pipe)

follows: $E(x) = \sum_{i=1}^{n} \binom{3}{i} X_i (1-t)^{3-i} t^i$. After the 4th iteration of sifting, we reach the termination condition. Figure 8.7 and Figure 8.8 show the final residue after de-noising.

In most cases, the equation (6.11) can be utilized to annotate the sampling locations based on RSSI value. However, in some cases, an abrupt jump or reverse of direction may be encountered in the computed distance estimates over time. To address such cases, we exploit the fact that sewer flow is laminar and the flow velocity is relatively steady. Assuming that a SewerSnort flows down with a constant speed V, we substitute d in Equation (6.11) with Vt. Then, we find the speed V based on the smoothed RSSI values that minimizes the errors in distance estimates. Then, we can mitigate the abrupt changes in estimates and eliminate the reverse of directions. With the equation and the enhancement assisted by characteristics of sewer flow, the experimental results showed less than 5% error which is adequate to solve the real-world problem.

CHAPTER 9

Deployment Study

9.1 Simulation Tool

The main objective of the simulation tool is to develop an efficient field deployment plan by testing and evaluating the plan before the deployment. The simulation tool provides workspace, task bar, and simulator. The workspace is used for developing a scenario, and the task bar is used for providing basic functionalities and advanced functionalities. The basic functionalities include inserting/deleting elements on developing a scenario, saving/retrieving scenarios, creating bitmap of scenario; and the advanced functionalities include analyzing floater's path, reporting statistics of the scenarios, and generating configuration files for simulator. Then, the simulator imports the configuration files to visualize the SewerSnort movement. Finally, the simulator generates a report for network connectivity and data upload in case of emergency such as illegal dumping or high concentrations of explosive gases.

In designing a simulation tool, we take into account the unique characteristics of WCS. Almost all models in the existing literature on mobile sensor networks assume that each sensor moves independently from the others. Typically, the path of each sensor is taken as an independent realization of a given stochastic process, such as a random walk, or random way point process. However, in sewer network few unique characteristics govern the mobility of sensor nodes. WCS exhibits a tree-like structure that prevents a floater from cycling through the pipelines. Also, WCS has been built for open channel flow. The hydraulic modeling of open channel flow is fundamentally represented by two equations namely, conservation of mass and conservation of momentum. From the equations, the main driving force of the sewer flow motion is gravity and flow depth. Since sewer

flow depth is affected by human lifestyle, the flow depth, in general, cycles through 24-hours.

First, we review the fundamental background of open channel flow and sewer flow from the aspect of understanding the mobility of floaters while they traverse down WCS. Then, we present the system architecture and functionalities of the simulation tool. In developing a simulation tool, we utilize C/C++ and JAVA SE 6. The simulation tool has three main components namely, workspace, task bar, and simulator. The task bar and workspace are written with C/C++ and simulator is written with JAVA SE 6.

9.1.1 Flow velocity in open channel flow

The flow of water in pipe is categorized by either pipe flow or open channel flow. Pipe flow is a flow which fluid is completely filled up in a conduit. On the other hand, open channel flow is a flow which has a free surface and there is an air passages in a conduit as illustrated in Figure 9.1. Fundamentally, WCS is designed to carry open channel flow and, in real-world, sewer is a primarily

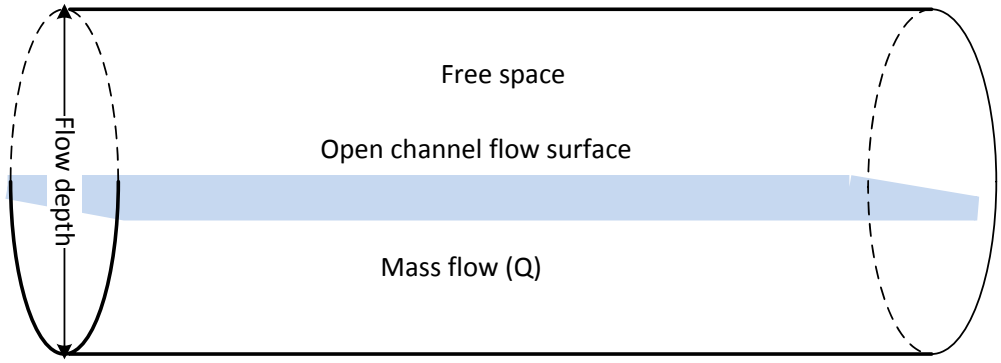

Figure 9.1: Illustration of open channel flow

open channel flow. The flow velocity in open channel flow is presented by conservation of mass and conservation of momentum as

$$\frac{\Delta F(h)}{\Delta h}\frac{\Delta h(x,t)}{\Delta t} + \frac{\Delta q(x,t)}{\Delta x} = 0 \tag{9.1}$$

where q(x, t) is the mass of flow at point x and time t, and h(x, t) is flow depth at point x and time t and F(h) is flow cross sectional area at flow depth h, and

$$\frac{1}{g}\frac{\Delta v}{\Delta t} + \frac{v}{g}\frac{\Delta v}{\Delta x} + \frac{\Delta h}{\Delta x} = I_S - I_R \tag{9.2}$$

where g is gravity, I_S is pipeline slope, and I_R is friction. In sewer flow, the flow velocity is

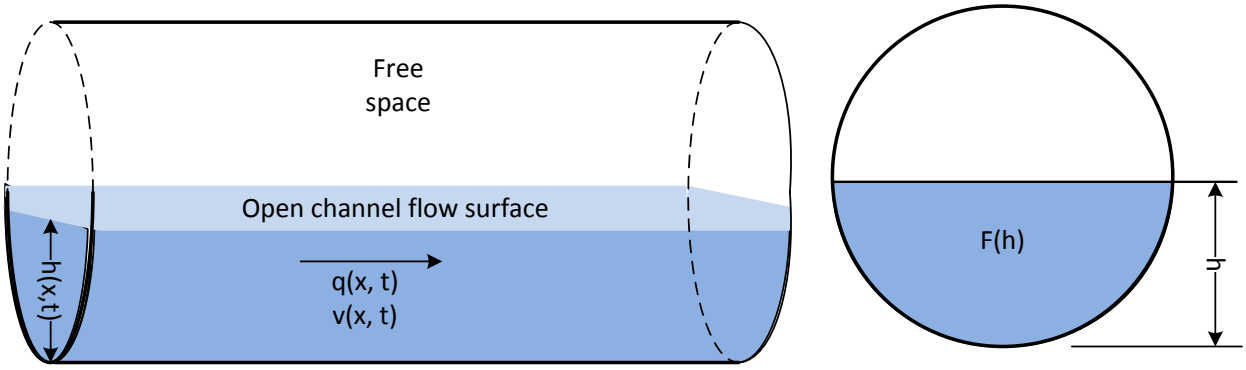

Figure 9.2: Illustration of open channel flow depth

determined by flow cross sectional area *F(h)*, the depth of flow *h*, the mass of flow *q*, gravity *g*, sewer slope I_S, and friction I_R. However, gravity *g*, sewer slope I_S, and friction I_R are constants. Also, flow depth is determined by flow mass at fixed pipe size. Thus, the flow velocity is mainly governed by cross sectional area and the mass of flow as

$$V = \frac{Q}{A} \tag{9.3}$$

where V = flow velocity, Q = flow mass, and A = flow cross sectional area.

In open channel flow, the flow velocity is distributed based on the flow depth due to friction along the wall of pipeline as illustrated in Figure 9.3(a) and 9.3(b). On the surface of flow, the velocity is maximized at the center of flow, and the velocity is decreased as it approaches to the wall of pipeline. The mean flow velocity is presented as

$$\overline{V}_{\text{flow}} = \frac{V_1A_1 + V_2A_2 + \ldots + V_nA_n}{A_1 + A_2 + \ldots + A_n}. \tag{9.4}$$

The cross sectional area can be deduced from the flow depth, and the flow depth can be deduced from the mass of flow since the size of pipe is fixed.

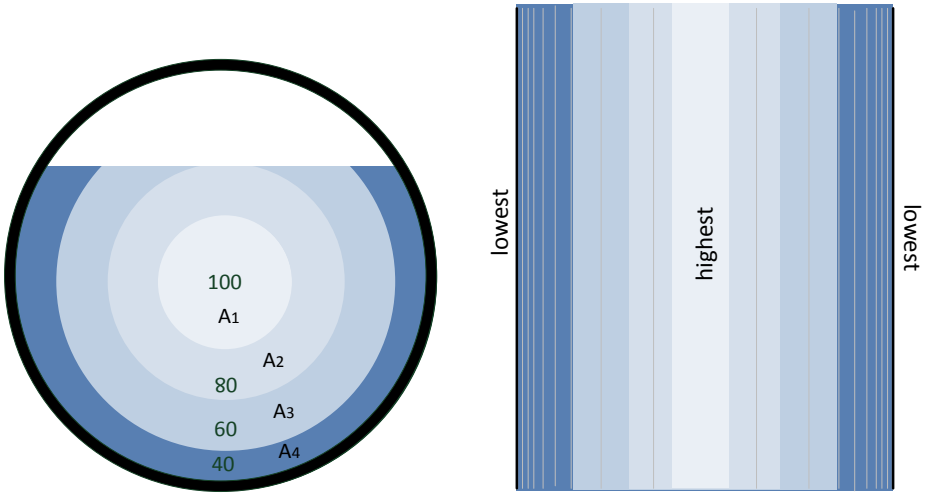

(a) Illustration of flow velocity distribution in open channel flow (100 is the maximum velocity. No particular measurement unit is associated with this value.)

(b) Illustration of flow velocity distribution on surface of flow in open channel flow

Figure 9.3: Illustration of flow velocity distribution in open channel flow (a) and (b)

Furthermore, the mass of flow in WCS is mainly affected by human lifestyle, and it typically cycles through 24 hours as illustrated in Figure 9.4, and the typical flow velocity ranges in terms of the time of a day is illustrated in Figure 9.5. Consequently, the speed of floater, when a floater traverses downstream, is governed by time of a day that floater is dispensed. For example, when a SewerSnort is dropped at 12:00 noon, it may start drifting down by 3.5 m/s, but will be slow down as time passed by. However, if a SewerSnort is dropped at 2:00 a.m., it may start moving down by 0.2 m/s, but will catch up with the speed as time passed. Besides human lifestyle, the flow rate profile is affected by location of the sites, day of a week, social events, and natural condition such as precipitation.

For the demonstration of simulation tool, we use a typical flow rate profile. Thus, the speed of SewerSnort is affected by the start time of a simulation. However, a specific flow rate profile associated with the site can be imported into the simulator to perform a simulation for that site.

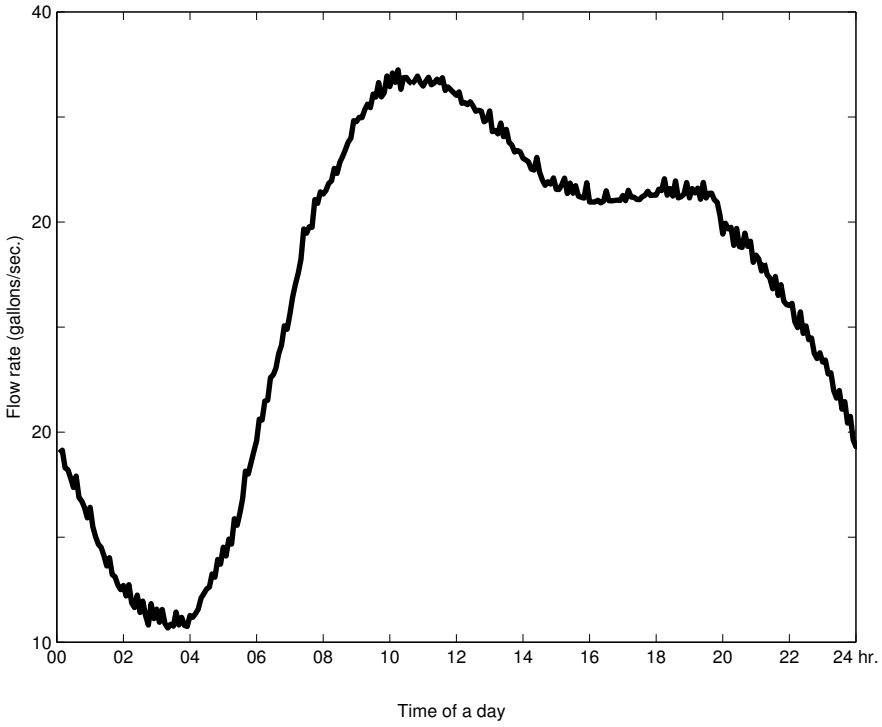

Figure 9.4: Example of typical sewer flow rate 24 hour cycle

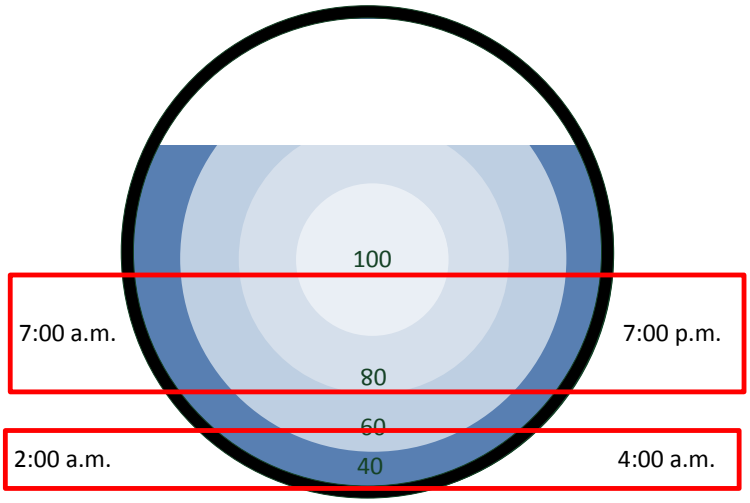

Figure 9.5: Typical sewer flow velocity range

9.1.2 Workspace

The workspace is to display a pipeline and to build a scenario. On the top left corner of the workspace, the current position of the mouse is shown as (longitude, latitude) coordinates with four decimal places as shown in Figure 9.6. Also, when a map file is loaded, the current working file name is shown on the top middle of the workspace as shown in Figure 9.6. As a mouse moves around, the new position of mouse is updated at (longitude, latitude) coordinates.

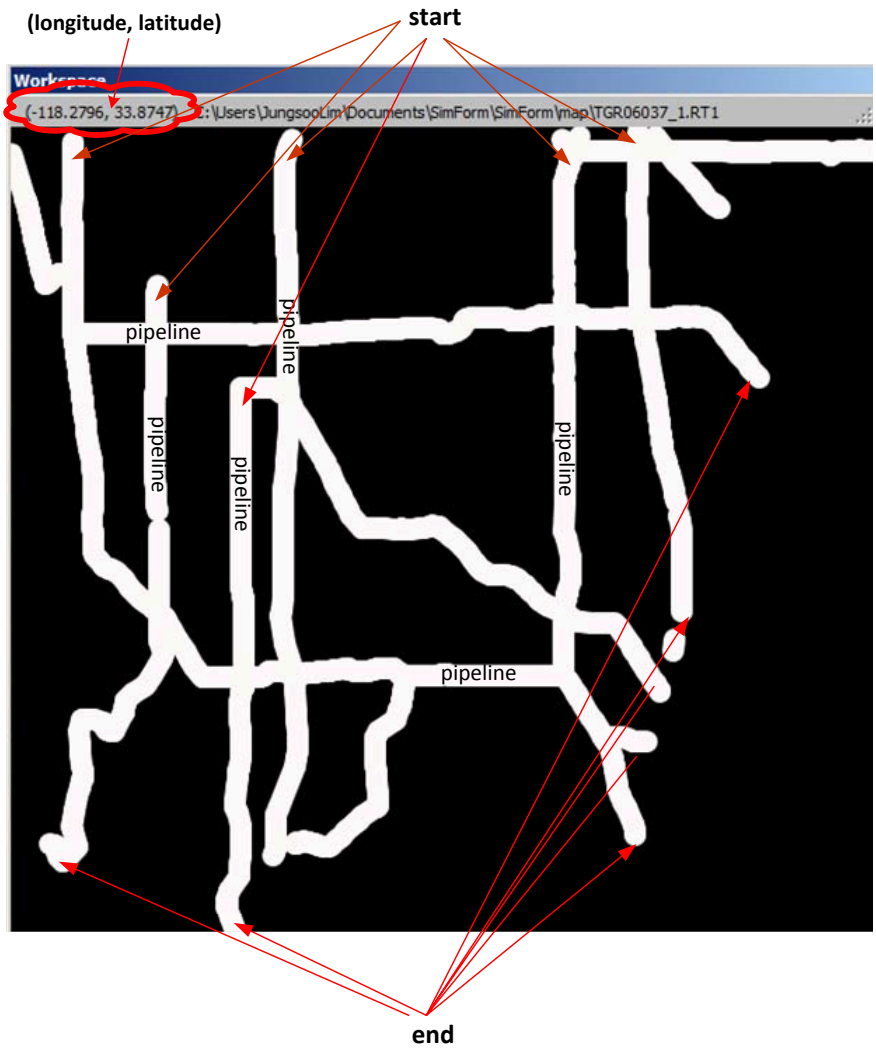

Figure 9.6: Workspace of simulator with a pipeline map (In this example, the north-west is located at the highest altitude.)

9.1.3 Task bar

The simulator provides utilities as shown in Figure 9.7. The simulation scenario can be saved or retrieved. Before a scenario is configured, a pipeline map is loaded on the Workspace. To show an example, we use TigerMap [66] since sewerline runs under the streets. Also, a bitmap of simulation scenario can be saved for future reference. A default simulation start time is set to be 12:00 Noon, but it can be changed as needed. The simulation ends when the journey of all SewerSnorts are ended. The default size of workspace is 600pt X 600pt, but the size of workspace can be increased or decreased as needed. After a map is loaded, the boundaries of map are specified by far north and south latitude, and far east and west longitude as illustrated in Figure 9.7.

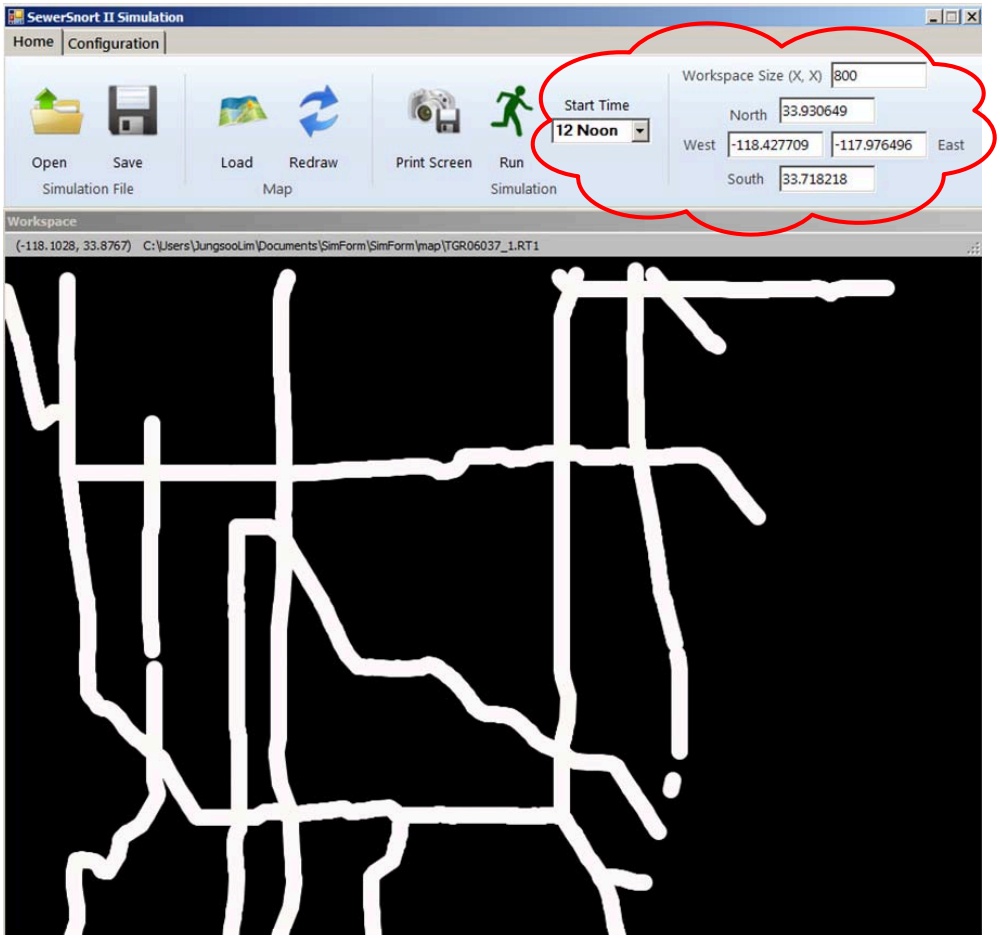

Figure 9.7: Home task bar of simulator and map boundaries with 800ptX800pt

To configure a scenario, we use "Configuration" task bar as shown in Figure 9.8. There are two types of node. One is a base station/gateway, and the other is a mobile floating sensor "SewerSnort." When an emergency (i.e. high concentration of explosive gas or possible illegal dumping) is detected, SewerSnort uploads information to the first reachable base station. Upon the completion of journey, SewerSnorts are retracted at the treatment plant, pumping station, or manholes using screening devices. To place an element on the workspace, select the element first. Then, find a position for it on the workspace by referring the (longitude, latitude) coordinates on the top left corner of the workspace.

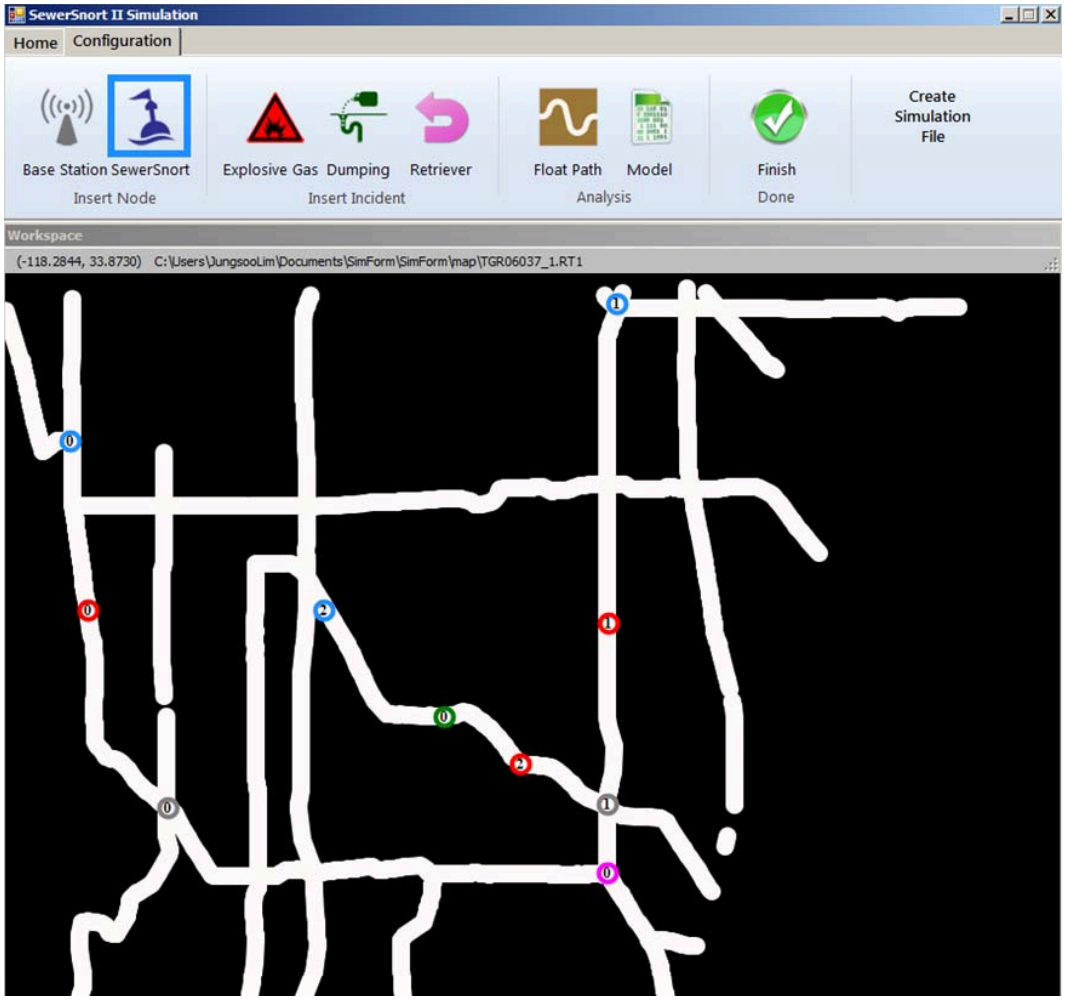

Figure 9.8: Example of a scenario

Before we run the scenario, the start time of a day can be set. The default start time is set to 12:00 noon, but it can be changed as needed. (Please refer to Section 9.1.1 for the effect of start time.) As we run the scenario, the travel path of SewerSnort is determined as shown in Figure 9.9.

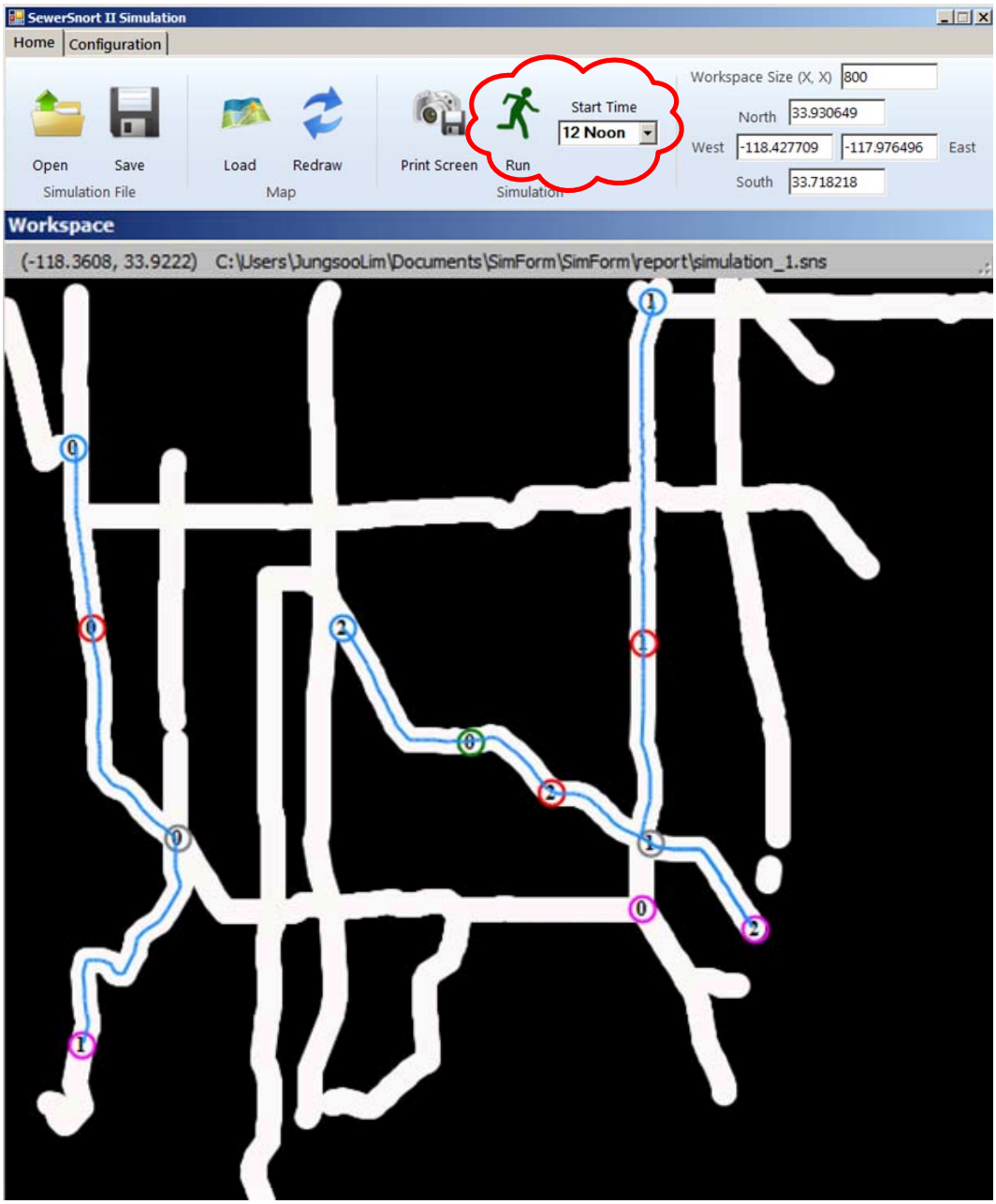

Figure 9.9: Example of SewerSnort paths

Upon the completion of running scenario, a scenario analysis is generated as shown in Figure 9.10. In the scenario analysis, we report the start time of simulation (i.e. scenario in Figure 9.10 starts at 7:00 a.m.); the total sewer line presented in the scenario; the total sewer line inspected by SewerSnorts; the coverage ratio of inspected sewer line to total sewer line; emergency detection/report log by specifying SewerSnort ID, location of emergency (i.e. (longitude, latitude) coordinates), and reported base station ID; and summary of any undetected emergency if exists.

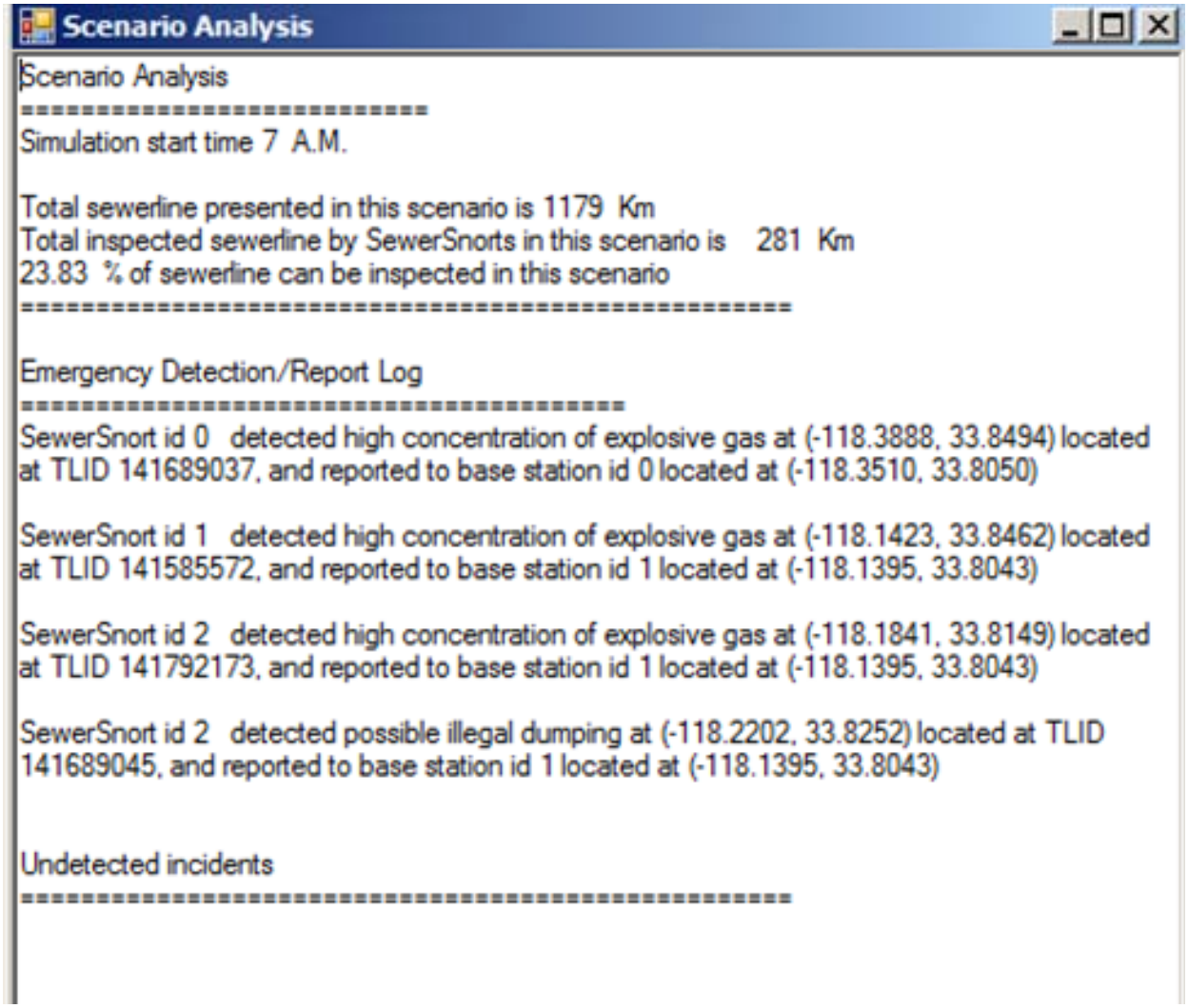

Figure 9.10: Example of scenario report

In addition, a SewerSnort path is analyzed in detail. The path analysis report provides simulation start time, SewerSnort ID, TIGER Line® ID (TLID), (longitude, latitude), accumulated distance of traversed path, and accumulated time of traversing as shown in Figure 9.11. As a SewerSnort travels downstream, the simulator collects the coordinates of paths and computes the accumulated distance SewerSnort traverses. Also, the simulator computes the accumulated travel time based on the speed determined by simulation start time.

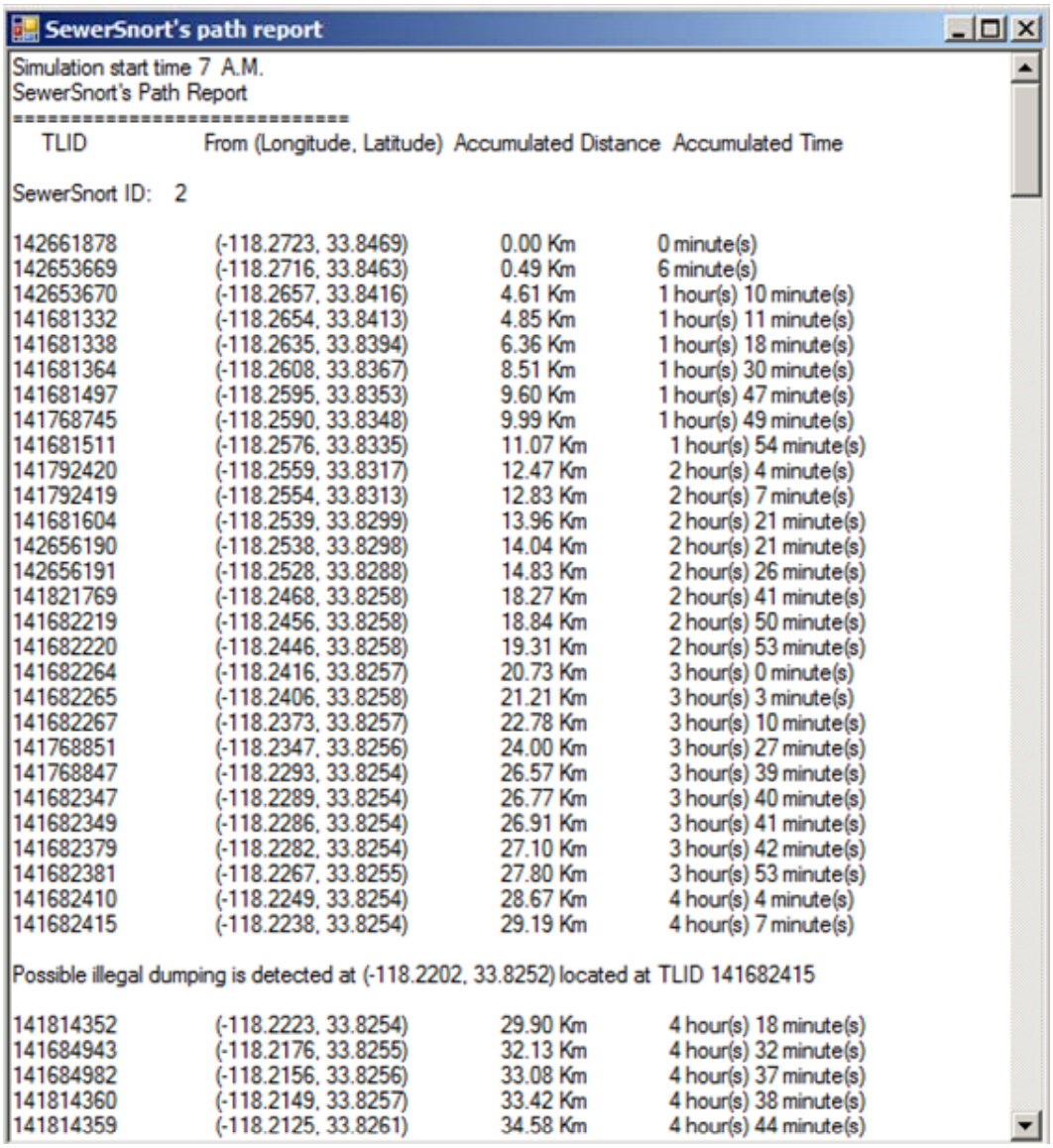
SewerSnort's path report

Simulation start time 7 A.M.
SewerSnort's Path Report
==========

TLID	From (Longitude, Latitude)	Accumulated Distance	Accumulated Time
SewerSnort ID: 2			
142661878	(-118.2723, 33.8469)	0.00 Km	0 minute(s)
142653669	(-118.2716, 33.8463)	0.49 Km	6 minute(s)
142653670	(-118.2657, 33.8416)	4.61 Km	1 hour(s) 10 minute(s)
141681332	(-118.2654, 33.8413)	4.85 Km	1 hour(s) 11 minute(s)
141681338	(-118.2635, 33.8394)	6.36 Km	1 hour(s) 18 minute(s)
141681364	(-118.2608, 33.8367)	8.51 Km	1 hour(s) 30 minute(s)
141681497	(-118.2595, 33.8353)	9.60 Km	1 hour(s) 47 minute(s)
141768745	(-118.2590, 33.8348)	9.99 Km	1 hour(s) 49 minute(s)
141681511	(-118.2576, 33.8335)	11.07 Km	1 hour(s) 54 minute(s)
141792420	(-118.2559, 33.8317)	12.47 Km	2 hour(s) 4 minute(s)
141792419	(-118.2554, 33.8313)	12.83 Km	2 hour(s) 7 minute(s)
141681604	(-118.2539, 33.8299)	13.96 Km	2 hour(s) 21 minute(s)
142656190	(-118.2538, 33.8298)	14.04 Km	2 hour(s) 21 minute(s)
142656191	(-118.2528, 33.8288)	14.83 Km	2 hour(s) 26 minute(s)
141821769	(-118.2468, 33.8258)	18.27 Km	2 hour(s) 41 minute(s)
141682219	(-118.2456, 33.8258)	18.84 Km	2 hour(s) 50 minute(s)
141682220	(-118.2446, 33.8258)	19.31 Km	2 hour(s) 53 minute(s)
141682264	(-118.2416, 33.8257)	20.73 Km	3 hour(s) 0 minute(s)
141682265	(-118.2406, 33.8258)	21.21 Km	3 hour(s) 3 minute(s)
141682267	(-118.2373, 33.8257)	22.78 Km	3 hour(s) 10 minute(s)
141768851	(-118.2347, 33.8256)	24.00 Km	3 hour(s) 27 minute(s)
141768847	(-118.2293, 33.8254)	26.57 Km	3 hour(s) 39 minute(s)
141682347	(-118.2289, 33.8254)	26.77 Km	3 hour(s) 40 minute(s)
141682349	(-118.2286, 33.8254)	26.91 Km	3 hour(s) 41 minute(s)
141682379	(-118.2282, 33.8254)	27.10 Km	3 hour(s) 42 minute(s)
141682381	(-118.2267, 33.8255)	27.80 Km	3 hour(s) 53 minute(s)
141682410	(-118.2249, 33.8254)	28.67 Km	4 hour(s) 4 minute(s)
141682415	(-118.2238, 33.8254)	29.19 Km	4 hour(s) 7 minute(s)
Possible illegal dumping is detected at (-118.2202, 33.8252) located at TLID 141682415			
141814352	(-118.2223, 33.8254)	29.90 Km	4 hour(s) 18 minute(s)
141684943	(-118.2176, 33.8255)	32.13 Km	4 hour(s) 32 minute(s)
141684982	(-118.2156, 33.8256)	33.08 Km	4 hour(s) 37 minute(s)
141814360	(-118.2149, 33.8257)	33.42 Km	4 hour(s) 38 minute(s)
141814359	(-118.2125, 33.8261)	34.58 Km	4 hour(s) 44 minute(s)

Figure 9.11: Example of SewerSnort path report part I

When a SewerSnort encounters an emergency such as high concentration of explosive gas or possible illegal dumping, it upload the information to the first available base station as shown in Figure 9.12.

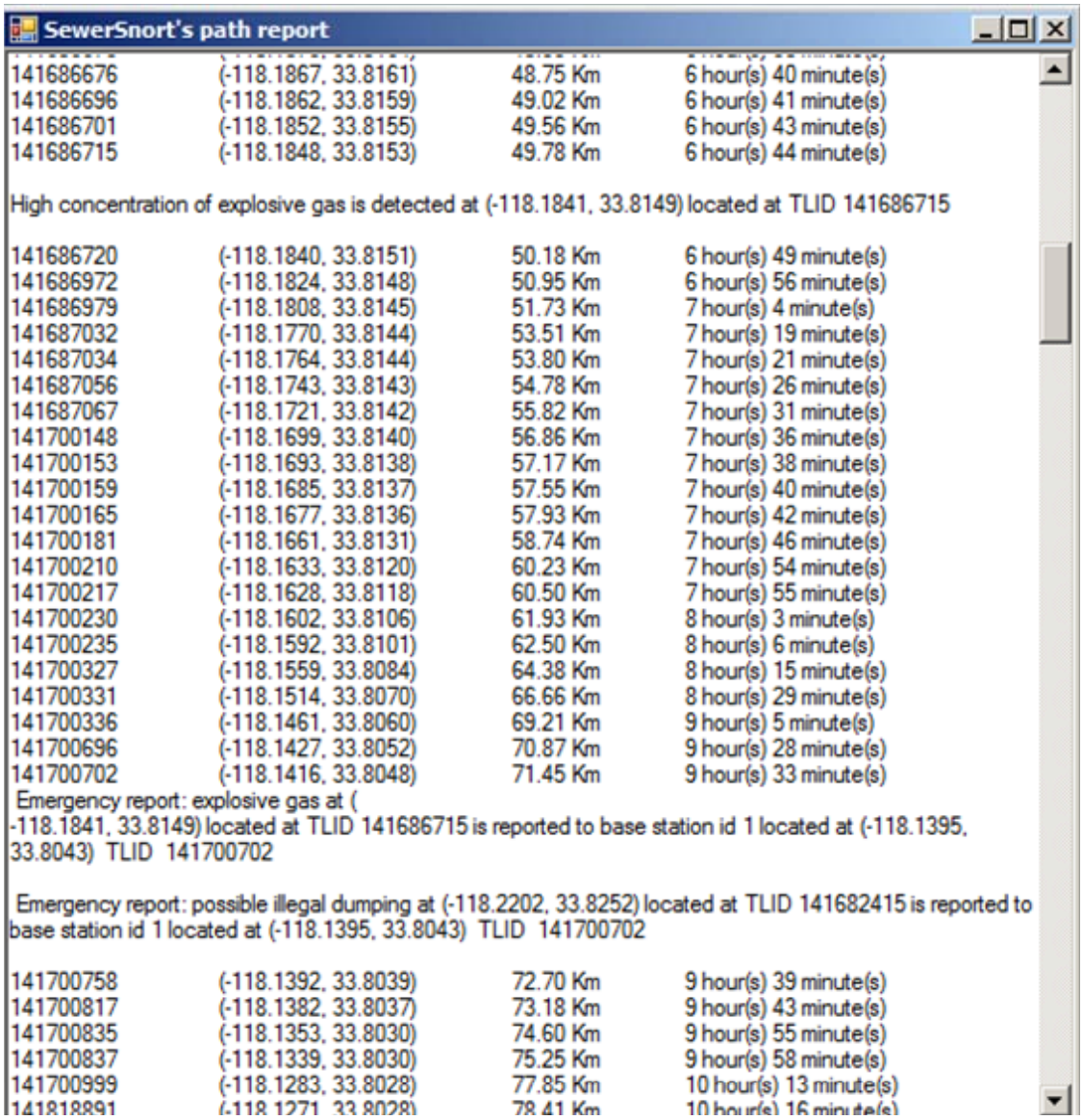

Figure 9.12: Example of SewerSnort path report part II

9.1.4 Simulation space

Multiple floaters can be used to increase the accuracy of diagnosis. In such case, the floaters may exchange probing messages during their journey and log the timestamp of last probing messages as illustrated in Section 6.6 to locate the lost floaters (i.e. The proximities of lost floater can be estimated based on the logs of survived floaters.). Then, the distance between the floaters should be within transmission range in order to hear from each other. Thus, we simulate multi floaters communication inside pipeline to assess the network connectivity among floaters. Also, we simulate the scenario based on the configuration and floaters' path analysis. Upon the completion of scenario configuration and floaters' path analysis, the simulation input files are created. Then, these input files are imported into SewerNet simulation space and the simulator provides an animation of the scenario.

9.1.4.1 Multi-floater communication simulation

When multiple floaters are dispensed, the distance between floaters should be within the transmission ranges to hear the probing messages. The distance between floaters is determined by the interval that the floaters are dispensed and the time of a day that they are dispensed. For example, if we were to drop four floaters every two minutes at 2:00 a.m., they may start traveling 20 - 60 meters apart. However, the distance between them will increase as the speed of flow increases. By 12:00 noon, they may travel over 400 meters apart where the distance is out of transmission range for ZigBee radio.

Hence, simulation space provides an assessment of the network connectivity from the convoy of the floaters. By clicking "Model" button in configuration task bar as shown in Figure 9.13(a), "Multi Float Connectivity Analysis" simulation space will be started as shown in Figure 9.13(b). Upon starting a multi floater simulation space, we are asked to provide two files. One is a flow rate file and the other is a log file. The flow rate file should contain 288 flow rates which represent flow rate for every 5 minutes for 24 hours starting from 00:00 and ending at 23:55. The log file is

to capture the messages generated during the simulation and be used for scenario analysis. If there exists a log file with the same name, the log file will be overwritten by the new file.

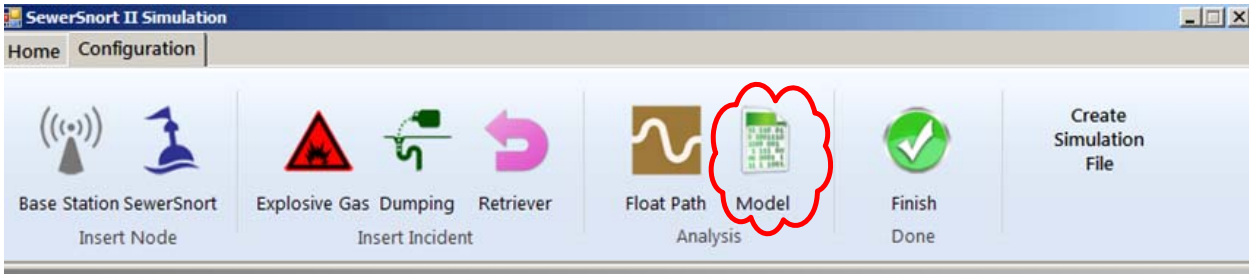

(a) Model button in configuration task bar for Multi-SewerSnorts scenario

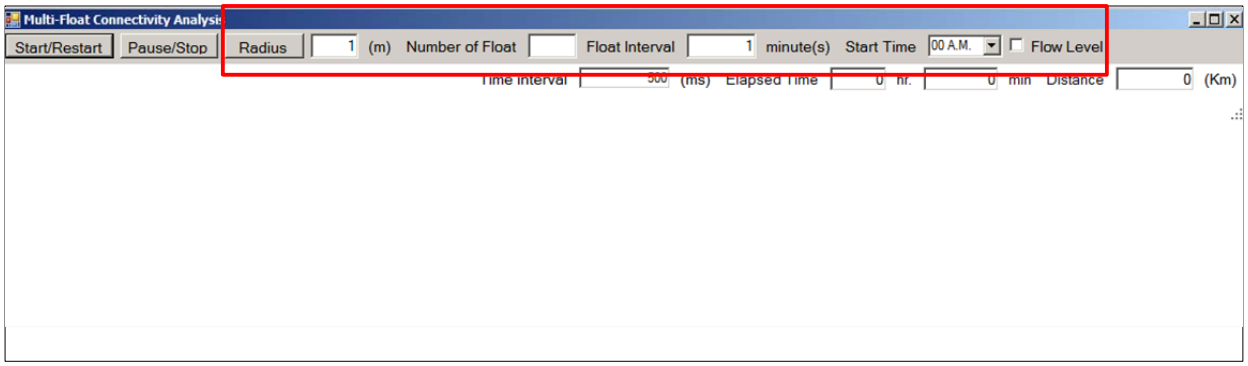

(b) Multi SewerSnorts simulation space

Figure 9.13: Multi SewerSnorts simulation (a) and (b)

Now, we need to fill in/select the following parameters:

- Radius - the radius of pipe by meter. The default radius is 1 meter.
- Number of Floats - how many floaters will be dispensed.
- Float Interval - the interval that floater is dispensed by minute(s). The default floater interval is 1 minute.
- Start Time - time of a day that floaters are dispensed. The default start time is 00:00 a.m.
- Flow Level - by selecting this option, the animation will be focused on the flow level.

- Time interval - this is for animation speed. To slow down the animation increase time interval, and vice versa. The unit is millisecond(s). The default animation time interval is 500 ms.

There are two control buttons. One is for "Start/Restart" and the other is for "Pause/Stop." The buttons are toggled. After filling out parameters without selecting "Flow Level", we will see the fructuations of flow level for 24 hours as shown in Figure 9.14(a) and 9.14(b). As the flow level increases, the flow velocity increases. Similarly, as the flow level decreases, the flow velocity decreases. The darker color represents slow stream while the lighter color represents fast stream. Also, the window is divided up by 288 vertical segments to represent the flow level of 5 minute interval.

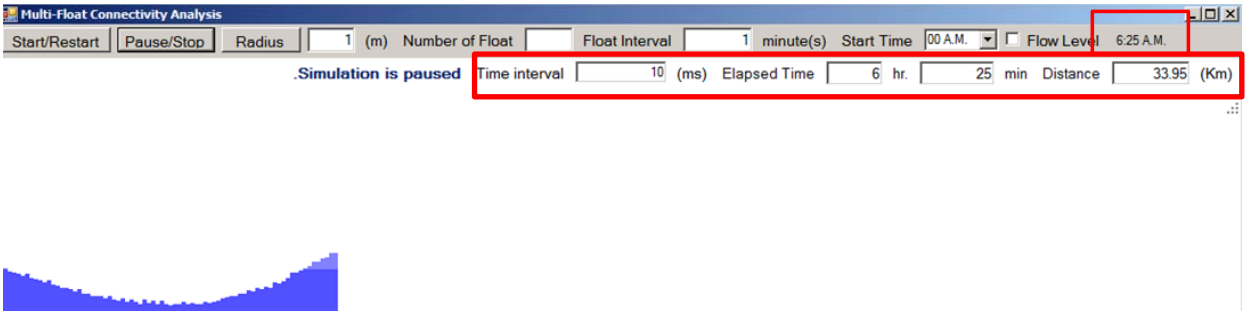

(a) Illustration of flow level

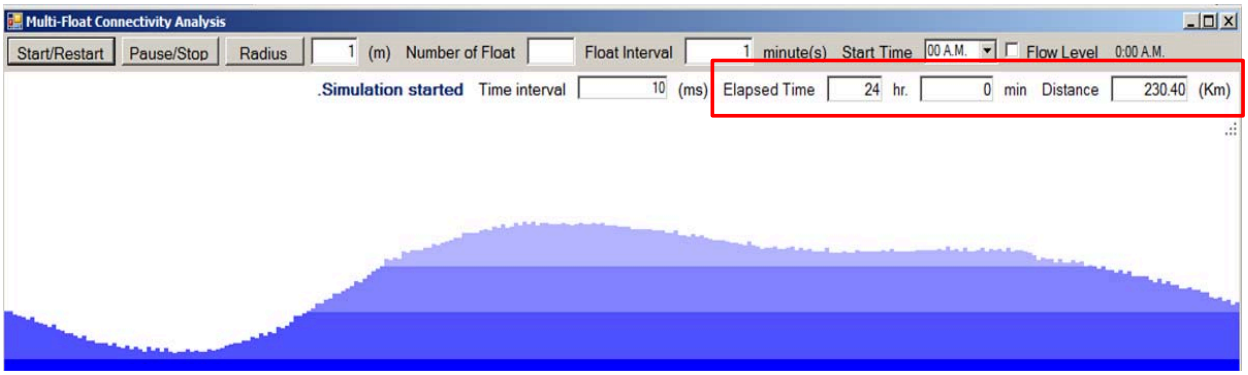

(b) Illustration of flow level for 24-hours

Figure 9.14: Example of flow level simulation (a) and (b)

As a simulation begins, the following variables are updated as illustrated in Figure 9.14(a):

- current time - the time of a day is updated and shown at the top right corner.
- Elapsed Time - the accumulated time for travel.
- Distance - the accumulated distance that floaters have been traversed.

Now, when we put a number of floats, the window is focused at the pipe segment where the floats are. The distance between floaters is determined by floater interval and simulation start time, and it is graphically shown in Figure 9.15(a) and 9.15(b).

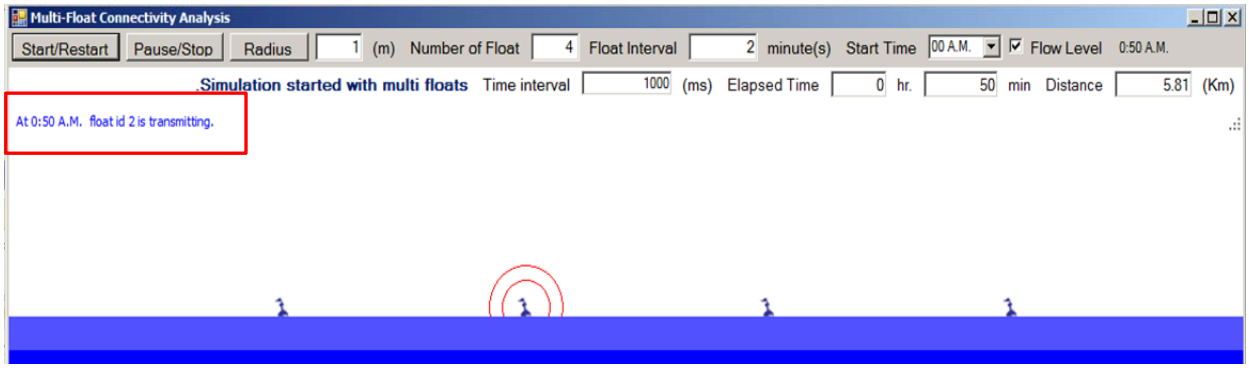

(a) Scenario with 2 minute interval starting at 00:00 a.m.

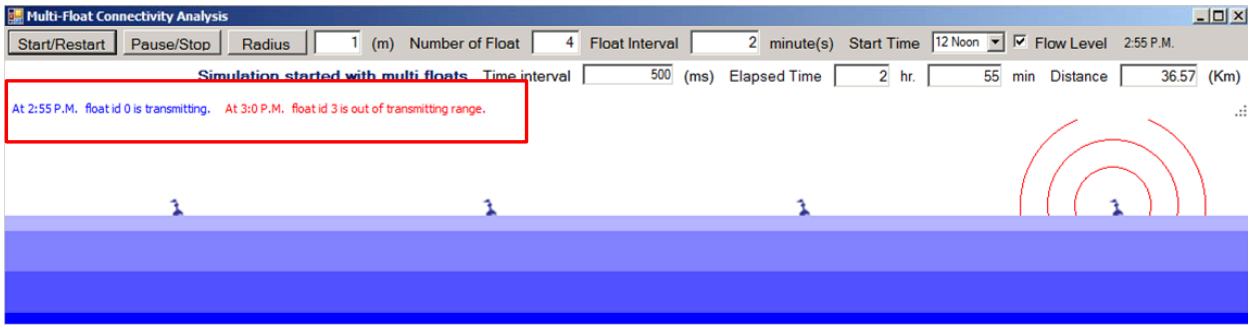

(b) Scenario with 2 minute interval starting at 12:00 noon

Figure 9.15: Examples of multi-floaters scenario (a) and (b)

When a large number of floaters is entered, the distance between floaters will be set to a minimum distance to show all floaters in the window as illustrated in Figure 9.16.

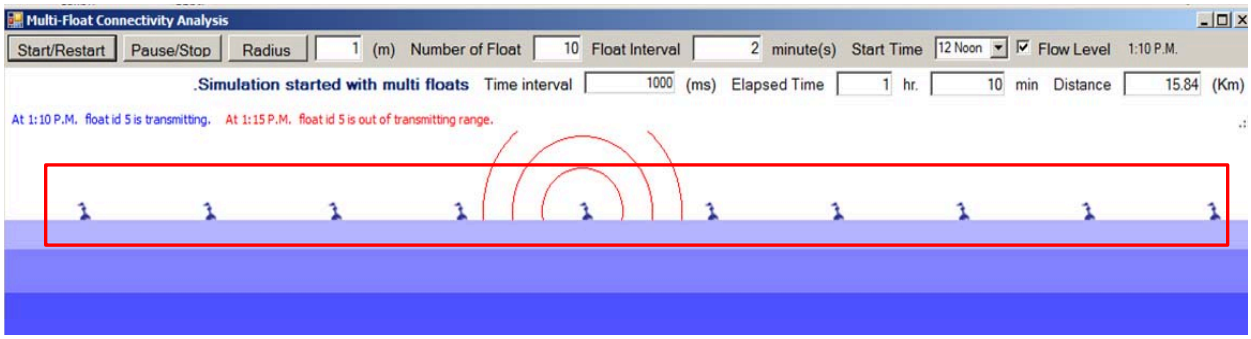

Figure 9.16: Scenario with 10 floater and 2 minute interval starting at 12:00 noon

When the floaters exchange probing messages, the system shows the floater id and the transmission time. Also, the system checks their transmission range. If the floater is out of transmission range, the system shows the communication failure message with floater id and transmission time as shown in Figure 9.15(b) and 9.16. All messages generated during the simulation are logged in the log file and can be used for further analysis.

9.1.4.2 Scenario Simulation

When we complete the scenario configuration, we generate simulation input files by clicking "Create Simulation File" button. as shown in Figure 9.17(a). It will create three files namely; road file, floater file, and static elements file such as base stations, dumping sites, or high explosive gas incidents. After creating input files, we import them into Sewernet simulator and run the simulation as show in Figure 9.17(b). There are three control buttons namely; "Start", "Pause", and "Reset." The Graphical User Interface (GUI) of SewerNet simulator provides the following functions:

- Load sewer map file
- Load floaters path
- Load different incidents inside the sewer and base station/gateway
- Display a timer for floater traversing time calculation

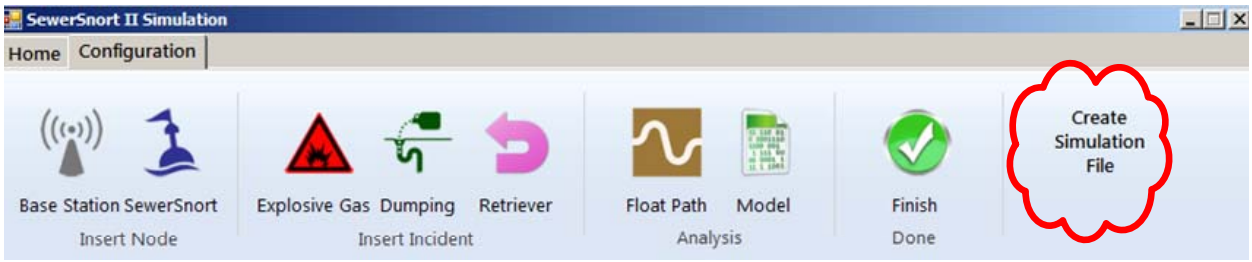

(a) Create input files for scenario simulation

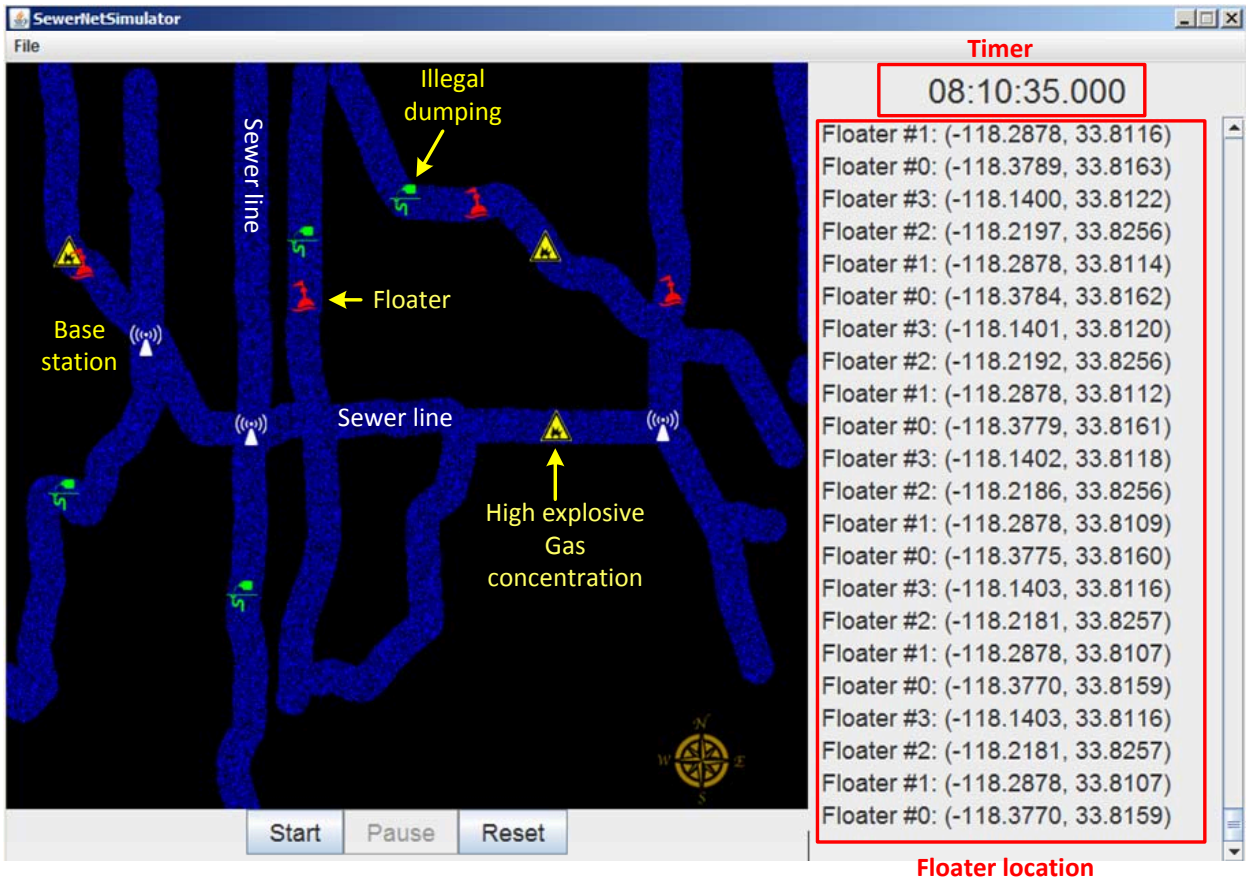

(b) Example of scenario simulation

Figure 9.17: Scenario simulation interface (a) and (b)

- Offer simulation control block (Start and Pause)
- Allow users to reset the simulator for next simulation
- Track the floater location in real-time and output the location log into files

9.2 Scenario Analysis

With the current technology, identifying some of the most pressing problems in WCS (i.e. illegal dumping, reporting emergency, estimates of greenhouse gas emission) is difficult or unfeasible. For example, illegal dumping can be detected as it occurs; however, the current technology requires a lengthy preparation to inspect the site while the problem is transient phenomena. In addition, the heavy and bulky equipment is not suitable to detect narrow pipeline. Moreover, a comprehensive inspection of WCS is prohibitively expensive using the current technology.

However, SewerSnort can address some of these issues. SewerSnort is light, small, low power, and low cost mobile sensing unit which requires only minimal preparation time for the deployment along any path of WCS. To catch the moment, a convoy of SewerSnort can be deployed with almost no time delay. In addition, SewerSnort effectively addresses the access limitation of the current technology; thus, it resolves "chimney effect" issue. Moreover, the low-cost mobile sensing unit makes comprehensive inspection of WCS feasible. In this section, we present how SewerSnort can be utilized in evaluating some of the pressing issues in WCS.

9.2.1 Monitoring illegal dumping

Illegal dumping is one of the most frequently committed environmental crimes, and yet it causes financial burden to our community. [1] Unfortunately, sewer is one of the common places where hazardous chemicals are dumped. In some cases, illegal substances are discharged persistently through an outlet attached to sewer. In other cases, illegal dumping is committed sporadically.

[1] According to the October 8, 2006 USA TODAY article "Illegal Dumps Alter Western Landscape" by Benjamin Spillman: ". . . In California alone, illegal dumping on private and public land costs at least $87 million annually, . . ."

Hence, we will consider both scenarios.

If the chemical is drained off continuously, SewerSnort may identify an illegal dumping and the dumping site as a SewerSnort traversing the area. When a SewerSnort detect a chemical with suspicious concentration, the SewerSnort can report the incident to a base station to prompt an alarm. However, if dumping occurs sporadically, they will be diffused in existing liquids as time passed by after the chemical is discharged in sewer. In such cases, we need to deploy multiple floaters. If we were to use multiple floaters, we can identify illegal dumping and estimate the dumping site as follows. For example, if the discharged chemicals were an acid liquids, the chemical will upset the pH level at the dumping site and surrounding area as illustrated in Figure 9.18. As time passed by, the chemical will be diffused with liquids in surrounding area as illustrated in

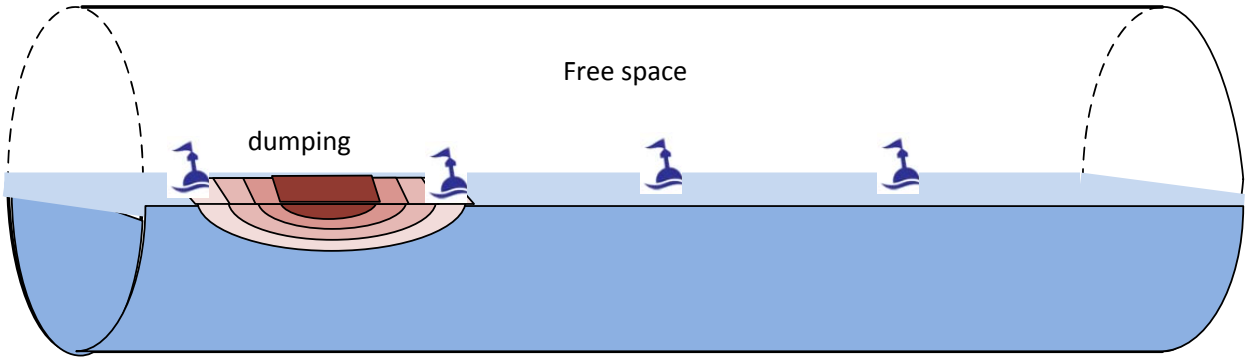

Figure 9.18: Illustration of illegal dumping

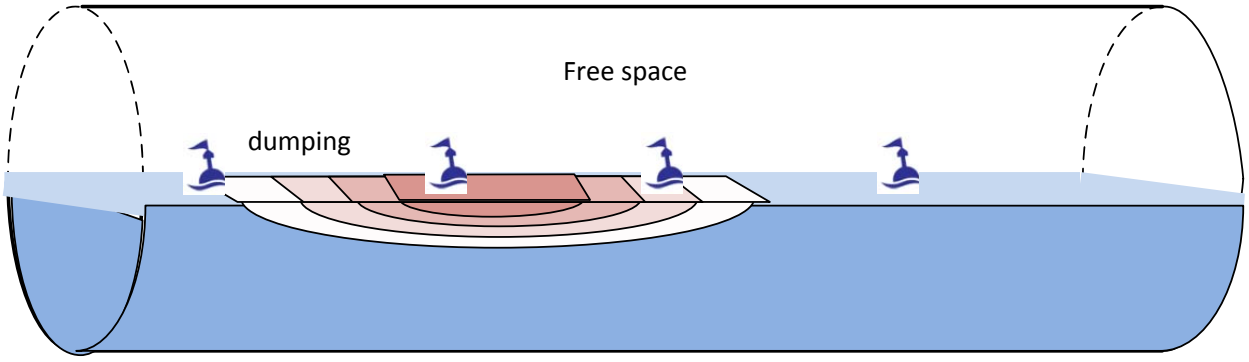

Figure 9.19: Chemical diffusion of illegal dumping

Figure 9.19 and the pH level will return to equilibrium state. Thus, by comparing the sample data and sample time among the floaters we can deduce the concentration gradient over time. Then, from the concentration gradient graph together with timestamp, we can estimate the proximity of the dumping site. For alkaline chemical dumping, pH will spike at dumping site and as they are diffused with surrounding liquids, pH level will reach to the equilibrium state eventually.

Apparently, to our best knowledge, there is no known technology of detecting illegal dumping occurring sporadically. However, a SewerSnort may allow fast and precise detection of illegal dumping; hence, prevent the contamination of our environment.

9.2.2 Greenhouse Gas emission modeling

9.2.2.1 Estimation of greenhouse gas emission

While wastewater is transported to the treatment plant or disposal site, organic materials are accumulated along the bottom of sewer. In these organic materials, various biochemical reactions occur that produce methane (CH_4) gas and carbon dioxide (CO_2) gas. These gas produced from WCS represents a considerable fraction of the Greenhouse Gases (GHG) released in the environment [20, 55].

In order to estimate the gas emission associated with WCS, a measuring plan should be established. However, measuring gas emission from WCS is very difficult. The amount of gas produced from WCS is estimated through several approaches as [19, 67, 67]

$$\begin{aligned} \text{annual emission} &= \text{annual volume of wasewater treated} \\ &\quad * \text{emission factor} \end{aligned} \tag{9.5}$$

, or

$$\begin{aligned} \text{annual emission} &= \text{annual sludge production (total ton /year)} \\ &\quad * \text{potential (g/ton)} * \text{emission factor} \end{aligned} \tag{9.6}$$

, or

$$\begin{aligned} \text{annual emission} &= \text{total population} \\ &\quad * \text{ gas emitted per person per year.} \end{aligned} \tag{9.7}$$

To improve the accuracy of estimate of the gas emission from WCS, various conceptual models have been developed and validated in laboratory [9, 36]. However, the models are based on the measurements of environmental variables, but collecting these environmental data from WCS is very difficult if not impossible with current technology.

However, we can improve the accuracy of the estimation of GHG emission from WCS using floaters. As a floater traverses downstream, it collects sample data for the gas of interest (i.e. hydrogen sulfide(H_2S), methane (CH_4), and carbon dioxide (CO_2).) The air pollutant concentrations can be expressed by either parts per million by volume (ppmv) or milligrams per cubic meter (mg/m^3). Likewise, parts per billion by volume (ppbv) or microgram per cubic meter ($\mu g/m^3$) is used as well. Thus, by measuring the concentrations of gas and the volume of the space, we can estimate the amount of gas emission. First, we divide the pipeline in equal length segment(i.e. 10

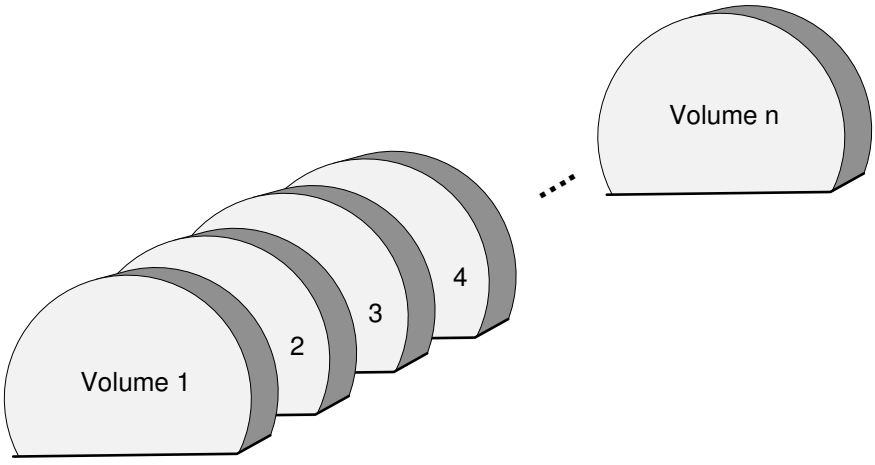

Figure 9.20: Illustration of pipe segment

meters) as illustrated in Figure 9.20. Then, we compute an average concentration from the sample data collected from floaters for each segment. Second, we compute the volume of pipe segment as

illustrated in Figure 9.21(a). Since a flow depth h can be estimated (please refer to Section 6.1.1 for flow level estimation), we calculate the volume of air space as followings:

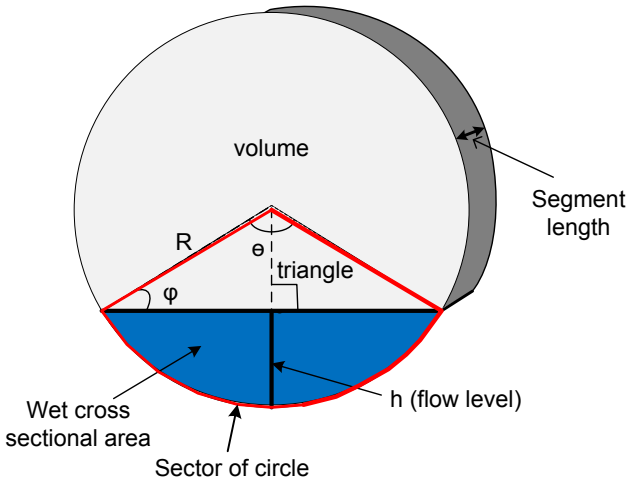

(a)

$R = radius$

$h =$ computed flow level

$\sin\theta = \frac{R-h}{R}$

$\phi = 90 - \theta$

sector of circle $= \frac{2\theta}{360}\pi R^2$

triangle $= R\cos\phi(R-h)$

wet cross sectional area $=$

sector of circle $-$ triangle

Figure 9.21: Compute the volume of pipe segment for air space

if flow level h $<$ R,

$$\text{volume} = (\pi R^2 - ((\frac{2\theta}{360}\pi R^2) - R\cos\phi(R-h))) * \text{segment length}, \tag{9.8}$$

else if flow level h = R,

$$\text{volume} = (\frac{\pi R^2}{2}) * \text{segment length}, \tag{9.9}$$

else

$$\text{volume} = ((\frac{2\theta}{360}\pi R^2) - R\cos\phi(2R-h)) * \text{segment length}. \tag{9.10}$$

Now, with the gas concentration measurements and the volume of space measurements, we can estimate the GHG emission to the sewer gas chamber as

$$\text{GHG emission to sewer gas chamber} = \sum_{i=1}^{n} m_i v_i \begin{pmatrix} m_i & \text{average gas concentration} \\ v_i & \text{segment volume} \end{pmatrix} \tag{9.11}$$

which is far more accurate than any of the previous approaches.

9.2.2.2 Monitoring sewer gas formation and release

As stated in Section 2.3.1, sewer gas formation and release are not spatially linked due to rapid transport of sewer gas in air-space. The liquid-phase composition of sewer gas occurs in the zone of debris accumulation and/or anaerobic activity, but the gas-phase of sewer gas may occur in a distant section from the gas formation zone because of rapid transport of gas in air-space mainly due to fresh air drafting in through manholes. Thus, to understand the spatial distribution of sewer gas formation and release it is crucial to acquire sample data from both liquid and air-space dynamically along the pipeline; however, to date, the areas mainly inspected are limited to manholes.

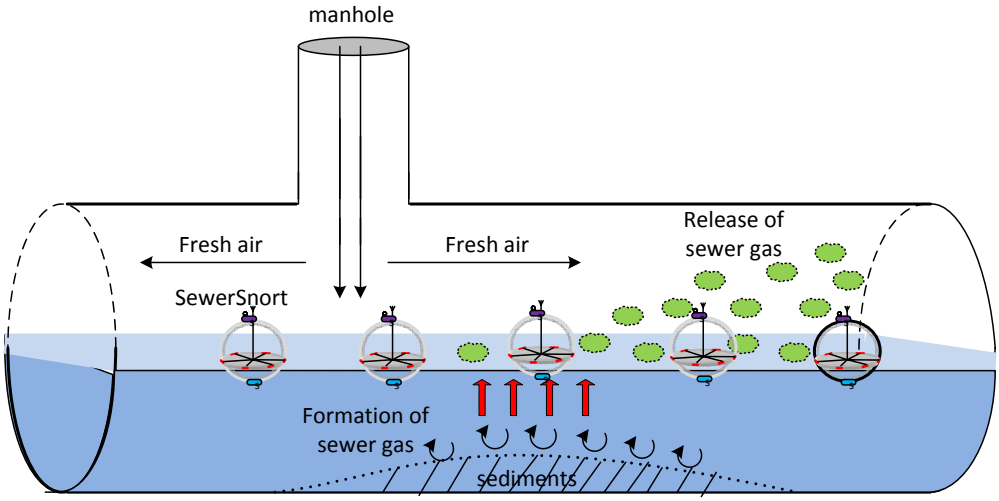

Figure 9.22: Illustration of data collection from liquid and air simultaneously

However, we can acquire the needed data to determine the section for formation and release of sewer gases in a spatially distributed sewer network using floaters. As a SewerSnort traverses downstream, it can acquire samples from both liquid and air simultaneously along the pipeline as illustrated in Figure 9.22. While SewerSnort is measuring dissolved oxygen in liquid to measure anaerobic activity, SewerSnort can measure H_2S, CH_4 in air to locate the section where they are released. Upon the completion of journey, the measurements from air space can be compared to measurements from liquid; hence, the section where sewer gases are produced can be determined. Moreover, the comprehensive dataset acquired from both liquid and air-space along the pipeline

may allow understanding the sewer internal dynamics and help determining the cause of sewer gases.

9.2.3 Preventive WCS monitoring

Up until now, monitoring WCS has been mainly focused on reactive response. However, a preventive and proactive WCS monitoring becomes feasible using floaters. SewerSnort is primarily a low power and low cost mobile sensing unit that is far less expensive and far easier to use than any current WCS inspection technology. A comprehensive inspection of WCS using SewerSnort is quite affordable, yet SewerSnort provides innovative fault detection methods with minimal efforts.

In addition, using the simulation tool, we can develop an efficient monitoring schedule. For example, a scenario can be configured such that SewerSnort traverses the entire sewer pipelines as illustrated in Figure 9.23. Then, the required resources to perform a comprehensive inspection can be estimated in terms of battery power and storage space. Thus, SewerSnort may allow preventive WCS monitoring where much of the system failures can be avoided.

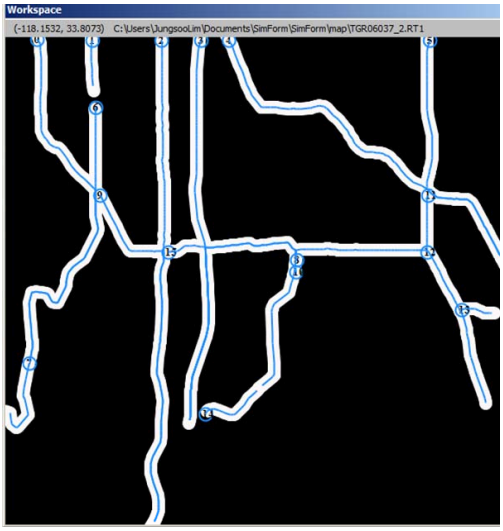

Figure 9.23: Example of preventive monitoring scenario

CHAPTER 10

Radio Propagation and Float Connectivity in the Sewer Environment

The purpose of this chapter is to investigate radio propagation in the sewer environment and determine how propagation impacts radio inter-float connectivity when multiple floats are introduced in a section of the sewer where a failure is suspected. As we mentioned earlier, the goal is to be able to get real time information about, for instance, gas formation in a section of the sewer, or about the injection of pollutants from an inlet by propagating the sensor data via the inter-float ZigBee network back to the place (say manhole) where the floats are introduced. Alternatively, the sensor data can be uploaded at any manhole along the path that is connected to the Internet.

The critical issue in maintaining connectivity along a string of floats is to make sure that they remain within communications reach while floating down the sewer. There are two main causes of disconnection: 1) the distance between two floats exceeds the safe communications threshold in case of line of sight; 2) there is a bend or corner on the path that blocks the line of sight; 3) the inter-float distance at the injection point is below threshold, however, because of flow acceleration in the sewer, the downstream float travels faster than the upstream float, thus the link exceeds the threshold limit. In this chapter, we first review the propagation properties in the sewer, which turns out to be quite an unusual and peculiar propagation medium. Then, we study the impact of bends of the pipes on connectivity. Finally, we study the problem of flow acceleration and the disconnection of the network.

10.1 Radio propagation in a sewer environment

Radio communications inside the sewer differ from terrestrial radio communications due to the constraints on signal propagation caused by the pipeline wall and the energy absorption by the liquid. The radio wave propagates inside the sewer as in a waveguide. Part of the wave's energy is absorbed by the water inside the pipeline. Radio propagation in circular waveguides has been studied by many researchers [12, 23]. However, most of the studies consider waveguides in a homogeneous propagation medium (i.e. air). In our case, the radio wave travels in water much slower than in air. The reduction of velocity at the air-water interface, a phenomena known as "refraction", causes a change in the direction of the wave and introduces a significant power loss.

To describe the radio signal propagation, two techniques have been developed: namely, ray tracing and modal analysis. The ray tracing technique traces radio waves by taking into account the system geometry information. Ray tracing is a powerful method to model the radio channel when the complete information about the environment is available. However, a relatively long, narrow pipe, with arbitrarily liquid level, may introduce multiple reflections and refractions. Taking into account all the reflected rays along the pipeline may overwhelm the tracing program capacity. In contrast, the modal analysis approach is based on theory. The analytical model allows us to characterize the radio frequency propagation in the proposed environment in an accurate and compact way. Thus, the modal analysis approach is the preferred choice for our system.

In this study, we develop an analytical model for communications inside the sewer. We account for the impact of liquid inside the pipe as well as for the waveguide effect created by the concrete walls. In addition, we account for the impact of pipe bends on radio propagation. Although an acute bend is not allowed (i.e. 90 degree or less) due to the high maintenance cost, and a minimum radius of curvature is required by authorities based on pipe length and type of materials; nevertheless, a pipe bend does occur in special circumstances for practical and economical reasons.

First, we review the characteristics of radio signal propagation in the sewer environment, and develop an analytical model based on a few reasonable assumptions leveraging previous studies.

We then use this model to compute the minimum number of floaters required to maintain the network connectivity.

10.1.1 Characteristics of radio propagation in a sewer environment

Compared to terrestrial wireless communications, radio communications inside the sewer exhibit few unique characteristics. First, the radio waveguide inside a sewer is considered to be a lossy waveguide due to the pipeline materials. Second, water inside the sewer will cause significant additional loss due the air-water interface. We review these two loss contributions in this section.

10.1.1.1 Lossy waveguide

The wall impedance is determined by the materials, the size, the shape, and the texture of the wall. The pipe material significantly affects the quality of transmissions. Since most sewers are made of concrete and concrete is categorized as a dielectric medium for radio wave propagation based on its electric parameters as shown in Table 10.1, the radio waveguide inside the sewer is considered to be a lossy waveguide when compared to lossless waveguide in optical fibers.

The medium for radio wave propagation is classified according to three electric parameters, namely: permittivity ε, permeability μ, and conductivity σ. Permittivity ε is a measure of how well the medium transmits an electric field; permeability μ is a measure of how a material responds to an applied magnetic field; and conductivity σ is a measure of free charges in the medium that will conduct electric current in the presence of an applied voltage. For example, free space (or vacuum) is categorized as a dielectric medium based on its electric parameters. Also, seawater is a better medium than freshwater for radio propagation according to their electric parameter conductivity. Thus, waveguide in sewer environment is considered to be lossy waveguide.

Table 10.1: Values of permittivity, permeability, and conductivity

Medium of Propagation	Permittivity (F/m)	Permeability (H/m)	Conductivity (S/m)
Free space(vacuum)	$\varepsilon_0 = 8.854 \times 10^{-12}$	$\mu_0 = 1.257 \times 10^{-6}$	0
Air	$1.006\varepsilon_0$	$\approx \mu_0$	≈ 0
Concrete	$5 \sim 10\varepsilon_0$	$4\pi \times 10^{-7}$	0.06
Fresh Water	$81.0\varepsilon_0$	$0.9999\mu_0$	10^{-3}
Treated Wastewater	?	?	$\approx 5 \sim 6$
Untreated Wastewater	?	?	$\approx 300 \sim 650$
Seawater	$70.0\varepsilon_0$	$0.9999\mu_0$	4

10.1.1.2 Power loss due to water

In free space, radio wave travels at the speed of light. However, when radio wave travels through water, its energy is absorbed by water. The absorbed energy causes the electrons in the medium to oscillate. As the electrons are oscillating, they generate a new electromagnetic wave with the same frequency. This new wave travels a short distance until it encounters new oscillating electrons. This process repeats continuously and effectively slows down the radio wave speed. This reduction of velocity causes refraction and/or reflection at the air-water interface as illustrated in Figure 10.1. This change of velocity introduces a significant power loss. The power loss due to the refraction

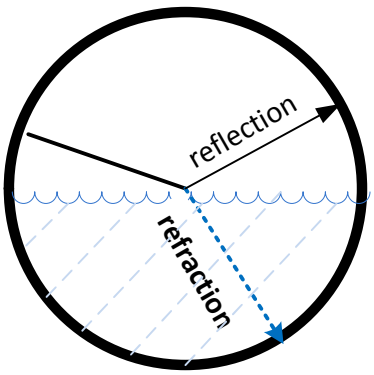

Figure 10.1: Reflection and refraction of radio wave

can be estimated in [59] as

$$RL = -20\log\left(\frac{7.4586}{10^6} \times \sqrt{\frac{f}{\sigma}}\right). \tag{10.1}$$

Some examples of the estimated power loss due to the refraction are shown in Table 10.2.

Table 10.2: Power loss due to the refraction at air-medium interface

Carrier Frequency	air-fresh water (dB)	air-seawater (dB)	air-treated wastewater (dB)
2.4 GHz	-55.00	-18.97	$\approx$ -18.01

10.1.2 Radio communication model inside sewer

When a radio wave passes through an air-water interface, the wave may be reflected inside the liquid due to the shallow water depth in the sewer as illustrated in Figure 10.2. Then, the radio

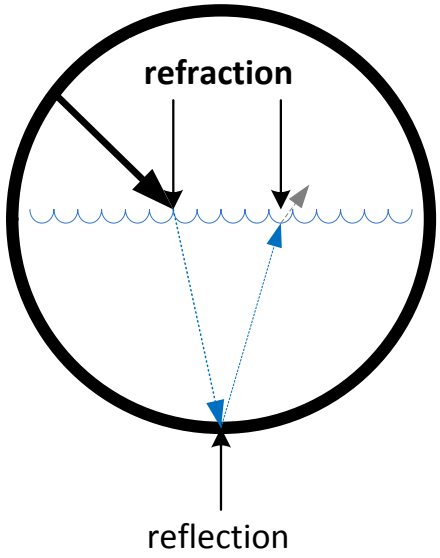

Figure 10.2: The impact of reflection and refraction of radio wave

wave will experience a water-air interface to emerge from water to air. The water-air interface will cause the same amount of power loss as the air-water interface. After passing through the air-water interface and the water-air interface, the radio signal emerging from the liquid will be significantly weakened and may quickly stop propagating at all as illustrated in Figure 10.2.

Thus, we assume that the radio wave that enters the liquid may be unable to contribute much to communication. Therefore, we account for the electric field strength in air as the sole source of energy for radio wave propagation. In addition, we assume horizontal polarization is used since the vertical polarization may lose its strength quickly due to the waveguide in the pipeline and the liquid at the bottom. Also, the lateral force may push the floaters to the pipeline wall, or the flow current may push the floaters to the center of pipeline. However, the speed of the radio wave is several orders of magnitude faster than the swaying movements of floaters. Thus, it is sufficient to account for the position of the floaters in terms of z-axis along the pipeline.

Also, although most sewer lines are made straight, curved paths are allowed for special circumstances. Hence, first we present a propagation model for a straight path. Then, we present a model for a curved path.

10.1.2.1 Propagation model for straight path

The electric field strength E composed of $E = E(air) + E(liquid)$ can be approximated as $E \approx E(air)$ since $E(air) \gg E(liquid)$. In this work, we use (ϕ, ρ) coordinate system as illustrated in Figure 10.3. Then, electromagnetic wave propagation along the pipeline (z-axial horizontal

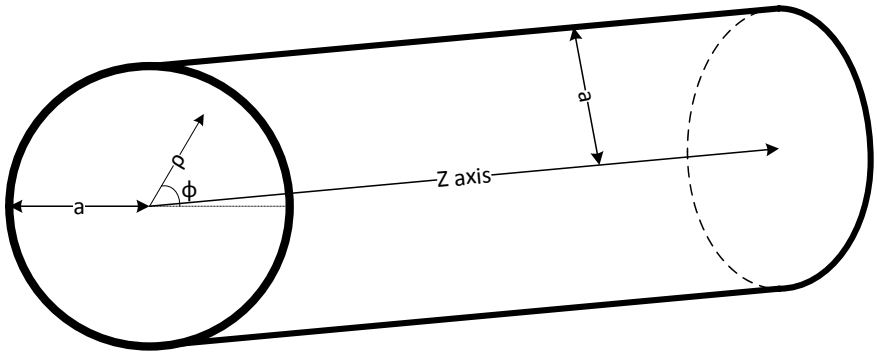

Figure 10.3: The cross section and side view

polarization) can be described by Maxwell's equations and Helmholtz's wave equations as

$$E_z(x) = \epsilon_{d_0}(\phi, \rho)e^{-\gamma x}(V/m) \tag{10.2}$$

, where $E_z(x)$ is the electric field strength at x along the z axis and $\epsilon_{d_0}(\phi, \rho)$ is the initial electric field strength, and γ represents a propagation constant which is a measure of the wave attenuation along the z axis.

Radio wave propagation model in circular cylindrical waveguide is defined in [8] as

$$\frac{\partial^2 \epsilon}{\partial \rho^2} + \frac{1}{\rho}\frac{\partial \epsilon}{\partial \rho} + \frac{1}{\rho^2}\frac{\partial^2 \epsilon}{\partial \phi^2} + \kappa_c^2 \epsilon = 0 \tag{10.3}$$

, where $\kappa_c^2 = \gamma^2 + \omega^2 \mu_0 \varepsilon_0$; $\omega = 2\pi f$; f = radio frequency; μ_0 = permeability in air; and ε_0 = permittivity in air. The solution of the above partial differential equation is approximated by Bessel function in [8] as

$$\epsilon(\phi, \rho) = J_n(\kappa_c \rho) \sin n\phi \qquad n = 0, 1, 2, \ldots \tag{10.4}$$

The propagation constant γ, also known as transmission parameter, transmission constant, or propagation coefficient, is expressed by a complex value as

$$\gamma = \alpha + \iota\beta \tag{10.5}$$

, where α (the real part) represents the attenuation constant, and β (the imaginary part) represents the phase constant. The attenuation coefficient for lossy cylindrical waveguides is defined in [8] as

$$\alpha_n = \frac{BR_c}{\eta_0 a \sqrt{1 - (\frac{f_c}{f})^2}} \tag{10.6}$$

by imposing boundary condition and radiation condition as

$$B = \left(\frac{f_c}{f}\right)^2 + \left(\frac{n^2}{(p_{nm}'^2 - n^2)}\right) \tag{10.7}$$

$$R_c = \sqrt{\frac{\mu_{\mathrm{r}} \pi f}{\sigma_{\mathrm{r}}}} \tag{10.8}$$

, where η_0 is the intrinsic wave impedance of free space (i.e. 337 Ω or 120$\pi\Omega$); a is the radius of the pipe; f_c represents a cut-off frequency; $p_{nm}^{'}$ presents m_{th} root of the n_{th}-order of modified Bessel function; μ_{r} is the permeability of concrete (i.e. $4\pi \times 10^{-7}(H/m)$); σ_{r} is the conductivity of concrete (i.e. 0.06 (S/m)), and f is the carrier frequency.

In order to propagate the radio wave inside the pipeline, a minimum frequency, known as cut-off frequency, is required and described as

$$f_c = \frac{c}{2\pi a} p_{n,m} \tag{10.9}$$

, where c is the speed of light; p_{nm} presents m_{th} root of the n_{th}-order of Bessel function; and a is the pipe radius. Some examples of cut-off frequency for various pipe sizes are shown in Table 10.3.

Table 10.3: Cut-off frequency and attenuation constant for various pipe radius

Pipe radius (m)	Cut-off Frequency (MHz) (with $p_{1,1}$)	Attenuation constant (dB/m) for 2.45 (GHz) with $p'_{0,1}$
0.8	21.88	0.8753
1.0	20.88	0.6001
1.2	19.70	0.3886
1.4	18.37	0.2267
1.6	16.90	0.1067
1.8	15.33	0.0231
2.0	13.68	0.0027

The phase constant is defined in [8] as

$$\beta_n = \frac{2\pi f}{c} \sqrt{1 - \left(\frac{f_c}{f}\right)^2} \tag{10.10}$$

, where f_c is cut-off frequency for transverse electric (TE) mode n and c is the speed of light.

The impact of liquid on the radio communications is proportional to the flow level. Fundamentally, more liquid inside pipe is translated to less air passages and reduced electric strength due to the power loss from the air-water and the water-air interface. The air space of the cross section S_0 and S as illustrated in Figure 10.4 can be measured as

$$S_0 = \pi a^2 \tag{10.11}$$

$$S = \pi a^2 - \left(\frac{1}{2}a^2\theta - a\cos\left(\frac{\pi}{2} - \frac{\theta}{2}\right)(a-h)\right) \tag{10.12}$$

, where a = radius of pipe and h = flow level as illustrated in Figure 10.4.

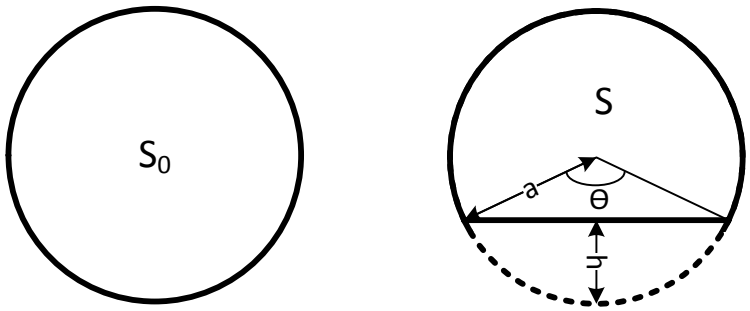

Figure 10.4: The cross section S_0 and S

In our analysis model, we assume only the radio waves in air space propagate to the receiver. Thus, the total electric field strength at distance d along the z axis for a straight pipeline with radius a and flow depth h can be estimated as

$$f_z(a,h,\theta,d) = 2\int_0^a \int_0^\pi J_1(\kappa_c\rho)\sin\phi\exp(-\gamma d(S_0/S))d\phi d\rho \tag{10.13}$$

with the first order Bessel function. Figure 10.5 presents the received signal strength (dB) at distance d (m) for 0.8 m radius pipe and 1.4 m radius pipe without liquid in pipe. The Figure 10.5 shows higher attenuation rate of signal strength in 0.8 m radius pipe than in 1.4 m radius pipe.

Also, the Figure 10.6 presents the received signal strength (dB) at distance d (m) for 1.4m radius pipe with flow level; zero, one-quarter, one-half, and three-quarter. The Figure 10.6 shows that the attenuation rate increases as the flow level increases.

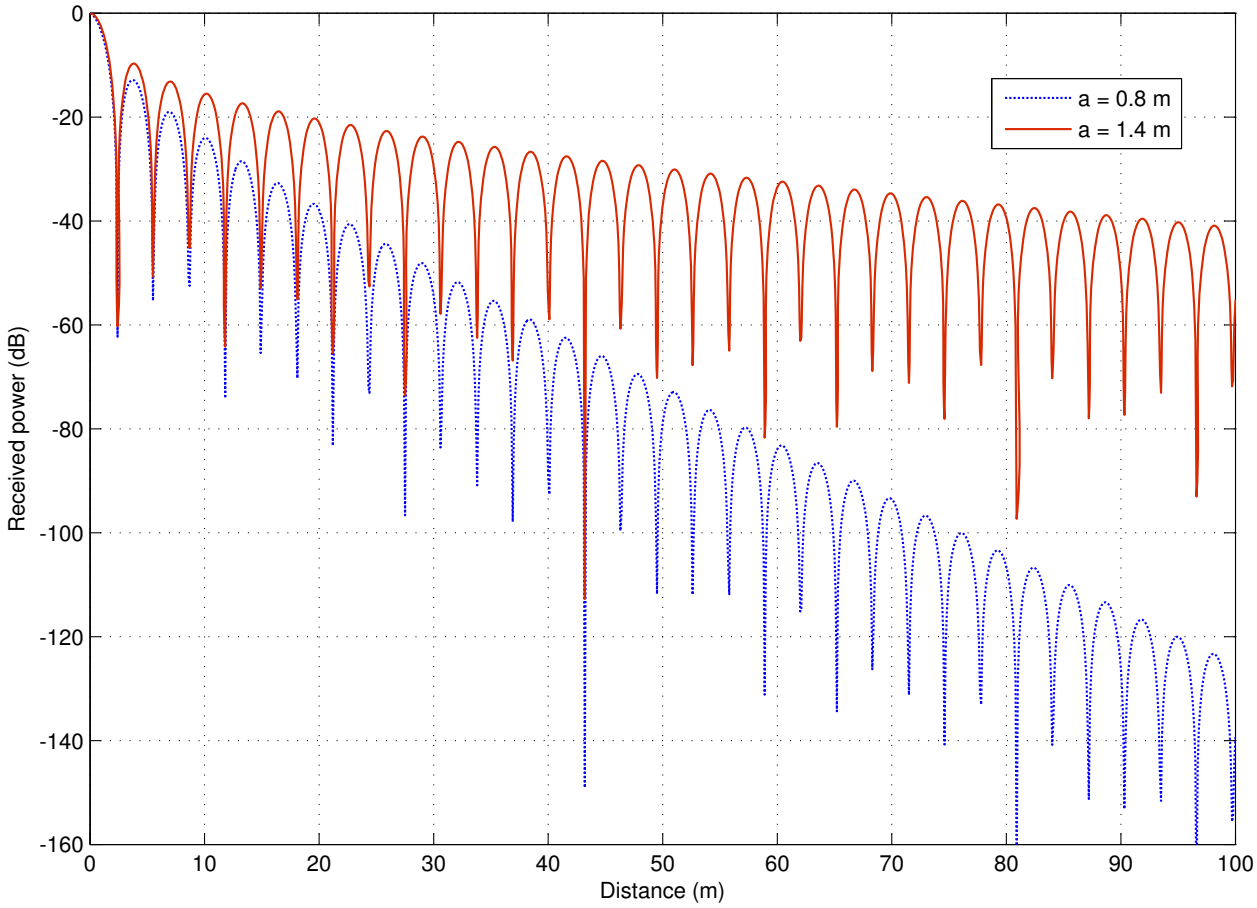

Figure 10.5: Received signal strength vs. distance with normalized amplitude of electric field with 2.45 GHz frequency for 0.8 m and 1.4 m radius pipe

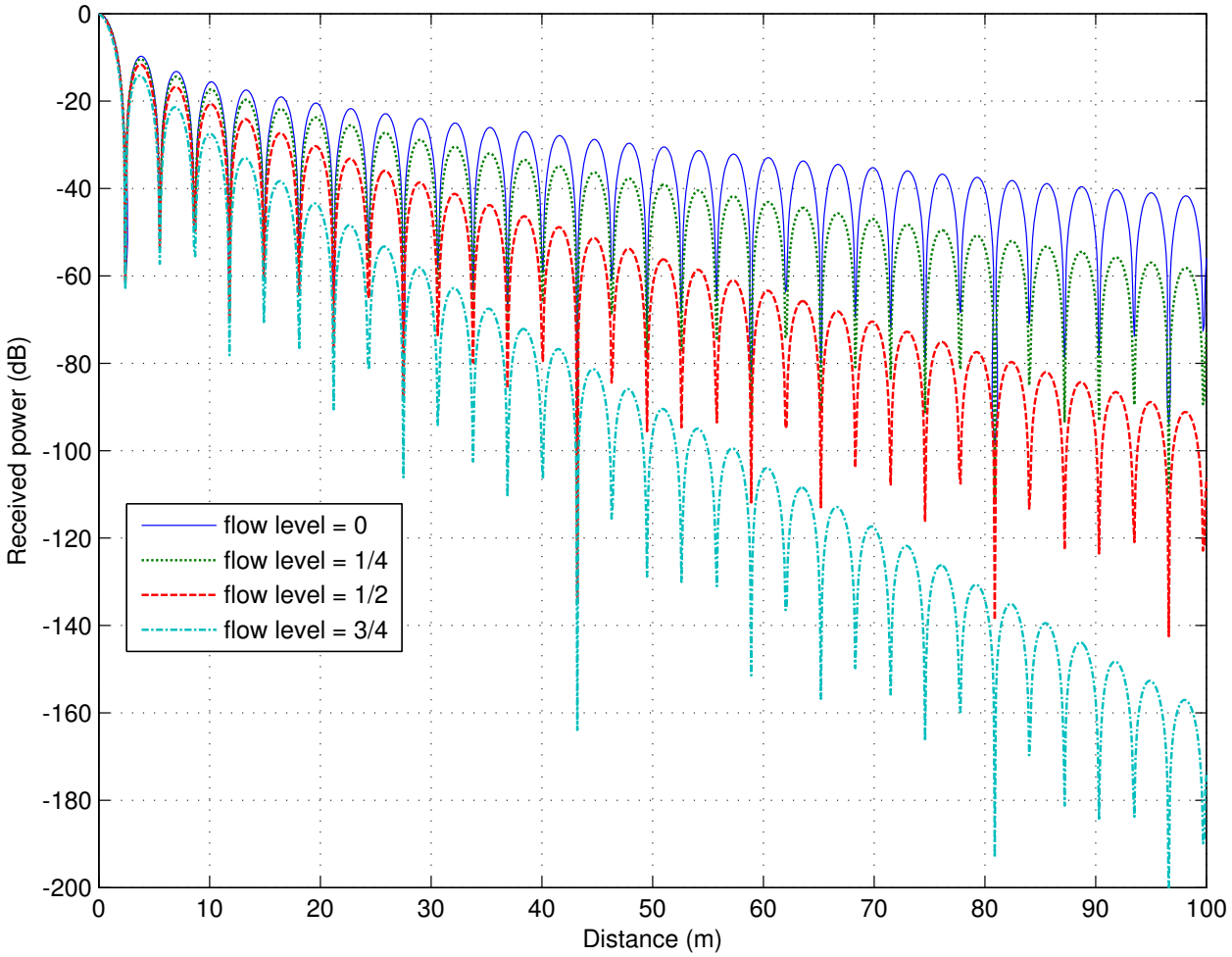

Figure 10.6: Received signal strength vs. distance with normalized amplitude of electric field with 2.45 GHz frequency and 1.4 m radius for flow level = 0, 1/4, 1/2, and 3/4

10.1.2.2 Propagation model for curved path

Although a bend of cement sewer pipe is not a smooth curve, the curvature of the bend is large enough to minimize the impact on flow. Thus, we draw a smooth curve along the bend such that the line is differentiable as illustrated at Figure 10.7. Then, R is a radius of curvature k at point P as illustrated in Figure 10.8.

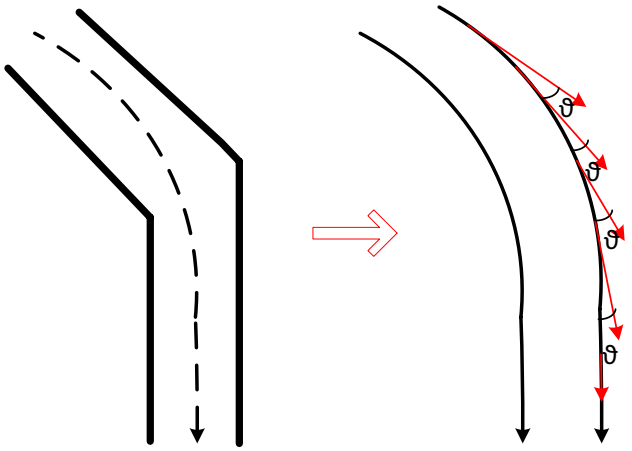

Figure 10.7: Illustration of bend at sewer

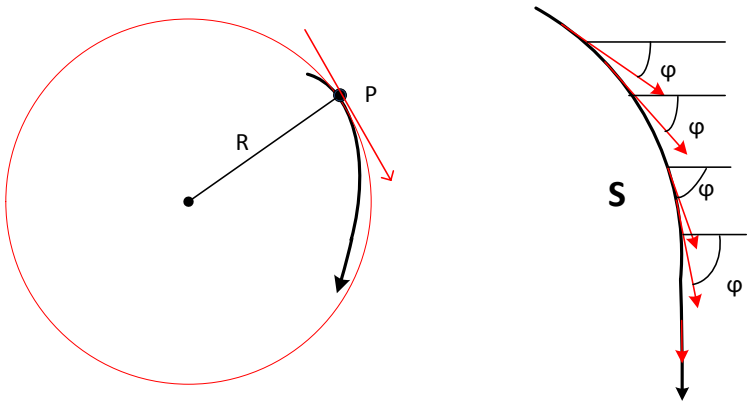

Figure 10.8: Illustration of radius of curvature

$$R = \frac{1}{k}, \qquad k = \left|\frac{d\varphi}{ds}\right|, \qquad k > 0 \tag{10.14}$$

Then, radio wave propagation along the curved pipeline can be described as

$$E_z(s) = w(\phi, \rho, \vartheta)e^{-\gamma s} \tag{10.15}$$

, where ϑ is a radian formed by tangent vector along the curve of pipeline as illustrated in Figure 10.7.

Let $x = \rho\cos\phi,$ and $y = \rho\sin\phi$. Then, the radio wave propagation model in curved rectangle tunnel is defined in [52] as

$$\frac{\partial^2 w}{\partial z^2} + \frac{\partial^2 w}{\partial y^2} - 2\kappa\left(\frac{\partial w}{\partial x} + \kappa\frac{y\cos\vartheta(x) + z\sin\vartheta(x)}{\rho(x)}\right) = 0 \tag{10.16}$$

, where κ is a wave number $2\pi/\lambda$. In [52], the solution of the partial differential equation 10.16 is approximated as

$$w(\phi, \rho, \vartheta) = \Psi(\rho\sin\phi)\Xi(\rho\cos\phi) \tag{10.17}$$

where:

$$\Psi(\rho\sin\phi) = C_1 Ai(q) + C_2 Bi(q) \tag{10.18}$$

$$\Xi(\rho\cos\phi) = D_1 Ai(p) + D_2 Bi(p) \tag{10.19}$$

, and

$$q = \left(\frac{2\kappa^2\cos\vartheta}{R}\right)^{\frac{1}{3}}(\rho\sin\phi) \tag{10.20}$$

$$p = \left(\frac{2\kappa^2\sin\vartheta}{R}\right)^{\frac{1}{3}}(\rho\cos\phi) \tag{10.21}$$

, $Ai(q)$, $Bi(q)$, $Ai(p)$, and $Bi(p)$ are Airy functions as defined in [1]; C_1, C_2, D_1, D_2, are arbitrary constants; and R is a radius of curvature.

Thus, the total electric field strength at distance s along the z axis for curved pipeline with radius a, flow depth h, can be estimated as

$$f_z(a, h, \theta, \vartheta, s) = 2\int_0^a \int_0^\pi \Psi(\rho\sin\phi)\Xi(\rho\cos\phi)\exp(-\gamma s S_0/S)d\phi d\rho \tag{10.22}$$

For example, with curvature k = 0.01 or R = 100 m the signal strength decays very rapidly as shown in the Figure 10.9.

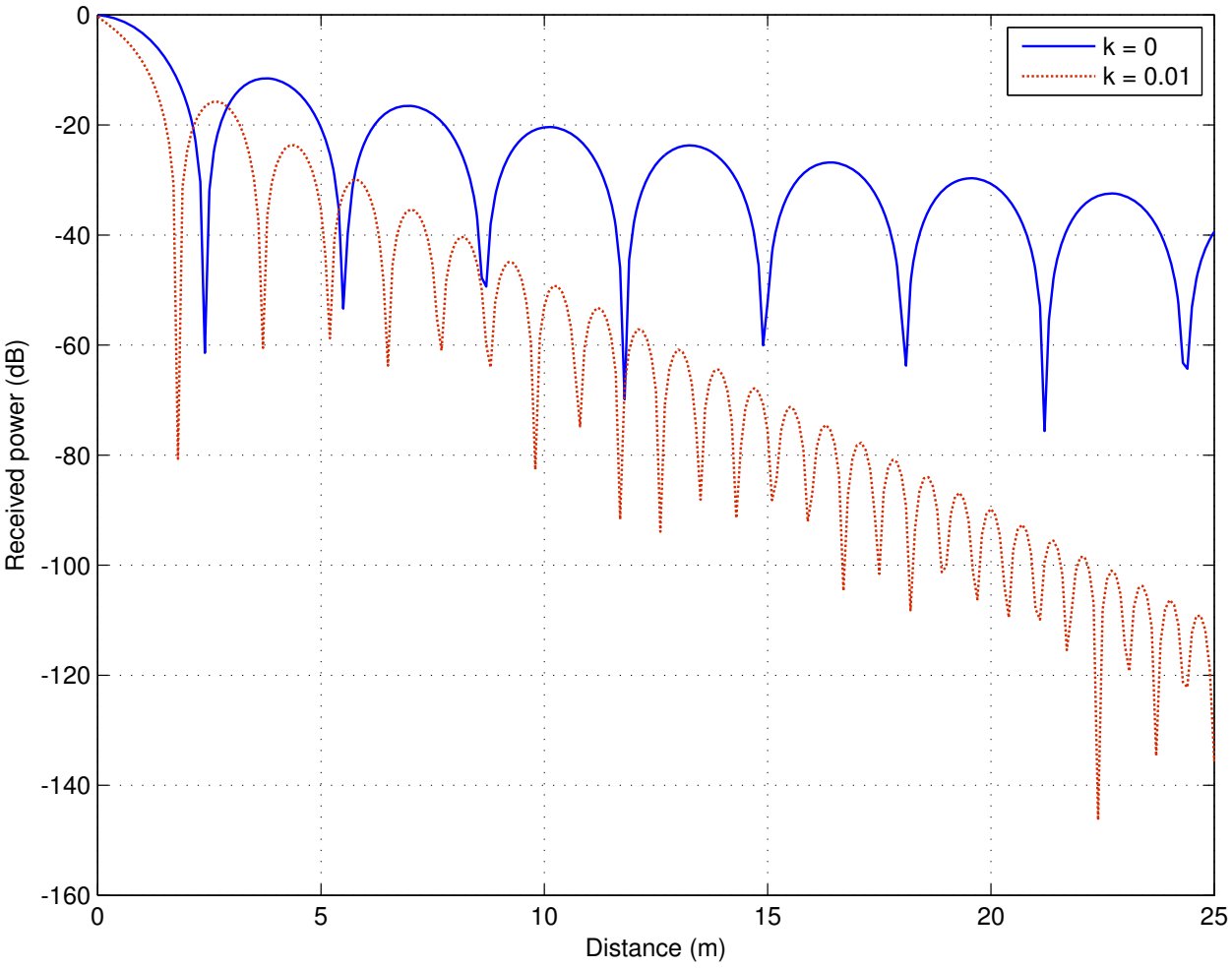

Figure 10.9: RSSI vs. distance with normalized amplitude of electric field with 2.45 GHz frequency for straight path and curved path: curvature k = 0 and k = 0.01(or R = 100 m), radius = 1.4 m, and $C_1 = C_2 = D_1 = D_2 = 1$

10.2 Maintaining network connectivity with flow accelerations

The communications range between floaters differs depending on the pipe radius, the wet cross sectional area, and the degree of curvature if the pipe is bent. For example, the communication range on a straight path is longer than the communication range on a curved path. Also, as the dry cross sectional area increases, the attenuation rate decreases. As illustrated in Figure 10.10, two floats may able to communicate along the straight path while they are apart by d_1 m. However, when they travel through the curved path, the communication range may be shortened (i.e. $d_1 > d_2 + d_3$ as illustrated in Figure 10.10). Thus, in order to maintain the network connectivity among

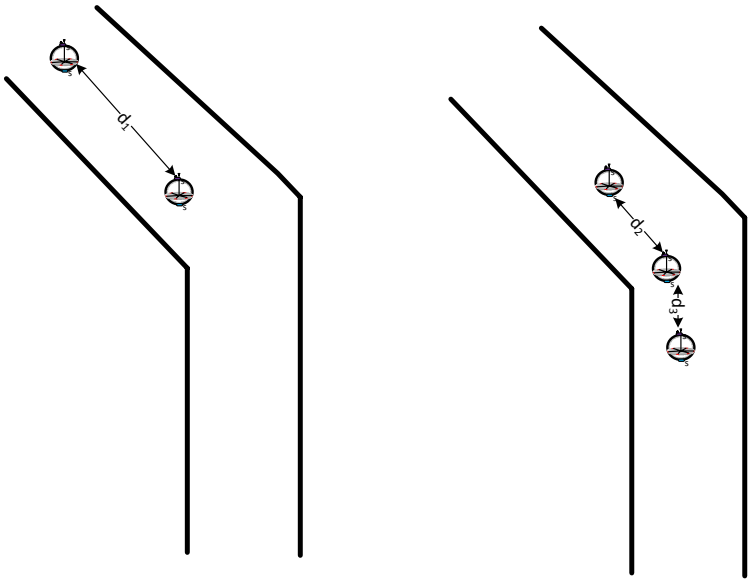

Figure 10.10: Illustration of communication range at straight path and curve

floaters during the journey, we estimate the needed number of floaters based on the analytical models developed in Section 10.1.2.

Assume that the floats are introduced in the sewer from a manhole and the point of interest (say, illegal dumping site) is L meters downstream. The flow velocity profile in the sewer can change as the floats navigate downstream. We want to find out at what intervals should we inject the floats so that we can get a continuous signal from the dumping site to our observation point. If L = length

of floaters' caravan L to the interest point, we can write:

$$\frac{dL}{dt} = V \tag{10.23}$$

, where V is flow velocity and dL is the incremental advancement of the float. From the Section 9.1.1, the flow velocity at open channel flow can be estimated as

$$V = (Q_{mass}(m^3/t))/A_{\text{wet cross sectional area}}(m^2). \tag{10.24}$$

Hence, the length of floaters' caravan L can be estimated as

$$L = \int \frac{Q}{A} dt = \sum_{i=1}^{n} \frac{Q_i}{A_i} t_i \tag{10.25}$$

, where Q_i = mass of water, A_i = wet cross sectional area, and t_i = time period. Now, the network connectivity for the total length of caravan L should be maintained, where L can be described as

$$L = L_1 + L_2 + \cdots + L_n = \sum_{i=1}^{n} L_i \quad \text{where } L_i = \frac{Q_i}{A_i} t_i. \tag{10.26}$$

Then, to maintain the network connectivity for the entire length L, $L_i \leq n_i \times r_i$, where n_i = the number of floaters and r_i = communication range. The communication range r_i can be found from equation 10.13 and equation 10.22 for L_i based on pipe radius, flow level, and curvature if pipe is curved. After computing r_i for each L_i, we can find the minimum communication range r_{min}. Then, the needed number of floaters N to maintain the network connectivity of the caravan during the entire journey can be found as

$$N = \left\lceil \frac{L}{r_{min}} \right\rceil. \tag{10.27}$$

First, we define U and W as

$$U = \int_0^a \int_0^\pi J_1(\kappa_c \rho) \sin\phi d\phi d\rho \tag{10.28}$$

$$W = \int_0^a \int_0^\pi \Psi(\rho \sin\phi) \Xi(\rho \cos\phi) d\phi d\rho \tag{10.29}$$

Second, we rewrite the equation 10.13 and equation 10.22 in terms of the estimated received power by a log scale model as,

$$P_z(a, h, \theta, d)(dB) = 10 * \log(2|U| \exp(-\gamma d(S_0/S)) \tag{10.30}$$

$$P_z(a, h, \theta, \vartheta, s)(dB) = 10 * log(2|W| \exp(-\gamma s(S_0/S)) \tag{10.31}$$

To transmit the data, the received signal strength should be greater than or equal to the threshold. Thus, we let $P_z \geq$ threshold and rewrite the equation in terms of communication range r as

$$r = \frac{10 \log U - P_z + 3}{4.34\gamma S_0/S} \quad \text{, for straight path} \tag{10.32}$$

$$r = \frac{10 \log W - P_z + 3}{4.34\gamma S_0/S} \quad \text{, for curved path.} \tag{10.33}$$

For example, if the caravan of floaters is 100 meter and it passes through the bent path with curvature = 0.01 with radius = 1.4 meter and the straight paths with radius = 1.4 meter as illustrated in the Figure 10.11, the communication range is approximately 22.84 meters for the straight path and 7.95 meters for the bent path if the threshold $\geq$ -55dB. Then, 13 floaters are required to maintain the network connectivity during the entire journey.

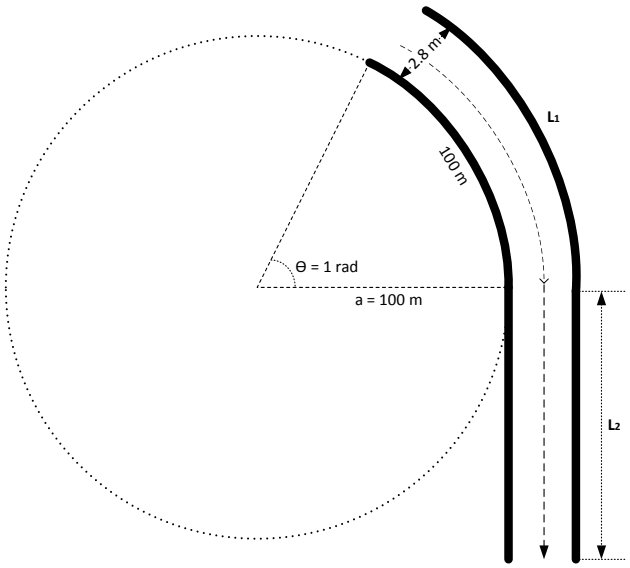

Figure 10.11: Illustration of communication ranges for various scenarios

To derive the min inter-float distance to a particular sewer section, one can use the above approach and extract from the database the parameters that characterize that specific section of pipe. If the parameters are not available, they can be measured at the beginning of the experiment (for brevity, we omit the description of the pipe mapping and calibration procedure). Another, more conservative approach is to estimate the worst possible line of sight loss, the worst pipe bend contribution to loss and the worst possible separation of the floats due to uneven flow speeds. Entering these worst case values in the above formula will provide a very conservative interval for float injection.

10.2.1 Intermediate repeaters

Unlike the curved path, for every sewer pipe-joint a manhole is required . Thus, we can deploy a repeater at pipe-joint under the manhole cover to assist the communication between the floaters while they are passing through the joints as illustrated in the Figure 10.12 and 10.13.

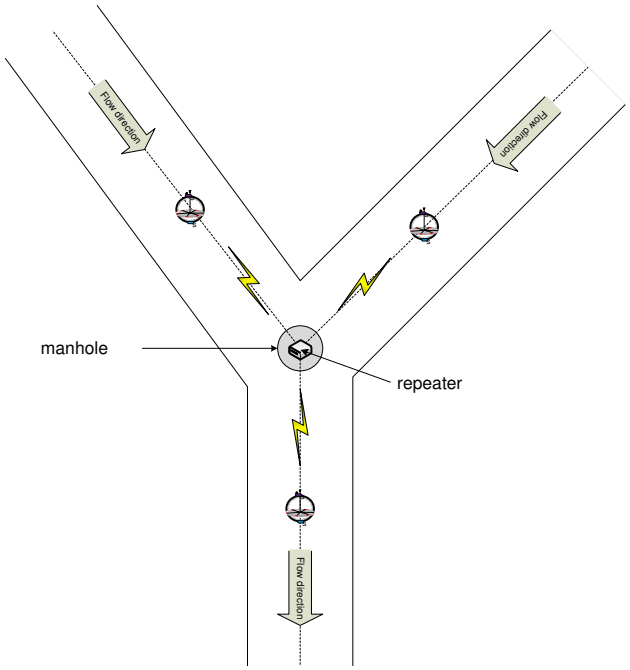

Figure 10.12: Example of Y-Junction

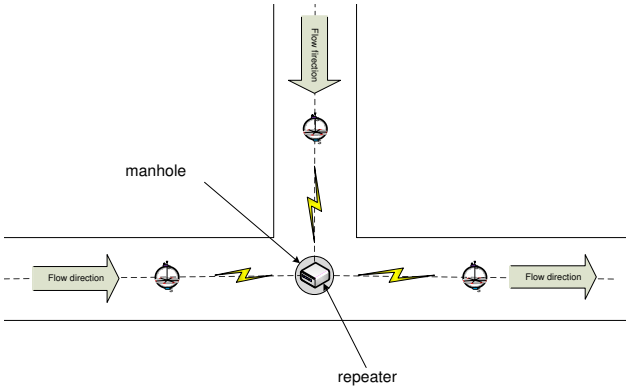

Figure 10.13: Example of T-Junction

10.3 Conclusions

We proposed an analytical model to estimate the received signal strength inside the sewer by accounting for its unique characteristics. The waveguide in the sewer is a lossy waveguide since most sewers are made of concrete and concrete is categorized as dielectric medium for radio wave propagation purposes. Also, the water inside the sewer absorbs most of the electric energy of the radio waves that are propagated into the water. In addition, pipe bends introduce rapid radio signal decays. Although most sewers are straight pipes, pipe bends are allowed in special circumstances. Thus, according to our analytical model the radio channel qualities are summarized based on pipe size, flow level, and pipe bend under various conditions as follows:

- **Pipe size:** Pipe size is inversely proportional to channel attenuation rate. As pipe size increases, the attenuation rate of radio signal decreases. Although, the attenuation rate increases rapidly, the radio wave propagation will not suffer from the cut-off frequency requirement to propagate the signal. The carrier frequency to be used on the floaters is mainly 2.4 GHz ISM band, and it is far higher than the cut-off frequency even for the smallest size of sewer pipe.

- **Flow level:** The impact of water inside sewer on radio channel quality is inversely proportional. The radio waves that are propagated into water are mostly absorbed by water. Thus,

as the flow level is increased, the communication range is decreased.

- **Pipe bend:** The pipe bends significantly impact the quality of radio channel. As the curvature increases, the signal strength decays very rapidly. However, the bends are smooth enough to minimize the impact on sewer flow in most circumstances. In the T-junctions or Y-junctions of sewer, a manhole is required to be installed. Thus, a repeater can be deployed under manhole cover to assist the network connectivity while the caravan passes through the junctions.

CHAPTER 11

Conclusion

In this work, we presented the first wireless mobile sensing system to monitor a wastewater collection system (WCS) based on a mobile floating sensing unit platform, SewerSnort. First, we reviewed the unique challenges associated with wastewater collection system environment. Second, we discussed the system design requirements by reviewing the issues and the limitations of current technologies. Third, we evaluated the feasibility of a mobile drifting sensor by analyzing the sewer flow statistics and presented the potential applications for discovery of emergencies and detection of functional deficiencies. Then, we designed a self-righting ball shaped hull that can handle the lateral force and can collect liquid samples as well as air samples; we proposed a GPS-free Received Signal Strength Indicator (RSSI) based localization scheme with enhancement of location estimation assisted by flow velocity for SewerSnort; we analyzed all required resources in terms of storage spaces and energy; we performed optimization of system to minimize the resource usages such as storage space for collected data and battery life by aggressively compressing data, adaptively adjusting sampling frequencies, and maximizing sleep time of beacon node; we designed the emergency notification system to deliver the urgent messages; we discussed how to locate lost floaters through base station or a convoy of floaters; we developed a decision tree to determine function deficiencies including sewer leaks, blockages, inflows, and possible explosions; and we developed an analytical radio propagation model inside sewer environment to assist maintaining the network connectivity among the floaters during their journey.

Additionally, we developed a simulation tool to assist a field deployment. The sewer network has unique properties such as having tree-like structure, operating on open channel flow, and having flow level that is cycling through 24 hours which is affected by human lifestyle. We have

incorporated these properties in designing the simulation tools. With the simulation tool, we can evaluate and test various scenarios to assist the field deployment. Thus, we can optimize the number of beacons and mobile sensors needed before the field deployment. Also, we analyzed various scenarios including monitoring illegal dumping, estimating greenhouse gas (GHG) emission, and scheduling preventive WCS monitoring to demonstrate the usages of the system. The proposed system provides us with an efficient method of monitoring GHG emission from WCS. Thus, GHG release can be minimized by evaluating and harnessing sewer gas release.

Experiments based on a dry land robotic emulator have demonstrated the feasibility of the system, with extremely accurate gas readings aboard the float and adequate location estimates (errors within 5% over hundreds of meters). The experiments and simulation results are encouraging and will stimulate further research in the field.

In the future, we will analyze communication patterns/requirements and develop an efficient networking protocol for mobile floating sensor networks to maximize network connectivity and coverage. Also, we will develop a more realistic mobility model for floater in sewer pipes, which will allow us better understanding of sensor coverage and networking protocol performance (e.g., network connectivity and packet delivery ratio), when a convoy of sensors is deployed. Finally, we will study how to incorporate dead-reckoning using accelerometer and gyroscope in order to reduce the needed number of beacons while maintaining the accuracy of the proposed localization scheme.

REFERENCES

[1] M. Abramowitz and I. Stegun. *Handbook of Mathematical Functions,*. Dover Publication, 1970.

[2] A. Ahrary, L. Tian, S. ichiro Kamata, and M. Ishikawa. Navigation of an Autonomous Sewer Inspection Robot Based on Stereo Camera Images and Laser Scanner Data. *Int'l Journal on Artificial Intelligence Tools*, 16(5):611–625, Aug. 2008.

[3] I. Akyildiz, Z. Sun, and M. Vuran. Signal propagation techniques fo wireless underground communication networks. *Physical Communication (Elsevier)*, 2:167–183, March 2009.

[4] American Society of Civil Engineers estimates the national investment was approximately 1.8 trillion in 1996.

[5] P. Bahl and V. Padmanabhan. RADAR: An In-Building RF-based User Location and Tracking System. In *INFOCOM'00*, Tel-Aviv, Israel, Mar. 2000.

[6] S. Chatterjee, A. Hadi, and B. Price. *Simple Linear Regression 3rd Ed. Ch. 2 in Regression Analysis by Example*. Wiley, 2000.

[7] P. Churchill and D. Elmer. Hydrogen Sulfide Odor Control in Wastewater Collection Systems. *NEWEA Journal*, 33(1):57, May 1999.

[8] R. E. Collin. *Field Theory of Guided Wave*. IEEE Press, second edition edition, 1991.

[9] R. Corsi, D. Chang, and E. Schroeder. A modeling approach for voc emission from sewers. *Water Environment Research*, 64(5):734–741, Jul. - Aug. 1992.

[10] H. Dizer and U. Hagendorf. Microbial contamination as an indicator of sewer leakage. *Water Research*, 25(7):791, 1991.

[11] L. Doherty, K. Pister, and L. Ghaoui. Convex position estimation in wireless sensor networks. In *IEEE INFOCOM'01*, volume 3, page 1655.

[12] D. G. Dudley and H. Y. Pao. Wireless propagation in circular tunnels. *IEEE Trans. Antennas Propagation*, 53(8):2400, August 2005.

[13] S. Edwini-Bonsu and P. Steffler. Air Flow in sanitary sewer conduits due to wastewater drag: a computational fluid dynamics approach. *Journal of Environmental Engineering and Science*, 3:331, 2004.

[14] A. Emslie, R. Lagace, and P.Strong. Teory of the propagation of uhf radio waves in coal mine tunnels. *IEEE Transactions on Antenna and Propagation*, 2(AP-23):192–205, 1975.

[15] C.-Y. Fan, R. Field, and F. hsiung Lai. Sewer-Sediment Control: Overview of an EPA Wet-Weather Flow Research Program. Technical Report EPA-600-J-03-188, US-EPA, National Risk Management Laboratory, Water Supply and Water Resource Division, Urban Watershed Management Branch, Edison, NJ, USA, 2006.

[16] M. W. Fincham. Big Boats, Narrow Channels. *Chesapeake Quarterly Online*, 4(2), Dec. 2005.

[17] D. Fox, W. Burgard, F. Dellaert, and S. Thrun. Monte Carlo Localization: Efficient Position Estimation for Mobile Robots. In *National Conference on Artificial Intelligence*, Orlando, FL, July 1999.

[18] D. Fox, W. Burgard, and S. Thrun. Markov Localization for Mobile Robots in Dynamic Environments. *Journal of Artificial Intelligence Research*, July.

[19] IPCC/OECD/IEA Good Practice Guidance and Uncertainty Management in National Greenhouse Gas Inventories. `http://http://www.ipcc-nggip.iges.or.jp/public/gp/bgp/5_2_CH4_N2O_Waste_Water.pdf`.

[20] A. Guisasola, D. de Haas, J. Keller, and Z. Yuan. Methane Formation in Sewer Systems. *Water Research*, 42(6-7):1421–1430, Oct. 2008.

[21] A. Guisasolaa, K. R. Sharmaa, J. Kellera, and Z. Yuana. Development of a model for assessing methane formation in rising main sewers. *Water Research*, 43, 2009.

[22] M. Hayashi. Temperature-Electrical Conductivity Relation of Water for Environmental Monitoring and Geophysical Data Inversion. *Journal of Environmental Monitoring and Assessment*, 96:119, August 2004.

[23] C. L. Holloway, D. A. Hill, A. Dalke, and G. A. Hufford. Radio wave propagation characteristics in lossy circular waveguides such as tunnels, mine shafts, and boreholes. *IEEE Trans. Antennas Propagation*, 48(9):1354, September 2000.

[24] D. J. Howes. *Improving Acoustic Doppler Velocity Meter Accuracy for Open Channel Discharge Measurement*. PhD thesis, Civil Engineering Department, University of California, Irvine, May 2010.

[25] I. Howitt, J. Khan, and S. Khan. Lumped Parameter Radio Wave Propagation Model for Storm Drain Pipe. In *Proceedings of First International Conference on Computer, Control and Communications*, Karachi, Pakistan, Nov 2007.

[26] N. E. Huang, Z. Shen, S. R. Long, M. C. Wu, H. H. Shih, Q. Zheng, N.-C. Yen, C. C. Tung, and H. H. Liu. The Empirical Mode Decomposition and the Hilbert Spectrum for Nonlinear and Non-stationary Time Series Analysis. *Royal Society of London Proceedings Series A*, 454(1971):903, 1998.

[27] T. Hvitved-Jacobsen. *Sewer Processes: Microbial and Chemical Process Engineering of Sewer Networks*. CRC, 2001.

[28] E. P. Ian F. Akyildiz. Wireless underground sensor networks: Research challenges. *Ad Hoc Networks*, 4(2006):669–686, July 2006.

[29] Purdue University: IDEAS Mirowave Laboratory). `https://engineering.purdue.edu/IDEAS/Enviro.html/`.

[30] Impact of Illegal Dumping. `http://www.calrecycle.ca.gov/LEA/Training/IllegalDump/2009AprMay/Presentations/LACity.pdf`.

[31] S. Jeong, C. Yang, J. Courter, S. Kim, B. Pipes, and W. Chappell. Multilayer Composite for Below Ground Embedded Sensor Networking. In *IEEE Int. Conference of Antennas and Propagation*, 2008.

[32] G. Jiang, O. Gutierrez, K. R. Sharma, and Z. Yuan. Effects of nitrite concentration and exposure time on sulfide and methane production in sewer systems. *Journal of Water Research*, 44:4241, June 2010.

[33] J. Kim, J. Lim, J. Friedman, U. Lee, L. Vieira, D. Rosso, M. Gerla, and M. Srivastava. SewerSnort: A Drifting Sensor for In-situ Sewer Gas Monitoring. In *IEEE SECON'09*, Rome, Italy, June 2009.

[34] F. Kirchner and J. Hertzberg. A Prototype Study of an Autonomous Robot Platform for Sewerage System Maintenance. *Autonomous Robots*, 4(4):319–331, Apr. 1997.

[35] E. Kjeldsen and M. Hopkins. An Experimental Look at Rf Propagation in Narrow Tunnels. In *MILCOM'06*, Washington DC, Sep. 2006.

[36] O. Lahav, Y. Lu, U. Shavit, and R. Loewenthal. Modeling hydrogen sulfide emission rates in gravity sewage collection systems. *Journal of Environmental Engeneering*, 10(1061):1382–1389, 2004.

[37] X. Li. RSS-Based Location Estimation with Unknown Pathloss Model. *IEEE Transactions on Wireless Communications*, 5(12), Dec. 2006.

[38] M. Lienard and P. Degauque. Natural wave propagation in mine environements. *IEEE Transactions on Antenna and Propagation*, 9(48):1326–1339, 2000.

[39] K. Lorincz and M. Welsh. MoteTrack: A Robust, Decentralized Approach to RF-Based Location Tracking. In *LoCA'05*, Munich, Germany, May 2005.

[40] N. S. M Dorfman and M. Merkel. Swimming in Sewage. Technical report, Natural Resources Defense Council, February 2004.

[41] J. Mastarone and W. Chappell. Urban sensor networking using thick slots in manhole covers. In *IEEE Antennas and Propagation Society International Symposium*, 2006.

[42] Memsic Corp, MEMS sensors). `http://www.memsic.com/`.

[43] Metcalf and I. Eddy. *Wastewater Engineering: Treatment and Reuse, 4th edition*. McGraw-Hill, 2003.

[44] MicroStrain Corp, mXRS measurement system). `http://www.microstrain.com/`.

[45] A. Nassiraei, Y. Kawamura, A. Ahrary, Y. Mikuriya, and K. Ishii. A New Approach to the Sewer Pipe Inspection: Fully Autonomous Mobile Robot "KANTARO". In *IECON 2006*, Paris, Nov. 2006.

[46] R. Negenborn. Robot Localization and Kalman Filters. Technical Report INF/SCR-0309, Utrecht University, 2003.

[47] Inventory of New York City GREENHOUSE GAS EMISSIONS. `http://www.nyc.gov/html/om/pdf/ccp_report041007.pdf`.

[48] A. S. of Civil Engineers. Protocols for Identifying Sanitary Sewer Overflows. Technical Report CX 82697-01-0, USEPA, June 2000.

[49] L. A. D. of Public Works Bureau of Sanitation. Year at a Glance 2008-2009, City of Los Angeles, Department of Public Works, Bureau of Sanitation. Technical Report YAG 2010-2011, City of Los Angeles, 2011.

[50] P. Pathirana, N. Bulusu, A. Savkin, and S. Jha. Node Localization Using Mobile Robots in Delay-Tolerant Sensor Networks. *IEEE Transactions on Mobile Computing*, 4(3), May/June 2005.

[51] N. Pletcher and J. M. Rabaey. *Ultra-Low Power Wake-Up Receivers for Wireless Sensor Networks*. PhD thesis, EECS Department, University of California, Berkeley, May 2008.

[52] A. Popov and N. Zhu. Modeling Radio Wave Propagation in Tunnels with a Vectorial Parabolic Equation. *IEEE Trans. Antennas Propagation*, 48(9):1403, September 2000.

[53] Datasheet. Electrochemical H_2S Sensor 032-0102-000, RAE Systems.

[54] T. Rappaport. *Wireless Communications: Principles and Practice, 2nd Ed.* Prentice Hall, 2002.

[55] D. Rosso and M. K. Stenstrom. The Carbon-sequestration Potential of Municipal Wastewater Treatment. *Chemosphere*, 70(8):1468–1475, Feb. 2008.

[56] T. Schmid, J. Friedman, Z. M. Charbiwala, Y. H. Cho, and M. B. Srivastava. Low-Power High-Accuracy Timing Systems for Efficient Duty Cycling. In *ISLPED'08*, Bangalore, India, Aug. 2008.

[57] T. Schmid, J. Friedman, Z. M. Charbiwala, Y. H. Cho, and M. B. Srivastava. XCXO: An Ultra-low Cost Ultra-high Accuracy Clock System for Wireless Sensor Networks in Harsh Remote Outdoor Environments. In *ISSCC/DAC'08*, San Francisco, CA, Feb. 2008.

[58] ewer Design Manual - Part F. `http://eng.lacity.org/techdocs/sewermanual/index.html`.

[59] T. Shaneyfelt, M.A.Joordens, K. Nagothu, and M. Jamshidi. RF communication between Surface and Underwater Robotics Swarms. Technical report, Automation Congress, Hawaii, December 2008.

[60] Stenstrom *et al.*United States Patent US005790476A Date of Patent: Aug. 4, 1998.

[61] I. Stoianov, L. Nachman, and S. Madden. PIPENET: A Wireless Sensor Network for Pipeline Monitoring. In *IPSN'07*, Cambridge, MA, Apr. 2007.

[62] Streetline City Infrastructure Technologies. `http://www.streetlinenetworks.com/site/index.php`.

[63] M. Sugano, T. Kawazoe, Y. Ohta, and M. Murata. Indoor Localization System using RSSI Measurement of Wireless Sensor Network Based on ZigBee Standard. Technical report, Graduate School of Information Science and Technology, Osaka University, Osaka, Japan, 2006.

[64] G.L. Sindt, P.E. "Chloride and TDS Water Quality Standard Update", January 15, 2008.

[65] B. Teichgräber, J. Stemplewski, H. Althoff, and N. Elkmann. Remote Controlled Inspection Device for Large Sewers. *Water Practice & Technology*, Sep.

[66] TigerMap - US CENSUS. `http://www.census.gov/geo/www/tiger/tiger2006se/tgr2006se.html`.

[67] US-EPA. Estimate of Global Greenhouse Gas Emissions from Industrial and Domestic Wastewater Treatment. Technical Report EPA-600-R-97-091, US-EPA Office of Enforcement and Compliance Assurance, September 1997.

[68] US-EPA. Report to Congress: Implementation and Enforcement of the Combined Sewer Overflow Control Policy. Technical Report EPA 833-R-01-003, US-EPA Office of Water, Dec. 2001.

[69] US-EPA. The Clean Water and Drinking Water Infrastructure Gap Analysis. Technical Report EPA-816-R-02-020, Office of Water, Sep. 2002.

[70] US-EPA. Wastewater Collection System Infrastructure Research Needs. Technical Report EPA-600-JA-02-226, US-EPA, National Risk Management Research Laboratoryt, 2002.

[71] US-EPA. Guide For Evaluating Capacity, Management, Operation, and Maintenance (CMOM) Programs At Sanitary Sewer Collection Systems. Technical Report EPA-305-B-05-002, US-EPA Office of Enforcement and Compliance Assurance, Jan. 2005.

[72] P. Varley. Responding to Disasters: The Story of the Guadalajara Sewer Explosion. Technical Report C16-94-1180.0 p3-6, Kennedy School of Government Case Program, 1994.

[73] J. Vollertsen, A. H. Nielsen, H. S. Jensen, and T. Hvitved-Jacobsen. Modeling the Formation and Fate of Odorous Substances in Collection Systems. *Water Environment Research*, 80(2):118–126, Feb. 2008.

[74] M. Ward, R. Corsi, R. Morton, T. Knapp, D. Apgar, C. Quigley, C. Easter, J. Witherspoon1, A. Pramanik, and W. Parker. Characterization of Natural Ventilation in Wastewater Collection Systems. *Water Environment Research*, 83(3):265, March 2011.

[75] In sewer gas model). `http://www.werf.org/am/template.cfm?section=Search\&template=/cm/ContentDisplay.cfm\&ContentID=9893`.

[76] L. Zhang, P. D. Schryver, B. D. Gusseme, W. D. Muynck, N. Boon, and W. Verstraete. Chemical and Biological Technologies for Hydrogen Sulfide Emission Control in Sewer Systems: A Review. *Water Research*, 42(1-2):1–12, Jan. 2008.

[77] Specification of ZigBee Technology). `http://www.ZigBee.org/`.